Chem Soc Rev

REVIEW ARTICLE

View Article Online
View Journal

Cite this: DOI: 10.1039/d0cs01370f

Overcoming barriers in photodynamic therapy harnessing nano-formulation strategies

Jianlei Xie,[a] Yingwei Wang,†[bc] Wonseok Choi,†[b] Paramesh Jangili,†[b] Yanqi Ge,[a] Yunjie Xu,[ab] Jianlong Kang,[a] Liping Liu,[d] Bin Zhang,[a] Zhongjian Xie,[a] Jun He,[c] Ni Xie,*[a] Guohui Nie,[a] Han Zhang *[a] and Jong Seung Kim *[b]

Photodynamic therapy (PDT) has been extensively investigated for decades for tumor treatment because of its non-invasiveness, spatiotemporal selectivity, lower side-effects, and immune activation ability. It can be a promising treatment modality in several medical fields, including oncology, immunology, urology, dermatology, ophthalmology, cardiology, pneumology, and dentistry. Nevertheless, the clinical application of PDT is largely restricted by the drawbacks of traditional photosensitizers, limited tissue penetrability of light, inefficient induction of tumor cell death, tumor resistance to the therapy, and the severe pain induced by the therapy. Recently, various photosensitizer formulations and therapy strategies have been developed to overcome these barriers. Significantly, the introduction of nanomaterials in PDT, as carriers or photosensitizers, may overcome the drawbacks of traditional photosensitizers. Based on this, nanocomposites excited by various light sources are applied in the PDT of deep-seated tumors. Modulation of cell death pathways with co-delivered reagents promotes PDT induced tumor cell death. Relief of tumor resistance to PDT with combined therapy strategies further promotes tumor inhibition. Also, the optimization of photosensitizer formulations and therapy procedures reduces pain in PDT. Here, a systematic summary of recent advances in the fabrication of photosensitizers and the design of therapy strategies to overcome barriers in PDT is presented. Several aspects important for the clinical application of PDT in cancer treatment are also discussed.

Received 31st January 2021

DOI: 10.1039/d0cs01370f

rsc.li/chem-soc-rev

1. Introduction

Photodynamic therapy (PDT) is a promising unique strategy for tumor therapy with high spatiotemporal selectivity and low side-effects. In PDT, several reactive oxygen species (ROS) are produced *in situ* to destroy cancer cells with the introduction of photosensitizers into tumor tissues and the delivery of light with suitable wavelength.[1] Ideally, PDT constitutes a non-invasive approach for cancer treatment. Both the photosensitizers and the light used in PDT are principally non-toxic when administered alone. Additionally, the cytotoxicity of PDT is restricted to light-exposed regions due to the very short lifetime (<200 ns) and diffusion range (about 20 nm) of ROS.[2] Therefore, the side effects of PDT are broadly acceptable compared to radiotherapy and chemotherapy. In particular, PDT is promising in that it can stimulate effective anti-tumor immune responses. Considering these advantages, PDT has been extensively investigated for cancer treatment and also utilized in several medical fields, including immunology,[3–5] urology,[6–8] dermatology,[9–11] ophthalmology,[12–14] cardiology,[15–17] pneumology,[18–20] and dentistry.[21–23]

However, the clinical application of PDT is largely restricted by several barriers. Traditional photosensitizers are mostly activated by light of short wavelengths with low tissue penetrability.[24] Therefore, the clinical application of PDT is currently restricted to superficial tumors, such as skin, head and neck tumors, *etc*.[25] Meanwhile, several other drawbacks of traditional photosensitizers, such as low water solubility, lack of tumor-targeting ability, and potential toxicity to normal tissues, also hinder the application of PDT in clinical practice. Moreover, PDT is unique in that it induces complex events in both the tumor tissues (tumor vascular damage,[26,27] tumor cell apoptosis,[28] necrosis or autophagy,[29–32] release of cell debris

[a] Key Laboratory of Optoelectronic Devices and Systems of Ministry of Education and Guangdong Province, Institute of Microscale Optoelectronics, and Otolaryngology Department and Biobank of the First Affiliated Hospital, Shenzhen Second People's Hospital, Health Science Center, Shenzhen University, Shenzhen 518060, P. R. China. E-mail: xn100@szu.edu.cn, hzhang@szu.edu.cn

[b] Department of Chemistry, Korea University, Seoul 02841, Korea. E-mail: jongskim@korea.ac.kr

[c] Hunan Key Laboratory of Nanophotonics and Devices, School of Physics and Electronics, Central South University, 932 South Lushan Road, Changsha, Hunan 410083, P. R. China

[d] Department of Hepatobiliary and Pancreatic Surgery, The 2nd Clinical Medical College (Shenzhen People's Hospital) of Jinan University, Shenzhen 518020, P. R. China

† J. X., Y. W., W. C., and P. J. contributed equally to this work.

and tumor specific antigen,[33] activation of the antioxidant system,[34,35] damage-repair system or pro-survival signaling,[36–39] *etc.*) and the hosts (retention, transformation, degradation or excretion of photosensitizers in the liver, kidneys and other organs,[40–43] activation of the immune system,[33,44] *etc.*), which may contribute to the tumor inhibition or resistance to the therapy. Therefore, the efficiency of PDT is also largely restricted by cellular responses and tumor resistance to the therapy, which are mediated by many different mechanisms. For example, the excretion of photosensitizers by transporters or exocytosis reduces their retention in tumor cells.[40,41,43] ROS generation may be dampened by the hypoxic tumor microenvironment.[45–47] Also, the activation of the antioxidant system in tumor tissues leads to scavenging of ROS.[34,35,48] Expression of heat shock proteins promotes the repair of proteins damaged by ROS.[36,37] Induction of pro-survival signaling pathways may reduce PDT induced tumor cell death.[39] The immune activation ability of PDT is also hampered by the immunosuppressive microenvironment of tumor tissues.[49] Another important but less concerned issue is the severe pain induced by PDT. During PDT treatment, the pain experienced by patients is sometimes intense or even intolerable, which causes the interruption or termination of the PDT process.[50–52] Therefore, the development of novel photosensitizer formulations and therapy strategies to overcome these barriers is critical for the clinical application of PDT.

Several kinds of nanomaterials possess promising optical and physicochemical properties (high ROS generation efficiency, being responsive to light of suitable wavelength, tumor targeting ability, moderate physiological stability and circulation time, excellent biocompatibility, *etc.*), making them attractive alternatives to traditional photosensitizers for PDT.[53–57] Also, various nanomaterials have been successfully used as carriers to improve the water solubility, tumor-targeting efficiency, and ROS production of traditional photosensitizers.[49,58–60] Therefore, considering the suggested advantages from nanomaterials, various nanoparticles, nanocomposites, and corresponding therapy strategies have been developed to overcome the barriers in PDT.[5,61–64] This review summarizes the recent advances in these issues. First, the principle of PDT and the development of photosensitizers are introduced. Then, various nanoparticles applied in PDT, either as carriers or as photosensitizers, are summarized, followed by the strategies for the fabrication of nanocomposites for PDT. Based on this, the physicochemical properties of these materials and their applications in the treatment of deep-seated tumors, modulation of cell death pathways, relief of tumor resistance to PDT, and the reduction of severe pain induced by PDT are summarized. Finally, several aspects important for the clinical application of PDT in cancer treatment are discussed.

2. Basic principles of PDT

Production of ROS by photosensitizers in response to light stimulation is the core reaction of PDT. Two types of photodynamic reactions have been reported based on the type of ROS

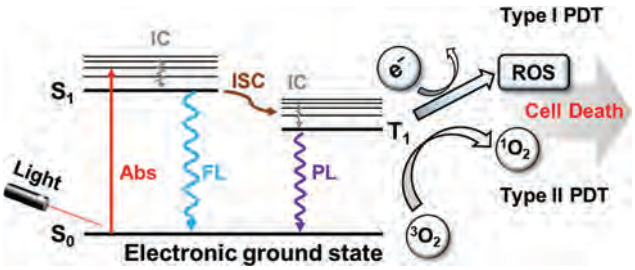

Fig. 1 Principles of type I and type II photodynamic reactions.

generation from the photosensitizers in the presence of light (Fig. 1). In a type I reaction, the ground-state photosensitizers are first activated to the singlet excited state upon exposure to light and then to the triplet excited state by intersystem crossing, in which electrons are transferred to surrounding substrates to produce radical anions and oxygenated products. In a type II reaction, the activated photosensitizers transfer energy to tissue oxygen to produce highly active singlet oxygen, which reacts with biological molecules to destroy cancer cells.[2,54]

The highly reactive ROS produced during PDT attack the surrounding bio-molecules, such as lipids, proteins, and DNA, to exert a cytotoxic effect (Fig. 2).[65,66] Lipids, especially unsaturated lipids, are sensitive to ROS.[67,68] The radicals generated in photodynamic reactions induce lipid peroxidation.[69] Meanwhile, unsaturated lipids might be directly added by singlet oxygen to form lipid peroxides. Lipid peroxidation damages the structure and function of bio-membranes.[67] Furthermore, these radicals might trigger free-radical chain reactions, leading to the secondary modification of proteins and polynucleotides.[65,69,70] Therefore, plasma membrane and membranous organelles, such as mitochondria, endoplasmic reticulum (ER), Golgi apparatus, and lysosomes, are vulnerable to PDT. Damage to these organelles leads to apoptosis, necrosis, or autophagy-mediated cell death.[67]

Proteins are also sensitive to the ROS produced during the PDT procedure (Fig. 2).[65,71] Amino acid residues, such as cysteine, methionine, tyrosine, histidine, and tryptophan, are the primary sites of oxidative modification of proteins.[72,73] ROS-mediated oxidation of proteins results in the formation of different products, depending on the amino acid sequence of each protein. Therefore, different proteins exhibit quite different sensitivities to ROS.[66] Cross-linking of proteins with other proteins or photosensitizers might also occur in response to PDT.[74] All these reactions damage the structure, catalytic activity, and biological functions of proteins, contributing to PDT-induced cell death.[72,75]

DNA is also an essential target of ROS in PDT (Fig. 2). Guanine (one of the DNA base pairs) is especially sensitive to oxidative damage. ROS-induced damage to mitochondrial and genomic DNA might also give rise to cancer cell apoptosis.[76,77]

3. Toward better photosensitizers

Generally, several characteristics are required for an ideal photosensitizer. First, a high quantum yield is required for photosensitizers to achieve efficient production of ROS.

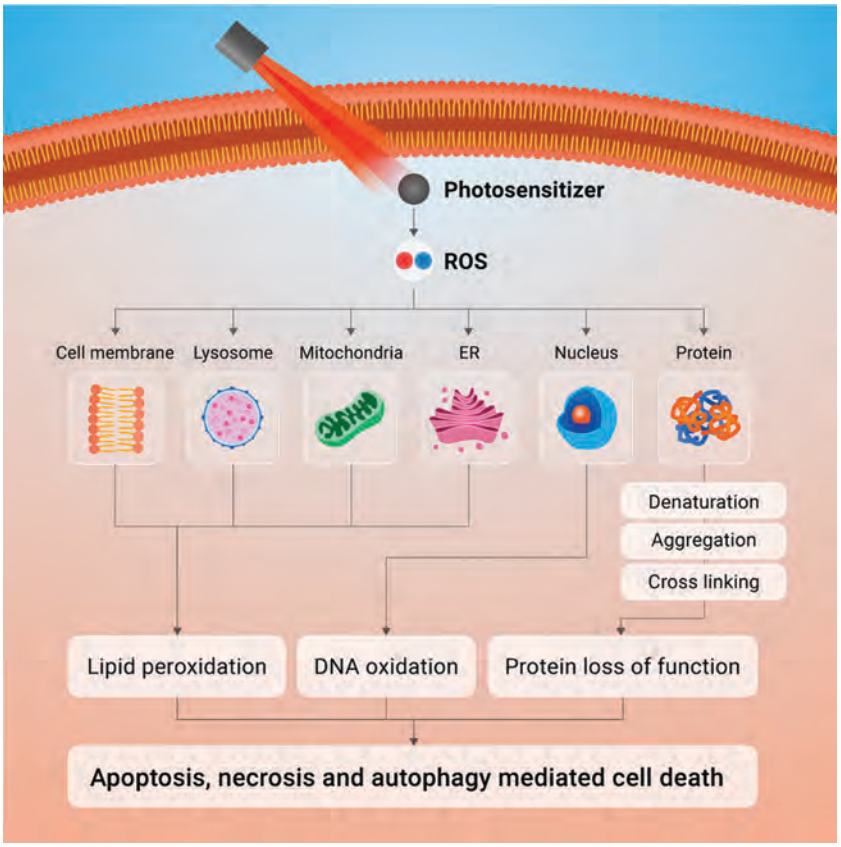

Fig. 2 Molecular targets of ROS in PDT. Lipids, proteins, and DNA are the main targets of ROS in PDT. Lipid peroxidation following PDT damages membrane structures, including cell membranes, lysosomes, mitochondria, and ER. ROS-mediated oxidation leads to the denaturation, aggregation, and cross-linking of cellular proteins, resulting in the loss of function of the targets. ROS might also attack both mitochondrial and genomic DNA. All these processes give rise to apoptosis, necrosis, or autophagy-mediated cancer cell death in PDT.

Second, activation by light with better tissue penetration ensures the application in deep tissues. Third, efficient accumulation in tumor tissues and precise targeting to certain organelles are critical for specific induction of tumor cell death with high efficiency. Fourth, suitable retention time in the body and negligible dark toxicity are important to minimize the side-effects.

In search of better photosensitizers, several generations of photosensitizers have been developed (Fig. 3).[53,54] The application of various nanomaterials in PDT, either as carriers or as photosensitizers, is a milestone in this field. Significantly, the fabrication of various nanocomposites and investigation of corresponding therapy strategies provide powerful tools to overcome the barriers in PDT.

3.1. Traditional photosensitizers

The first generation of photosensitizers included porphyrin and hematoporphyrin (Fig. 3).[53] Several of these photosensitizers have been approved for the clinical treatment of esophageal, bladder and lung cancers, and the early stages of cervical cancer after investigations for many years.[53] However, the clinical application of these photosensitizers is restricted by several drawbacks, such as relatively poor absorption of light with high tissue penetration, low efficiency of ROS production, lack of tissue specificity, and long retention time in the human body.[54,78]

A group of macrocyclic compounds composed of porphyrin-based structures and several non-porphyrinoid compounds were developed and introduced as the second generation of photosensitizers considering the shortcomings of the first generation of photosensitizers (Fig. 3).[53] Generally, the quantum yields of second-generation photosensitizers are higher than those of the first generation. Meanwhile, efficient activation by light of longer wavelengths improves the therapeutic effect on deeper tissues. Moreover, the shorter retention time in the body reduces the phototoxicity to normal tissues. However, the lack of tumor specificity still restricts the clinical application of the second generation of photosensitizers.[54]

Recently, considerable efforts have been made to develop novel photosensitizers with better tumor-specific delivery or targeting efficacy. It is a popular strategy to modify the existing photosensitizers with targeting moieties. Recently, the application of nanomaterials either as carriers or as photosensitizers strongly promotes the development of PDT.[54,79]

3.2. State-of-the-art nanomaterials in PDT

With the development of nanotechnology, a series of nanomaterials have been reported to exhibit an efficient ROS generation

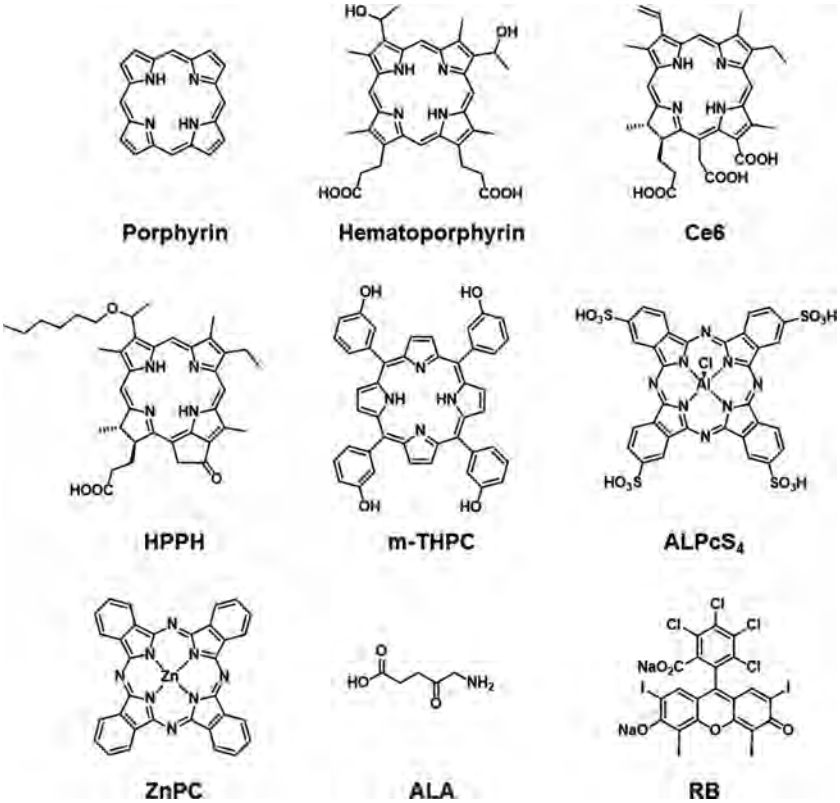

Fig. 3 Molecular structures of representative traditional photosensitizers. Molecular structures of representative photosensitizers of the first (porphyrin and hematoporphyrin) and second (Ce6, HPPH, m-THPC, ALPcS4, ZnPC, ALA, and RB) generations are presented [Ce6: Chlorin e6; HPPH: 2-[1-hexyloxyethyl]-2-devinyl pyropheophorbide-a; m-THPC: *meta*-tetra(hydroxyphenyl)-chlorin; ALPcS4: aluminum phthalocyanine tetrasulfonate; ZnPC: Zn(II)-phthalocyanine; ALA: aminolevulinic acid; RB: Rose Bengal].

ability in response to light excitation, enabling their use as photosensitizers in PDT.[61,80–84] Moreover, nanomaterials are also ideal carriers for traditional photosensitizers.[54,85] Nanomaterial-mediated PDT of cancers is associated with several advantages. First, nanomaterials exhibit better tumor-targeting efficacy, and passively transport and accumulate in tumors through the enhanced permeability and retention (EPR) effect due to their particle size and the abnormal vascular structure of tumors.[58,86,87] The targeting efficacy of nanomaterials can also be effectively modulated through surface modification and functionalization to achieve enhanced tumor-killing efficiency and reduced toxicity to normal tissues.[83,88] Second, nanomaterial-based photosensitizers exhibit better photostability than traditional ones. Hence, less photo-bleaching is observed upon light exposure.[80,89] Third, the optical properties of nanomaterials are highly adjustable, which provides the system with more possibilities and capabilities.[87,90] Fourth, the multifunctional feature of nanomaterials enables diagnostic imaging of the treatment process and further improvement of the specificity and therapeutic effects.[91,92] Furthermore, the large surface area of nanomaterials enables high drug loading capability so that traditional photosensitizers and other drugs can be delivered into tumors for combinational therapy.[25] Several experiments have been conducted to investigate the potential applications of nanomaterials as carriers or as photosensitizers in PDT.

3.2.1. Nanocarriers for photosensitizers. Nanomaterials are suitable for drug loading and delivery due to their large surface-to-volume ratios. The pharmacokinetics of traditional photosensitizers can be effectively optimized by loading them on suitable nanoparticles.[58,93–96] Accumulation of nanoparticles in tumors through the EPR effect gives rise to passive tumor targeting of photosensitizers. Moreover, surface modification of nanoparticles with various targeting moieties significantly enhances the targeting efficacy of photosensitizers. Many nanoparticles fabricated with naturally occurring or synthetic materials have been used as carriers of photosensitizers for cancer PDT (Table 1).[97]

3.2.1.1 Inorganic nanoparticles for photosensitizer delivery. Several kinds of inorganic nanoparticles, such as silica nanoparticles,[98] metal oxide nanoparticles,[99] and gold nanoparticles,[100] have been widely investigated in tumor theranostics. These nanoparticles constitute ideal carriers for photosensitizers due to their highly adjustable morphology, excellent loading capacity, and biocompatibility.[1,59,101]

Silica nanoparticles, such as mesoporous silica nanoparticles, can act as excellent drug carriers because of their excellent biocompatibility, large surface area, and high pore volume.[101] As ''generally regarded as safe'' (GRAS) materials, they are biodegradable and can be surface-modified for more efficient drug loading, targeted drug delivery, and controlled

Table 1 Summary of representative nanocarriers of photosensitizers

Nanomaterial	Photosensitizer	Functionalization	Size (nm)	Light (nm)	Administration	Cancer	Remarks	Ref.
Hollow silica nanoparticles	Phthalocyanine	—	35	730	Intratumoral	Sarcoma	Highly efficient dual PDT and PTT	103
Mesoporous silica nanoparticles	ICG	PEG–folic acid	193.40	808	Intratumoral	Breast cancer	Ultrasonic/NIR fluorescence imaging and PDT/PTT	105
Iron oxide nanoparticles	PpIX	—	37	632	Intravenous	Breast cancer	Magnetic resonance imaging-guided PDT	99
Iron oxide nanoclusters	Ce6	DA–PAA–PEG	100	704	Intravenous	Breast cancer	Red-shift of the absorption/excitation peak from 650 nm to 700 nm	108
Micelles	PpIX	—	123.9	He–Ne laser	Intravenous	Lung cancer	Prolonged blood circulation and enhanced tumor-targeting ability	113
Liposomes	Aggregation-induced emission photosensitizers	—	160–200	480, 810	Intravenous	Breast cancer	Controlled photosensitivity of the photosensitizers and reduced side effects	507
Human serum albumin nanoassemblies	Ce6	—	100	660	Intravenous	Breast cancer	Fluorescence, photoacoustic, and magnetic resonance triple-modal imaging-guided PDT	115
DNA origami	BMEPC	—	115 (edge), 2 (height)	440	—	Breast cancer	Restricted intramolecular rotation of BMEPC, intensified fluorescence emission and radical production	117

drug release. Meanwhile, they are suitable for enhancing the solubility of poorly water-soluble drugs and traditional photosensitizers.[93,102]

For example, hollow silica nanospheres have been used for the delivery of a highly hydrophobic photosensitizer, phthalocyanine. Enhanced water-dispersity of the photosensitizer was achieved with this strategy. Efficient loading and delivery of phthalocyanine into tumor cells enabled highly effective dual PDT and photothermal therapy (PTT) of sarcoma *in vivo* with 730 nm laser irradiation.[103] Dual-modal imaging-guided combined PDT/PTT of cancer was also achieved with mesoporous silica nanoparticles as carriers through the manipulation of cargoes and surface modification (Fig. 4). Both perfluorohexane and indocyanine green (ICG) were loaded into mesoporous silica nanoparticles for ultrasonic/near-infrared (NIR) fluorescence imaging to achieve this goal (Fig. 4b and c). In response to NIR light irradiation, the production of ROS was catalyzed by ICG, while hyperthermia was produced from the polydopamine coating of the nanoparticles (Fig. 4d and e). Dramatic tumor inhibition was observed with this combined strategy (Fig. 4f).[104,105]

Metal oxide (such as iron oxide) nanoparticles are also used as carriers for tumor targeting of photosensitizers. The excellent contrast enhancement of iron oxide nanoparticles also makes imaging-guided PDT of cancer possible.[106,107] More importantly, the efficient response of iron oxide nanoparticles to the magnetic field enables enhanced targeting of tumors. Yan *et al.* reported the application of protoporphyrin IX (PpIX)-loaded super-paramagnetic iron oxide nanoparticle (SPION) nanoclusters in magnetic resonance imaging-guided PDT. Highly efficient loading of PpIX onto SPIONs ensured enhanced ROS production and significant inhibition of tumor growth *in vivo*.[99] Li *et al.* also reported the application of iron oxide nanoclusters in the targeted delivery of photosensitizers for PDT. The photosensitizer Ce6 was loaded onto polyethylene glycol (PEG) functionalized iron oxide nanoclusters. Interestingly, the absorption/excitation peak of Ce6 shifted from ~650 nm to ~700 nm after this process, enabling activation by NIR light. The cellular uptake of Ce6 was also significantly accelerated by combining with these nanoparticles. The tumor-targeting efficiency of these nanoparticles was also improved with the assistance of a magnetic field. More favorable tumor therapy effects were achieved with this nanocomposite both *in vitro* and *in vivo*.[108]

The localized surface plasmon resonance (LSPR) effect of specific inorganic nanoparticles, such as gold nanoparticles, also enables energy transfer from the nanoparticles to the loaded photosensitizers apart from simply being used as a carrier of photosensitizers. This gives rise to enhanced ROS production efficiency and therapeutic effect in PDT.[59,60]

Despite their extraordinary physicochemical properties, further investigation is still needed to confirm the biocompatibility of inorganic nanoparticles in the human body. Due to the high stability of several inorganic nanoparticles, the pharmacokinetics *in vivo* and long-term impacts to the immune system and important organs (especially the liver, kidneys, and lungs) should be further clarified for clinical application.

3.2.1.2 Organic nanoparticles for photosensitizer delivery. Organic nanoparticles, such as polymeric micelles, nanospheres, nanocapsules, liposomes, and dendrimers, are also important carriers to deliver photosensitizers in PDT (Fig. 5). Organic nanoparticles might be prepared with various naturally occurring or synthetic organic molecules, such as polyesters, polyacrylamides, phospholipids, proteins, nucleic acids, polysaccharides, *etc.*[5,49,58,63,109] With different formulations, hydrophilic and hydrophobic chemicals can be effectively

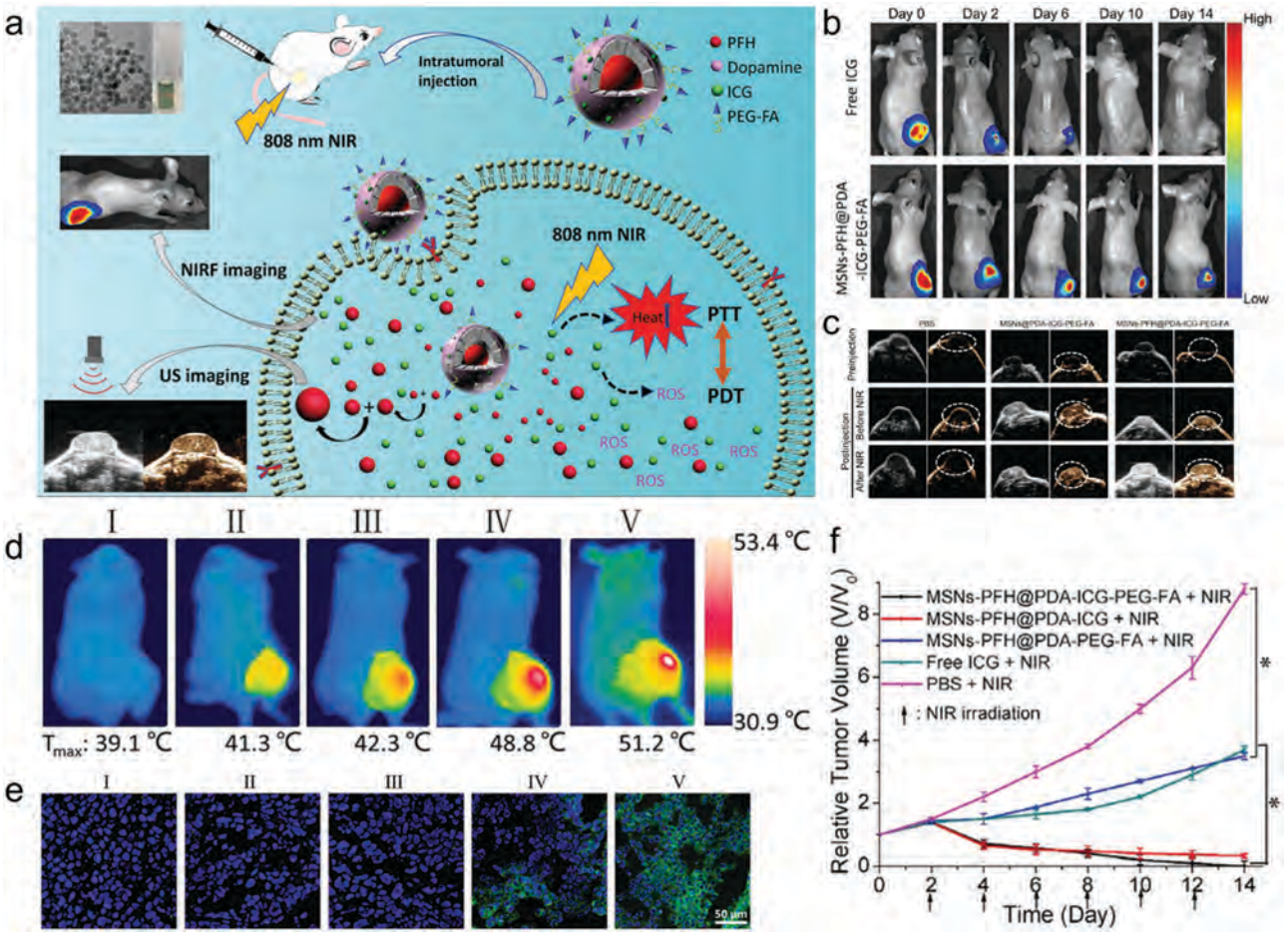

Fig. 4 Mesoporous silica nanoparticles as carriers for dual-modal imaging-guided combined PDT/PTT of cancer. (a) Schematic illustration of the theranostic system constructed with mesoporous silica nanoparticles. (b) *In vivo* bio-distribution of the nanoparticles depicted with NIR fluorescence imaging. (c) *In vivo* ultrasonic images of the tumor. (d) *In vivo* PTT efficacy of the nanoparticles. (e) *In vivo* PDT efficacy of the nanoparticles depicted by 2,7-dichlorodihydrofluorescein diacetate (DCFH-DA) staining in tumor sections. (f) Tumor growth curves following the indicated treatments. Reproduced with permission.[105] Copyright, 2019, Wiley-VCH.

loaded into organic nanoparticles, enabling their full application in PDT.[5,58,110]

For example, micelles are molecular aggregates dispersed in colloidal solutions. In aqueous solutions, micelles are formed with the hydrophilic heads of molecules in contact with the solvent, while the hydrophobic tails aggregate at the center. Therefore, hydrophobic drugs, such as photosensitizers, can be loaded in the core of micelles and delivered to tumors.[111,112] Tsai *et al.* investigated the application of pH-sensitive micelles in PDT. The photosensitizer PpIX was encapsulated in either non-pH-sensitive or pH-sensitive micelles for cancer cell treatment. PpIX was localized in lysosomes with non-pH-sensitive micelles. However, nuclear localization of PpIX was observed when delivered with pH-sensitive micelles. Delivery with micelles also gave rise to prolonged blood circulation and enhanced tumor targeting ability, effecting better anti-tumor activity.[113]

Bio-molecules, such as proteins, nucleic acids, and polysaccharides, are also used for photosensitizer delivery. Serum albumin is a globular protein abundant in blood plasma and has widely been used to deliver drugs, genes, peptides, and imaging agents.[114] Serum albumin is suitable for the delivery of hydrophobic drugs, such as photosensitizers, with no need for toxic solvents. Hu *et al.* prepared human serum albumin nanoassemblies to deliver the photosensitizer Ce6. Ce6 was loaded onto these nanoparticles through S–S bond cross-linking and hydrophobic interactions. Excellent reduction response and enhanced tumor targeting and retention were observed within this nanocomposite. *In vitro* and *in vivo* investigations confirmed the enhanced anti-tumor efficacy of this nanocomposite.[115] Folic acid moiety was tagged to albumin to enhance the uptake of the co-delivered photosensitizer by tumor cells to enhance the targeting efficiency of albumin nanoparticles. This targeted delivery strategy results in improved cytotoxicity.[116]

Nucleic acids, such as DNA, are also successfully used for photosensitizer delivery. A DNA origami was designed to form two- or three-dimensional nanostructures suitable for drug loading by taking advantage of the interaction between complementary base pairs. For example, Zhuang *et al.* successfully loaded the photosensitizer 3,6-bis[2-(1-methylpyridinium)ethynyl]-9-pentylcarbazole diiodide (BMEPC) onto a DNA origami. With this strategy, aggregation-induced photobleaching of BMEPC was effectively reduced.

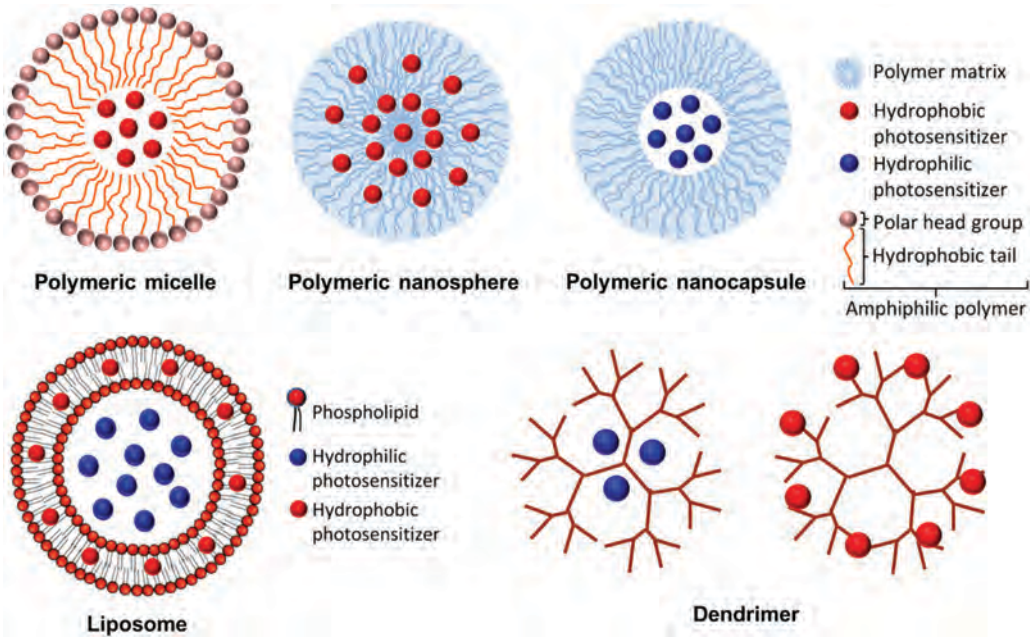

Fig. 5 Organic nanoparticles for the delivery of hydrophobic or hydrophilic photosensitizers in PDT. Reproduced with permission.[54] Copyright, 2015, American Chemical Society.

More interestingly, the intramolecular rotation of BMEPC was also restricted after loading onto the DNA origami, resulting in enhanced ROS production and cytotoxicity following light stimulation.[117] Kim *et al.* prepared a self-assembled DNA tetrahedron to deliver the photosensitizer methylene blue for cancer PDT utilizing the advantage of the DNA binding property of the photosensitizer.[118] It was demonstrated that the developed DNA nano-construct effectively inhibited the tumor growth *in vivo*. DNA photocleavage after the therapy effectively reduced the potential side effects.[117] The highly programmable sequence, diverse nanostructures, moderate stability, and excellent biocompatibility of DNA based nanocarriers make them promising for future applications.

3.2.2. Nanomaterials as photosensitizers. Several nanomaterials can generate ROS themselves under light stimulation, making them suitable for use as photosensitizers for PDT due to their unique optical properties (Table 2). Compared to traditional photosensitizers, nanomaterial-based photosensitizers have better photostability, passive tumor targeting ability mediated by the EPR effect, and convenient for further modification and combined therapy.

3.2.2.1 Noble metal nanoparticles as photosensitizers. In addition to being carriers for photosensitizers, several kinds of noble metal nanoparticles are also directly used as photosensitizers in cancer PDT. Gold nanostructures are the most representative noble metal photosensitizers. Under laser irradiation, the strong LSPR of gold nanoparticles allows their enhanced light–matter interaction in a specific wavelength range, resulting in enhanced light absorption and photothermal conversion.[119–121] When light excites on the surface of gold nanoparticles, the energy from LSPR can be transferred to the oxygen molecule in the ground state effectively to produce singlet oxygen, which is a typical type II PDT process.[122–126] Interestingly, the size or other morphological parameters finally determine the LSPR band of gold nanostructures, making it possible to activate them with light of higher tissue penetrability to enable application in deeper tissues. This feature endows gold nanoparticles with tunable and multiple function potential in diagnostic applications.[127,128] Vankayala *et al.* reported the efficient production of singlet oxygen with gold nanorods (NRs) upon NIR light stimulation. Eradication of B16F0 melanoma was observed with gold NR-mediated PDT. The highly potent anti-tumor effects achieved with this strategy enabled the use of a low-energy light-emitting diode array instead of a high-power laser as a light source (Fig. 6).[81] Two-photon excited singlet oxygen production was also achieved with the gold NRs. Significantly higher singlet oxygen production levels were observed compared with the traditional photosensitizers, such as RB and ICG. The gold NRs exhibited good biocompatibility and efficient cellular uptake after functionalization with polyvinylpyrrolidone. This nanocomposite efficiently destroyed HeLa cervical cancer cells.[129]

In addition, gold nanostructures with different morphologies were constructed to optimize the PDT performance. Gold nanoechinus,[130] gold nanoshells,[131] gold bipyramids,[132] and gold nanocages[131] were reported to achieve highly efficient singlet oxygen generation and tumor elimination. The light resource also plays a critical role in the PDT process. Under X-ray irradiation, enhanced generation of hydroxyl radical and superoxide anion can be observed than under UV light irradiation.[133]

Light-stimulated ROS production and PDT-mediated killing of cancer cells [breast (MCF-7) and lung (A549)] were also validated with silver nanoparticles as photosensitizers.[134]

Table 2 Summary of representative nanomaterial-based photosensitizers

Nanomaterial	Functionalization	Targeting	Size (nm)	Light (nm)	Administration	Cancer	Remarks	Ref.
Gold NRs	Lipofectamine 2000	—	37.3 (length), 11 (diameter)	915	Intratumoral	Melanoma	First demonstration of gold NR-mediated PDT	81
TiO_2 nanoparticles	—	IL13R antibody	5	Visible light	—	Brain cancer	Visualization with synchrotron X-ray fluorescence microscopy at the submicrometer scale	82
ZnO nanoparticles	Phospholipid DOPC	—	21	255	—	Cervical cancer	UV-stimulated PDT	140
Fullerene	DSPE-mPEG	—	100	730	Intravenous	Cervical cancer	Photoacoustic imaging-guided PDT and PTT	87
Graphene oxide	PEG	Folate	100	980	Intravenous	Melanoma	Fluorescence imaging-guided PDT and PTT	64
Graphene quantum dots	—	—	2–6	405, 637	Subcutaneous	Breast cancer	High quantum yield of ~1.3, broad absorption band spanning the UV region and the entire visible region, strong deep-red emission	144
BP nanosheets	—	—	2 (height)	660	Subcutaneous	Breast cancer	High quantum yield of about 0.91, photodegradable	61
BP quantum dots	PEG	—	2.5	625	Intratumoral	Breast cancer	Prominent NIR photothermal and red light-triggered photodynamic properties	183
DBP-UiO NMOFs	—	—	100 (diameter), 10 (thickness)	640	Intratumoral	Head and neck cancer	Highly potent PDT agents for the treatment of resistant cancers	84
SPNs	Cell membranes of activated fibroblasts	—	47 (diameter)	808	Intravenous	Breast cancer	Enhanced tumor accumulation, stronger bioimaging ability and combined PTT/PDT	195

3.2.2.2 Metal oxide nanoparticles as photosensitizers. Metal oxide nanoparticles, such as titanium dioxide (TiO_2) and zinc oxide (ZnO) nanoparticles, can also catalyze ROS production when stimulated with a light of suitable wavelength.[80] The photocatalytic activity of TiO_2 was first reported in 1972.[135] Due to its vibrant photocatalytic properties, TiO_2 has widely been used in many energy-conversion processes, such as photo-degradation, CO_2 reduction, and solar cells.[54] Under UV light irradiation, the large photon energy permits ground state electron transition from the valence band to the conduction band by crossing the band gap of TiO_2. The excited carriers, holes, and electrons are formed in the valence band to the conduction band of the semiconductor. Before the recombination of holes and electrons, the holes react with the surrounding water to produce radicals and the electrons are transferred to the surrounding oxygen to form superoxide anions.[136,137] Such a type I PDT reaction in TiO_2 endows it with the potential for wide application in the treatment of hypoxic tumor tissues, though its potential in the treatment of deep-seated tumors is still limited by the relatively short wavelength of corresponding light sources.[82,138,139] For example, TiO_2 nanoparticles (5 nm) were also used as photosensitizers in brain cancer (glioblastoma) PDT (Fig. 7). An antibody against the glioblastoma multiforme surface marker IL13α2R was covalently tethered to the nanoparticles with a dihydroxybenzene bivalent linker to enhance the targeting efficiency of brain cancer (Fig. 7). Visible light-stimulated production of ROS with this nanocomposite gave rise to the programmed death of cancer cells.[82]

ZnO nanoparticles are also used as photosensitizers for PDT with bandgap energy and photocatalytic activity similar to TiO_2. A lipid bilayer was used to coat the nanoparticles to enhance the stability of ZnO nanoparticles in biological media. The lipid-coated ZnO nanoparticles were effectively internalized by human epithelial carcinoma cells through a liposomal pathway. ROS production and enhanced cancer cell death were observed following stimulation with ultraviolet (UV) light.[140] Moreover, doping of ZnO nanoparticles with silver stimulated the production of ROS in the daylight.[141]

3.2.2.3 Carbon-based nanomaterials as photosensitizers. Carbon-based nanomaterials, such as fullerenes, graphene, and graphene oxide are also widely used in tumor theranostics.[142–144] These materials are mostly hydrophobic. However, it is usually quite convenient to modify the surface of carbon-based nanomaterials through either electrostatic interactions or covalent bonding.[83] Many studies have been conducted to investigate the application potential of various carbon-based nanomaterials for the loading and delivery of photosensitizers and imaging agents.[54,143] Meanwhile, several kinds of carbon-based nanomaterials can also catalyze ROS production in response to light stimulation, making them potent photosensitizers for cancer PDT.[83]

3.2.2.3.1 Fullerenes. Fullerenes are allotropes of carbon, consisting of hollow cages of carbon atoms. Due to their unique structure and properties, fullerenes have attracted much attention in various fields since their discovery in 1985.[145] Fullerenes are ideal carriers for the delivery of drugs and photosensitizers.

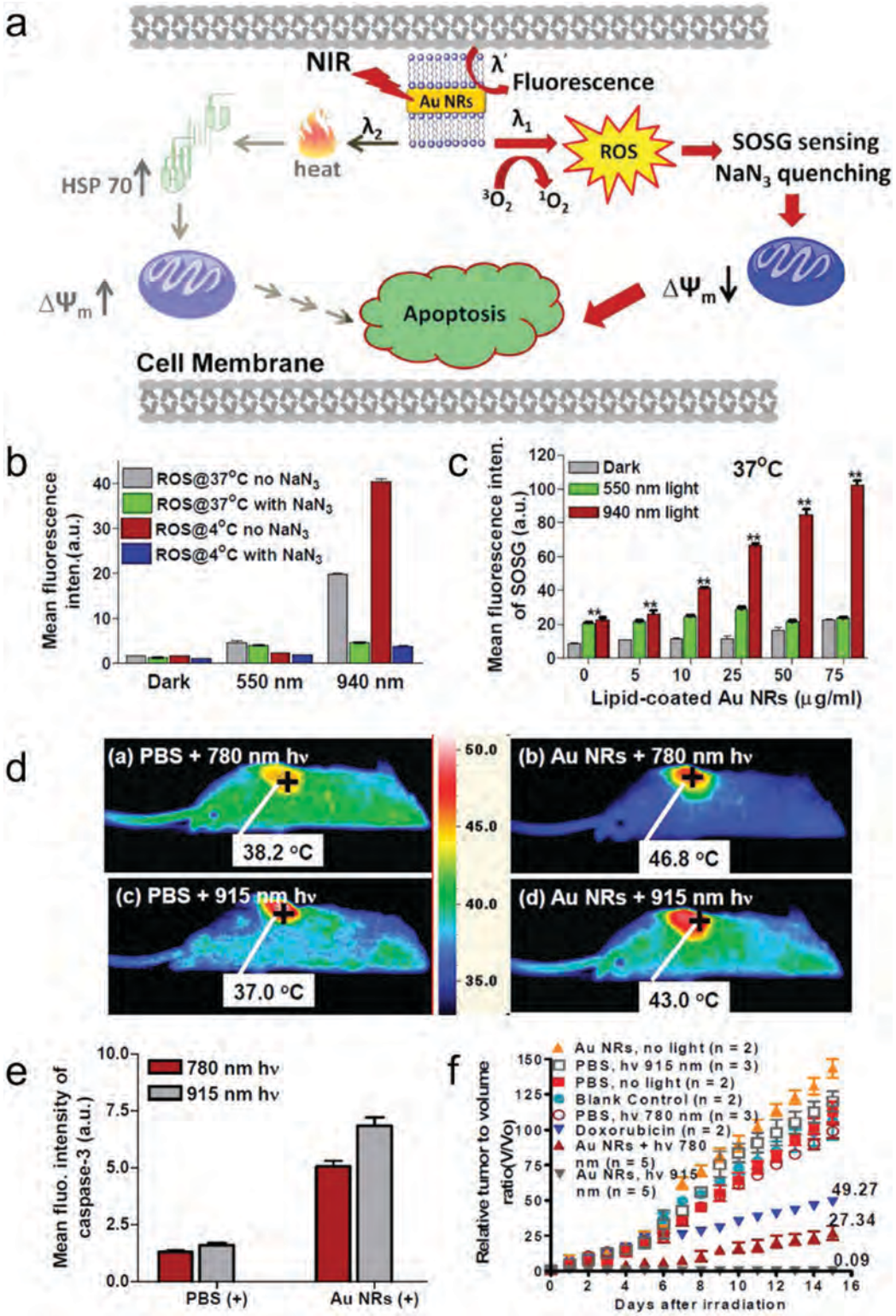

Fig. 6 NIR light excited PDT with gold NRs. (a) Cellular processes involved in the PDT- and PTT-induced cell death upon photo-irradiation of cells incubated with gold NRs. (b) ROS production was determined by DCFH-DA fluorescence. (c) Singlet oxygen sensor green fluorescence in HeLa cells treated as indicated. (d) Photothermal images of mice following the indicated treatments. (e) The apoptotic index was determined with the mean fluorescence intensity of caspase-3 staining in tumor tissues. (f) Relative tumor-to-volume ratios following the indicated treatments. Reproduced with permission.[81] Copyright, 2013, Wiley-VCH.

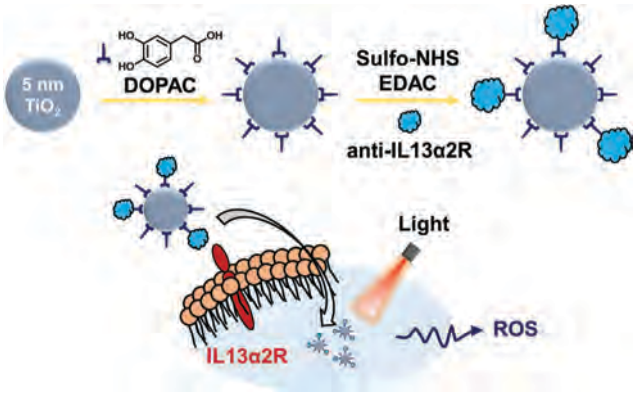

Fig. 7 Schematic representation of the preparation of a brain cancer-targeting nanocomposite with TiO_2 as a photosensitizer for PDT. Reproduced with permission.[82] Copyright, 2009, American Chemical Society.

Interestingly, the loading of porphyrin onto fullerenes changed their photochemical properties, leading to the enhanced production of singlet oxygen and increased tumor cell penetration.[142] Moreover, the extended π-conjugation of fullerenes enables the absorption of light in the UV or blue spectrum to form a triplet state and generate ROS. Both type I and type II photodynamic reactions can be induced to produce free radicals and singlet oxygen. Therefore, fullerenes can be used as photosensitizers for the PDT of tumors even in the hypoxic microenvironment.[146] Antennae–fullerene complexes were prepared for light-stimulated PDT using long wavelengths due to the low tissue penetration of UV and blue light.[147] For example, Shi *et al.* reported the fabrication of fullerene-based nanoparticles conjugated with an NIR-absorbing antenna for photoacoustic imaging-guided synergetic PTT and PDT. Functionalization with 1,2-distearoyl-*sn-glycero*-3-phosphoethanolamine (DSPE)-mPEG enhanced the biocompatibility of nanoparticles. Upon intravenous injection, the nanoparticles accumulated in tumors through the EPR effect, generating photoacoustic imaging signals around the tumors. With NIR light-induced electron transfer from antennas to fullerenes, enhanced ROS and heat generation efficiency was achieved, resulting in marked inhibition of tumor growth.[87]

3.2.2.3.2 Graphene and its derivatives. As the first group of two-dimensional nanomaterials, graphene and its derivatives have been widely used in ultrafast photonics,[148–152] optoelectronics,[153–155] and biomedicine.[156,157] Considering its amazing irreplaceable physicochemical properties,[158,159] graphene has been investigated as a drug delivery vehicle and a photosensitizer for cancer treatment. The large surface area[160–163] and various surface functional groups[164–166] of graphene-based materials enable efficient loading of chemical drugs, photosensitizers, and large biological molecules, such as small interfering RNA (siRNA), antibodies and other functional proteins. Microenvironment responsive moieties and tumor-specific drug delivery, release, and activation can also be achieved through the incorporation of targeting ligands, leading to enhanced tumor therapy efficacy and reduced side effects.[143]

Tremendous research has been conducted to investigate the utilization of graphene-based nanomaterials as carriers of photosensitizers for cancer PDT. Delivery with graphene-based nanomaterials improves the stability, bioavailability, and photodynamic efficiency of traditional photosensitizers.[143] It is crucial to pre-quench the photosensitizers for selective activation in tumors following light stimulation to reduce off-target effects from non-specific activation and the poor targeting efficiency of photosensitizers. Du *et al.* reported that integrating the photosensitizer Ce6 onto the surface of graphene quantum dots or graphene oxide gives rise to fluorescence quenching and mild phototoxicity. However, the photoactivity of Ce6 could be selectively recovered in reducing conditions. The resulting nanosystem exhibited improved tumor accumulation, enhanced tumor therapy efficiency, and reduced side effects.[167] Yu *et al.* prepared a cancer integrin $\alpha_v\beta_6$-targeting peptide-modified graphene oxide for the delivery of the photosensitizer HPPH to improve the tumor-targeting efficacy. The resulting nanocomposite exhibited significantly enhanced tumor uptake and PDT-mediated tumor suppression in both subcutaneous and lung metastatic rodent models. More interestingly, dendritic cells were activated by the therapy, leading to further inhibition of tumor growth and lung metastasis.[168] Furthermore, Choi *et al.* prepared graphene oxide quantum dot-based core–shell nanoparticles for cell imaging and photosensitizer delivery. The nanoparticles consisted of upconversion nanoparticles (UCNPs) as the core and graphene oxide quantum dots as the shell. Cell imaging was achieved by implementing upconversion luminescence of the UCNPs, while singlet oxygen was generated by hypocrellin loaded on the graphene oxide quantum dots through π–π interactions. The EPR effect enables the accumulation of the as-prepared nanomaterials in tumors. Improved anti-tumor therapeutic effects were achieved with this multifunctional nanocomposite.[169]

Graphene-based nanomaterials might also generate ROS following light stimulation; therefore, they might also be used as PDT photosensitizers. For example, nano-sized graphene oxide was shown to catalyze singlet oxygen generation through a type II photodynamic reaction in response to 980 nm NIR light stimulation, enabling its application in the PDT of deep-seated tumors. A photothermal effect was also observed in this condition. Besides, the photoluminescence of nano-sized graphene oxide in the visible and short NIR region was used for multi-color fluorescence imaging *in vivo*. After the functionalization of nanoparticles with PEG-folate, precise targeting of tumor cells was achieved. A combination of PDT and PTT with this nano-sized graphene oxide gives rise to effective cancer cell killing *in vitro*, efficient tumor destruction *in vivo* and increased survival of tumor-bearing mice after the therapy.[64]

Graphene quantum dots (GQDs) were also found to produce singlet oxygen through a multistate sensitization process with a quantum yield of ~1.3, enabling their application as photosensitizers in PDT. The GQDs exhibited a broad absorption

band spanning both UV and the entire visible region, with a strong deep-red emission. *In vitro* and *in vivo* studies indicated that GQDs are potent PDT agents for imaging and treatment of cancers with efficient ROS generation.[144]

Several strategies have been reported to enhance the PDT effect of GQDs. Kuo *et al.* prepared nitrogen-doped GQDs to enhance the production of ROS. A higher amount of ROS was generated upon light stimulation, resulting in dramatically improved antimicrobial effects. Interestingly, higher nitrogen-bonding compositions of GQDs gave rise to a better photodynamic effect than the lower compositions. Meanwhile, the intrinsically emitted luminescence and high photostability made the nitrogen-doped GQDs promising agents in biomedical imaging.[170] Rare earth-doped UCNPs combined with GQDs were used to overcome the limitation of the relatively low tissue penetration depth of the light source. In this nanocomposite, UCNPs emitted visible UV light upon NIR light excitation, which stimulated the production of singlet oxygen by GQDs. A hydrophilic rhodamine derivative, tetramethylrhodamine, was covalently modified to the nanocomposite to enhance the efficiency of cell targeting, leading to mitochondrial targeting of the material. The destruction of mitochondria by the generated singlet oxygen resulted in the apoptosis of cancer cells in response to NIR light stimulation. Highly improved tumor therapeutic efficacy was observed *in vivo* with this nanocomposite.[171]

A combination of graphene derivatives with other carbon-based photosensitizers might enhance the tumor therapeutic effects. For example, graphene oxide has been used in combination with fullerene C60 to prepare a new graphene oxide–C60 hybrid. After functionalization with mPEG, the hybrid has been proved to be effective in combined PDT and PTT of cancer.[172] In this hybrid, graphene oxide mediates the photothermal effect, while the conjugated C60 mediates the generation of singlet oxygen in response to light stimulation in an aqueous solution. The hybrid exhibited excellent stability and enhanced inhibition of cancer cells than both of them individually. In another similar research, C60 was conjugated with graphene oxide *via* host–guest chemistry (Fig. 8). Graphene oxide was first functionalized with folic acid to enable tumor cell targeting.

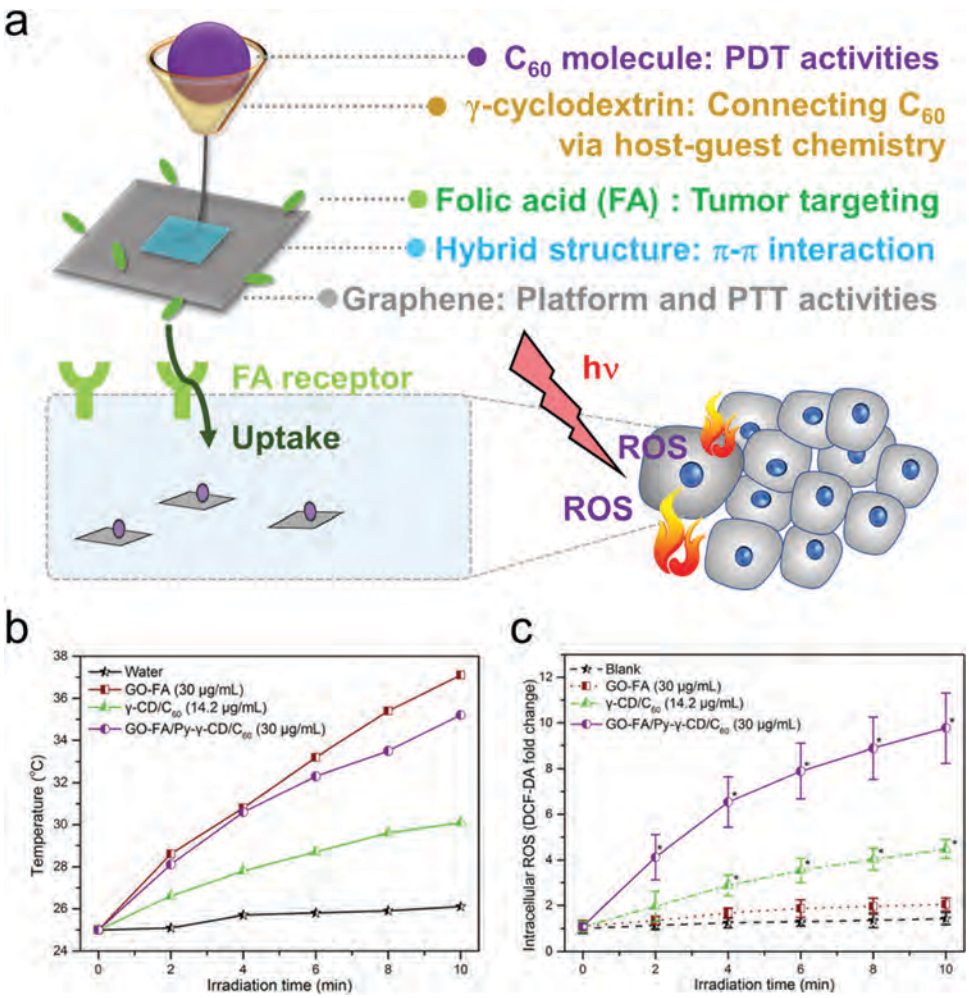

Fig. 8 Graphene/C60 nanohybrid for combined PDT/PTT. (a) Schematic illustration of PDT/PTT combined with the graphene/C60 nanohybrid. (b) PTT effect of the nanohybrid. (c) Intracellular ROS production of the nanohybrid. Reproduced with permission.[173] Copyright, 2017, The Royal Society of Chemistry.

Then, γ-cyclodextrin (γ-CD) was attached to its surface *via* π–π interactions to generate a hybrid structure for drug loading. Finally, C60 molecules were loaded onto the above structure to generate a host–guest complex (Fig. 8a). Increased cellular uptake of the nanocomposites was observed as a result of folic acid modification. Upon light stimulation, efficient ROS production was observed in the cells (Fig. 8c), resulting in dramatic inhibition of cancer cells.[173]

3.2.2.4 Black phosphorus. With the excellent physicochemical properties of layer-dependent bandgap, large surface area, carrier mobility balance, on/off ratio, and excellent biocompatibility, black phosphorus (BP) has aroused widespread interest in the fields of ultrafast photonics,[155,174–176] optoelectronics,[177–179] and biomedicine.[180,181] The application of BP in cancer PDT has also been investigated as a new two-dimensional nanomaterial. In 2015, Wang *et al.* reported that ultra-thin BP nanosheets exhibit excellent photodynamic properties (Fig. 9). When irradiated with a laser of 660 nm wavelength, efficient production of singlet oxygen with consumption of the surrounding oxygen through a type II photodynamic reaction was detected both in the solution and in cancer cells (Fig. 9c and d). Dose-dependent cytotoxicity to tumor cells was also observed (Fig. 9e). The PDT of breast cancer (MDA-MB-231) with BP nanosheets gave rise to tumor cell apoptosis and tumor growth inhibition *in vivo* (Fig. 9f and g).[61] Combination of the photodynamic properties of BP with its photothermal and drug-loading properties enabled more efficient tumor cell killing.[182] To extend the potential application of BP in tumor PDT, a dual-triggered self-supported oxygenic nanosystem based on BP nanosheets was developed recently to overcome the limitations of oxygen dependent ROS generation of the intrinsic hypoxic tumor microenvironment. BP nanosheets in this strategy were used

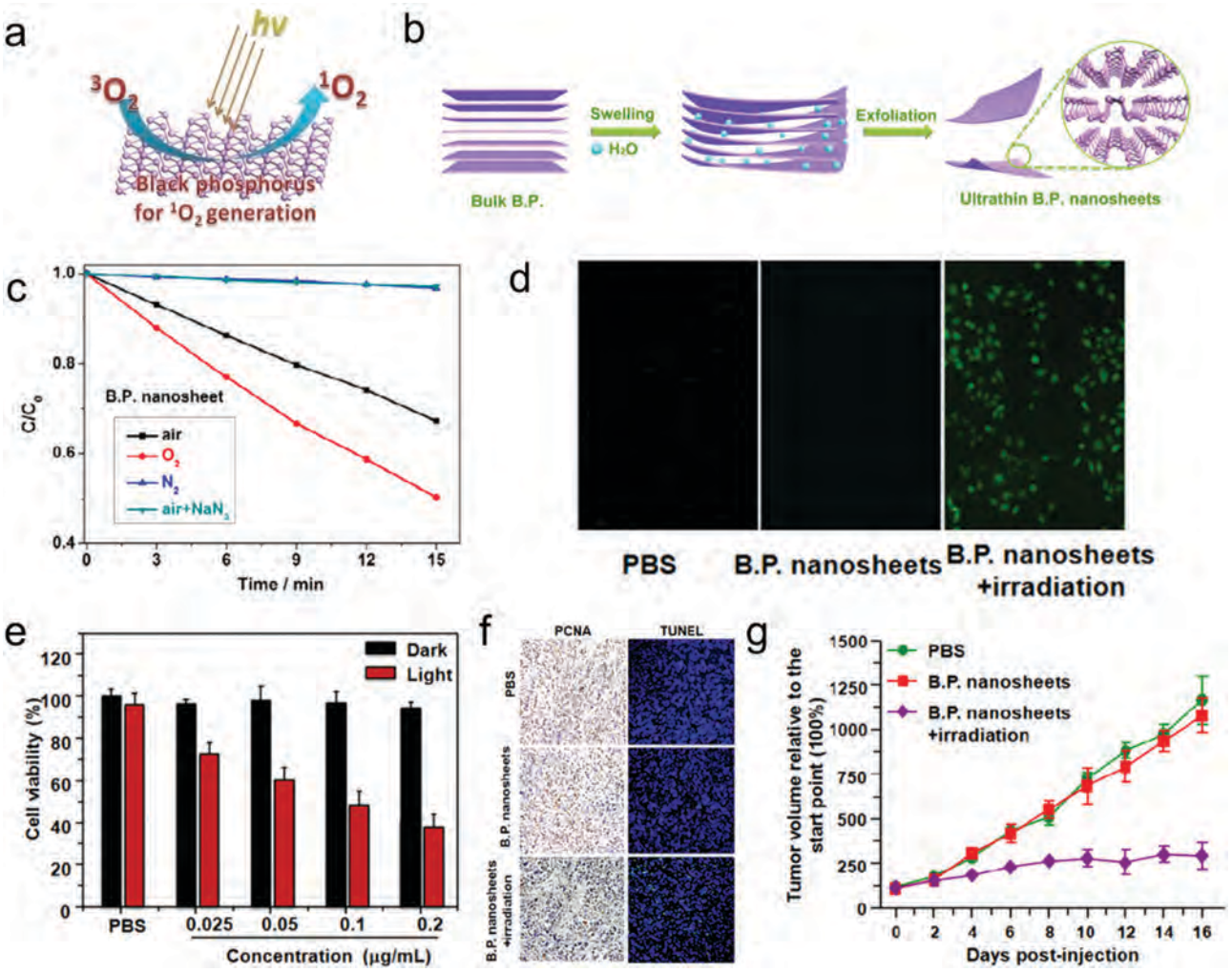

Fig. 9 BP nanosheets as photosensitizers for cancer PDT. (a) Schematic illustration of singlet oxygen production catalyzed by BP nanosheets. (b) Preparation of ultra-thin BP nanosheets with liquid exfoliation. (c) Characterization of singlet oxygen production. (d) Detection of ROS generation in cells with DCFH-DA. (e) Cell viability after PDT with different amounts of BP nanosheets. (f) Cell proliferation and apoptosis in tumor tissues [PCNA: proliferating cell nuclear antigen; TUNEL: terminal transferase uridine triphosphate nick-end labeling]. (g) Changes of tumor size following PDT with BP nanosheets [PBS: phosphate-buffered saline]. Reproduced with permission.[61] Copyright, 2015, American Chemical Society.

as both a photosensitizer and a nanocarrier. The functionalization of BP nanosheets with folate and a blocker DNA duplex of 5′-Cy5-aptamer-heme/3′-heme-labeled oligonucleotides enabled specific recognition of tumor cells and O_2 generation from the excessive intracellular H_2O_2 in tumor tissues, leading to a dramatic increase in PDT efficacy in the hypoxic environment of cancer cells and tumors.[45]

Moreover, in addition to BP nanosheets, BP quantum dots (BPQDs) can also produce ROS, expanding the use of BP as a photosensitizer in certain cancers. BPQDs have been successfully used in cancer PDT.[183,184] Li *et al.* reported the functionalization of BPQDs with PEG to improve the biocompatibility and physiological stability to be used as a photosensitizer in phototherapy. The resulting nanoparticles exhibited excellent PTT and PDT effects. PDT/PTT combined therapy with these nanoparticles gave rise to significantly improved therapeutic efficacy of cancer both *in vitro* and *in vivo*. BPQDs loaded with fluorescent molecules also enabled reliable imaging of cancer cells. Meanwhile, the cytotoxicity and side effects of PEGylated BPQDs to the main organs were negligible.[183] Guo *et al.* also confirmed the excellent physiological stability and acceptable cytotoxicity of BPQDs. It was shown that BPQDs could be quickly eliminated from the body through renal clearance because of their ultrasmall size. The excellent ROS generation and efficient cancer cell killing ability of BPQDs upon light irradiation were also confirmed both *in vitro* and *in vivo*.[184]

Compared with several kinds of other nanophotosensitizers, such as gold nanoparticles and carbon-based nanoparticles, an interesting property of BP based nanophotosensitizers is their moderate stability. When exposed to oxygen and water, rapid degradation of BP occurs, resulting in the production of phosphate.[185] This process can be modulated using light of different wavelengths.[186] Moreover, BP-based nanocomposites with adjustable stability (with half-life from days to weeks) can also be prepared through surface modification with different strategies, enabling their application in various clinical conditions.[181,187] Nevertheless, further investigation is still needed to clarify the impact of burst phosphate release by BP to protein phosphorylation, cellular signal transduction, and tissue homeostasis.

3.2.2.5 Nanoscale metal–organic frameworks. Nanoscale metal–organic frameworks (NMOFs) are a group of crystalline hybrid materials made up of metal centers and organic bridging ligands. NMOFs, as photosensitizers or as photosensitizer nanocarriers, have been used in PDT due to their modulable structure, easy surface modification, highly porous nature, and excellent biocompatibility. Because of their highly functional characteristics, MOF-based nanomaterials are promising for fabricating photosensitizers with favorable characteristics for PDT.[57,62]

The application of NMOFs for cancer PDT was first reported in 2014, in which a Hf-porphyrin NMOF, DBP-UiO, was used as a photosensitizer for the treatment of resistant head and neck cancers. Singlet oxygen production with surrounding oxygen through a type II photodynamic reaction was achieved upon light stimulation of DBP-UiO nanoplates. The PDT-mediated tumor inhibition was investigated both *in vitro* and *in vivo*.[84] In another work, an NMOF composed of Hf and tetrakis(4-carboxyphenyl)porphyrin (TCPP) was fabricated as a photosensitizer for tumor treatment. The PDT effect of TCPP was combined with the radiotherapy effect of Hf^{4+}, enabling combined PDT/radiotherapy of cancer. Finally, PEG was used to functionalize the nanostructure to enhance the stability and biocompatibility of the material. An improved anti-tumor effect was observed upon intravenous injection of the nanomaterial.[188] Recently, an NMOF-based tumor-responsive image-guided PDT platform was reported with minimum ROS exhaustion from the endogenous antioxidant, glutathione (GSH). A Cu(II) carboxylate-based MOF (MOF-199) was used as a nanocarrier for the loading and delivery of the photosensitizer. The Cu(II) in the MOFs scavenged the GSH and simultaneously released the encapsulated photosensitizer by inducing MOF-199 decomposition. An efficient cancer killing effect was observed both *in vitro* and *in vivo* through the resulting enhanced ROS accumulation in cancer cells and tumors.[189]

Different from most other nanophotosensitizers, the composition, nanostructure, and physicochemical properties of NMOFs are highly divergent and programmable, making them promising for the construction of multifunctional nanoplatforms with various characteristics for more efficient tumor theranostics.[57] On the other hand, the incorporation of heavy metal atoms requires a detailed investigation of their long-term impacts on health.

3.2.2.6 Semiconducting polymer nanoparticles. Semiconducting polymer nanoparticles (SPNs) are mainly made up of hydrophobic semiconducting polymers. In certain conditions, amphiphilic polymer matrices are also needed for the fabrication of the nanoparticles.[190] Because of their excellent optical properties, photostability and biocompatibility, SPNs are also widely investigated in various biomedical applications, including biosensing, fluorescence imaging, photoacoustic imaging, and PTT mediated tumor inhibition.[191–193] With the capability of catalyzing ROS generation following light stimulation, various SPNs are treated as promising photosensitizers for PDT.[190,194]

Through the conjugation of SPNs with targeting ligands, drugs or other components, multifunctional nanocomposite photosensitizers with better therapeutic performance can be fabricated to overcome various barriers in PDT. For example, Li *et al.* prepared SPN based nanocomposites to overcome delivery barriers in the tumor microenvironment. To achieve this goal, the cell membrane of activated fibroblasts was coated onto the SPNs, enabling specific targeting of cancer-associated fibroblasts. This strategy enhanced the tumor accumulation and combinational PTT/PDT efficiency of the nanocomposites.[195] To overcome the limitation from the hypoxic tumor microenvironment, Zhu *et al.* prepared oxygenic hybrid SPNs by conjugation with MnO_2 nanosheets. Oxygen was generated through MnO_2 nanosheet mediated H_2O_2 conversion. The generation of

singlet oxygen by the nanocomposites was therefore enhanced, enabling efficient inhibition of tumor by PDT.[196] Cui *et al.* developed a hypoxia-activated PDT strategy with SPNs, and a chemodrug conjugated by hypoxia-cleavable linkers. Enhanced tumor inhibition was achieved through the synergistic effect of PDT and chemotherapy.[197] Jiang *et al.* synthesized an SPN based nanoinhibitor through the incorporation of a carbonic anhydrase IX (CA-IX) antagonist. Specific targeting of CA-IX positive cancer cells was achieved with this strategy. Meanwhile, CA-IX inhibition potentiated the tumor inhibition efficiency of PDT.[198]

SPNs are also promising in the construction of stimuli-responsive nanoenzymes to achieve a better tumor inhibition efficiency. For example, Li *et al.* designed photoactivatable pro-nanoenzymes with SPNs to promote the tumor inhibition efficiency of PDT. During PDT, the RNA degradation activity of the pro-nanoenzyme was also induced by NIR light irradiation, leading to the inhibition of metastasis. The therapeutic efficiency was thus improved.[199]

3.3. Synthetic chemistry of nanomaterials for PDT

To achieve ideal PDT performance of nanomaterials during cancer treatment, it is necessary to produce nanomaterials (as carriers or as photosensitizers) with high quality and suitable morphology. To date, various methods have been employed to synthesize nanomaterials for PDT. These strategies can be classified into top-down approaches (mechanical cleavage, liquid phase exfoliation, *etc.*) and bottom-up approaches (chemical vapor deposition (CVD), wet-chemical synthesis, *etc.*) (Fig. 10).

3.3.1. Top-down synthesis

3.3.1.1 Mechanical cleavage. The micromechanical cleavage approach is the most representative top-down synthesis method to delaminate materials down to few-layers, even atomically thin monolayers. Novoselov and Geim have synthesized single-layer graphene *via* mechanical cleavage in 2004;[200] since then, this method has been widely used to fabricate different kinds of 2D nanomaterials, such as BP, transition metal dichalcogenides (TMDs), arsenene, and antimonene.[201–206] Mechanical force is applied *via* a scotch tape to break the van der Waals-like interactions between layers, while the in-plane interaction is still undamaged (Fig. 10a). It is a facile way to obtain ultrathin few-layer or monolayer 2D nanostructures with a lateral size of hundreds of nanometers. Very recently, by improving the synthesis process, the size of monolayer 2D materials as large as dozens of millimeter with high crystal quality can be reached.[207] However, the relatively low yield significantly limited the application of the mechanical cleavage method in the biomedical field. Nevertheless, some researchers still performed biomedical sensor investigations based on 2D materials obtained with mechanical cleavage.[208]

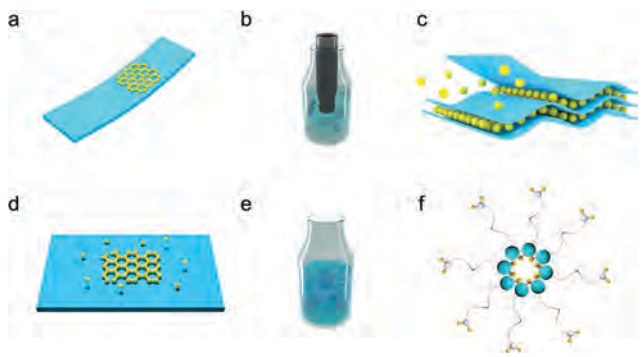

Fig. 10 Schematic illustration of the typical synthesis methods of nanomaterials. Top-down synthesis: (a) mechanical cleavage; (b) liquid phase exfoliation; and (c) selective etching assisted exfoliation. Bottom-up synthesis: (d) CVD; (e) wet-chemical synthesis; and (f) self-assembly.

3.3.1.2 Liquid phase exfoliation. The liquid phase exfoliation method is one of the most widely used approaches for 2D materials synthesis. Compared to the mechanical cleavage method, the advantage of the liquid phase exfoliation method is that it enabled the production of 2D materials in large quantities with relatively high quality and low cost.[209,210] The intercalation solvent and ultrasonication are the key factors in liquid phase exfoliation. During the intercalation process, the intercalation solvent would extend the interlayer space and weaken the interlayer interaction. After that, the ultrasonication further breaks the van der Waals interactions to obtain ultra-thin 2D nanosheets (Fig. 10b). To further increase the yield of 2D materials, various emerging approaches were developed such as salt-assisted exfoliation, intercalation-assisted exfoliation, ion exchange-based exfoliation, *etc.*[211] Owing to the abovementioned advantages, liquid phase exfoliation was widely used in the synthesis of 2D nanocarriers and photosensitizers, such as graphene,[208,212] graphene analogues,[213,214] 2D TMD nanosheets,[215–217] BP,[61,218–220] and others.[221,222]

3.3.1.3 Selective etching assisted exfoliation. Since the report of 2D Ti_2C_3 in 2011, the family of 2D transition metal carbide and nitride compounds (termed MXenes) have been widely investigated.[221] The MXene family shares the same chemical formula $M_{n+1}X_nT_x$ (n = 1–3), where M represents an early transition metal (such as Ti, Zr, Hf, V, Nb, Ta, Cr, Mo and so on), X is carbon and/or nitrogen and T_x stands for the surface terminations (for example, hydroxyl, oxygen or fluorine). For the MAX phase, the metal atom layers always insert between the two layers of MXene. To obtain an ultra-thin MXene layer, the selective etching assisted exfoliation method was proposed. As shown in Fig. 10c, the MAX phase was immersed in a strong acid solution (like hydrofluoric acid) to etch the metal atom layer. The accordion-like multi-layer MXene will be exfoliated to few-layer even monolayer MXene by further intercalation process. Such a universal approach can produce 2D MXene materials with nanoscale-lateral size and atomic-scale thickness for almost all the members of the MXene family. Moreover, the synthesized MXene shows excellent optical properties, drug carrier ability, and biocompatibility. After surface functionalization with organic molecules, the MXene can be well used as both a carrier and a photosensitizer for PDT.[223–226]

3.3.2. Bottom-up synthesis

3.3.2.1 CVD. CVD is the most representative bottom-up approach for the synthesis of various nanomaterials. The CVD

process was achieved *via* a chemical reaction between a solid or molten substrate and gas-phase small molecules. Huge efforts have been made to explore the emerging methods for the fabrication of nanomaterials with layer controllability and large-area uniformity.[208,222,227] CVD is widely applied in the synthesis of 2D materials. In the early stage, the widely used method is the one-step vapor phase reaction method. Using this approach, vapor phase precursors are transferred to the next thermal zone and deposited onto the substrate to form 2D material layers such as graphene, BP, and hexagonal boron nitride, as shown in Fig. 10d.[228–230] Two-step CVD was also proposed for the synthesis of 2D TMDs, in which the transition metal was deposited on the substrate, followed by chemical reaction in the vapor phase chalcogen atmosphere.[231,232] This emerging CVD processing enables the fabrication of 2D TMDs with large lateral size and excellent thickness controllability. CVD is also suitable for the preparation of doped or multi-component nanoparticles. Nanomaterials fabricated with CVD have been investigated for various biomedical applications including PDT and biosensing.[233–235] However, similar to the previously mentioned mechanical cleavage method, the relative low yield of the CVD approach limits its large scale application for nanomaterials synthesis.

3.3.2.2 Wet-chemical synthesis. Wet-chemical synthesis refers to synthesis processes in which nanomaterials were obtained through chemical reactions among certain precursors in solution phase (Fig. 10e). Hydro/solvothermal synthesis and 2D-templated synthesis are two most widely applied wet-chemical synthesis strategies.[236,237] Wet-chemical synthesis is suitable for achieving a high yield and large amount production of various nanomaterials, such as TMDs.[238] Conventional metal and metal oxide photosensitizers can also be obtained based on the wet-chemical synthesis method.[81,82,140,239] Recently, wet-chemical synthesis based 2D and 0D material fabrication was also used extensively. For example, graphene quantum dots and fullerenes have been synthesized as excellent 0D photosensitizers under hydrothermal reaction experimental conditions.[90,146,240] Rich-defect MoS_2 ultra-thin nanosheets were also synthesized by a hydrothermal reaction with hexaammonium heptamolybdate tetrahydrate as a precursor.[217] Featured by high yield and low cost, the wet-chemical synthesis process shows promising potential in large-scale and industrial production of nanomaterials for applications in PDT as carriers or as photosensitizers.

3.3.2.3 Self-assembly. Self-assembly refers to the process in which organized structures formed in a disordered system through interactions between the components in the system (Fig. 10f). This process is controlled by both the intrinsic characteristics of the precursors and extrinsic stimulations such as changes in temperature, pH, and mechanical force. The self-assembly strategy enables the large-scale production of materials with high quality and low cost. It is widely applied in the preparation of nanoparticles suitable for usage as building blocks of nanocomposites, especially those composed of lipids, polymers, peptides, proteins, and nucleic acids.[241–244] The self-assembly strategy is also an effective way to construct nanocomposites by assembling single nanoparticles and other components together. The constructed nanocomposites always show superior properties by integrating nanoscale building blocks.[245] For example, Li *et al.* decorated 2D MoS_2 nanosheets with DNA which enabled the self-assembly of MoS_2 to construct a 3D nanoplatform. After self-assembly, the superstructure showed enhanced drug loading capacity and resistance to damage from intracellular enzymes. The self-assembled superstructure was disassembled in cancer cells by triggering high levels of ATP, resulting in tumor specific release of drugs.[246] Very recently, our group demonstrated a tumor microenvironment triggered self-assembly BP platform by anchoring polyoxometalate (POM) nanoparticles onto the surface of BP (POM@BP). When exposed to the tumor microenvironment (acidic tumor microenvironment), the POM@BP will self-assemble to form larger clusters with extended retention in tumor tissues and enhanced photothermal performance.[247] Nanoparticles and nanocomposites prepared through self-assembly are also widely applied in PDT as carriers or as photosensitizers.[248–250]

3.4. Strategies for the fabrication of nanocomposite photosensitizers for better PDT

Through the conjugation of nanocarriers and photosensitizers with other functional components, the physicochemical and biochemical properties of the resulting nanocomposite photosensitizers can be significantly optimized. Various covalent and non-covalent approaches are used in the surface modification of nanomaterials. In particular, multi-functional nanocomposites can be fabricated through the combination of photosensitizers with various polymers, targeting ligands, small molecule drugs, metals, nanoparticles, siRNA, proteins, *etc.* The unique physicochemical and biochemical properties of these nanocomposites enable effective modulation of light responsibility, ROS production, tumor microenvironment, cellular signal transduction, and tumor responses. Various barriers in PDT can be overcome with these novel photosensitizer formulations and corresponding therapy strategies.

3.4.1. Polymers. Polymers are most widely used components in the preparation of nanocomposite photosensitizers with enhanced properties. Various polymers, such as PEG, polydopamine (PDA), and poly(lactic-*co*-glycolic acid) (PLGA), have been applied in the construction of nanocomposite photosensitizers to achieve better physiological and chemical stability, biocompatibility, targeting efficiency, and ROS production.[48,98,112,251,252] For example, many pristine nanoparticles tend to aggregate in a physiological medium. Surface modification of these nanoparticles with hydrophilic polymers is an effective strategy to enhance their physiological stability and ensure their application in PDT.[83] Certain nanomaterials, such as BP nanoparticles, are intrinsically unstable under ambient conditions. Coating with suitable polymers reduces their contact with oxygen and water and improves their chemical stability.[187,251] Polymers also provide sites for further

conjugation of nanocomposite photosensitizers with various functional components, largely expanding the functionality of photosensitizers.[5,253]

In the preparation of nanocomposite-based photosensitizers, polymers can be incorporated through various mechanisms.[251,252,254] For example, polymers can interact directly with nanoparticles through electrostatic interactions, van der Waals forces, or hydrogen bonds.[83,252] Meanwhile, polymers can also be attached to nanoparticles through covalent interactions.[5,112] Certain polymers, such as PDA, can be synthesized on the surface of nanoparticles through *in situ* polymerization.[253]

3.4.2. Targeting ligands. Lack of tumor targeting ability is one of the most important drawbacks of traditional photosensitizers.[255] Nanomaterials could accumulate in tumors through the EPR effect.[58] However, this cannot fully meet the needs of clinical applications. To further improve the tumor targeting efficiency of nanoparticle-based photosensitizers, a variety of tumor targeting strategies are developed. As the most widely used active targeting strategy, various targeting ligands have been investigated for tumor-specific delivery of nanoparticles.[100,256,257]

Generally, targeting ligands are coated on the surface of photosensitizers and recognized by certain tumor specific surface markers following administration.[100] Therefore, various small molecule ligands, peptides, proteins, and oligosaccharides with high affinity to tumor specific surface markers are used as the targeting ligands of photosensitizers.[91,258,259] With high variability, specificity, affinity, and biocompatibility, antibodies can also act as ideal targeting ligands in PDT.[260,261] Aptamers, oligonucleotides with certain 3D conformation and affinity to specific targets, have also been widely used as targeting ligands in recent years.[262,263]

Tumor specific delivery of photosensitizers can be achieved with targeting ligands. For example, several cell surface receptors, such as folic acid receptor, transferrin receptor, and CD44, are overexpressed in certain tumor types. Therefore, photosensitizers coated with corresponding ligands (folic acid, transferrin, hyaluronic acid, *etc.*) can be recognized through ligand–receptor interactions and taken up by tumor cells through receptor mediated endocytosis.[223,264]

To enhance PDT induced tumor cell death, targeted delivery of photosensitizers to certain organelles can also be achieved with suitable ligands. For example, mitochondria are a kind of organelle that is critical for both energy supply and apoptosis regulation. Meanwhile, they are extremely sensitive to ROS. Therefore, photosensitizers with surface modification of mitochondria targeting ligands can be specifically delivered to mitochondria and catalyze the production of ROS *in situ* following light stimulation to induce tumor cell apoptosis with high efficiency.[220]

For the PDT of certain tumors, targeting ligands are also required for photosensitizers to overcome anatomical barriers *in vivo*. For example, brain delivery of traditional photosensitizers is blocked by the blood–brain barrier. Therefore, targeting ligands, such as RGD peptide, are utilized in the surface modification of photosensitizers to promote brain delivery in the PDT of brain tumors.

3.4.3. Small molecule drugs. Small molecule drugs are powerful tools for the modulation of various physiological and pathological processes.[265–267] Therefore, they are also widely applied in the construction of multifunctional nanocomposites for PDT.[268,269] Small molecule drugs are also promising tools to overcome tumor resistance to PDT through the modulation of physiological processes in tumor cells. For example, several transporter proteins, such as P-glycoprotein (P-gp) and ATP-binding cassette superfamily G member 2 (ABCG2), participate in the excretion of traditional photosensitizers by tumor cells.[41,270,271] Therefore, the co-delivery of corresponding small molecule inhibitors with nanocomposite photosensitizers may promote the retention of photosensitizers in tumor cells to enhance PDT efficiency. The antioxidant system also participates in resistance to PDT through the degradation of ROS.[34,272] Therefore, small molecule inhibitors of antioxidant enzymes, such as superoxide dismutase (SOD), GSH peroxidase (GPX), and GSH-S-transferase (GST), may also be used in the construction of multifunctional nanocomposite photosensitizers to enhance the therapeutic efficiency of PDT.

Small molecule drugs are usually loaded onto inorganic nanoparticle-based photosensitizers through electrostatic interactions, van der Waals forces or hydrogen bonds. They can also be effectively loaded into organic nanoparticles such as liposomes, micelles, and dendrimers.[58,244] Moreover, they may also be conjugated with photosensitizers through covalent bonds.[109] In particular, chemical bonds responsive to the tumor microenvironment (acid, GSH, H_2O_2, *etc.*) or external stimuli (NIR light, heat, *etc.*) are also utilized in the delivery of small molecule drugs to modulate the PDT efficiency.[48,109,112]

3.4.4. Nanoparticles. Nanoparticles with desirable physical or chemical properties are also applied in the decoration of nanocomposite photosensitizers to overcome the barriers in PDT. In particular, UCNPs are widely used in the PDT of deep-seated tumors. After the absorption of two or more low energy photons, photons with higher energy are emitted by UCNPs to stimulate the production of ROS by the co-delivered photosensitizers.[273] Therefore, better PDT efficiency for deep-seated tumors was achieved.

On the other side, the formation of heterostructures has been shown to promote ROS generation through enhanced separation of photogenerated electron–hole pairs and improved light harvesting. Therefore, coupling of certain kinds of nanoparticles may be an effective strategy to fabricate photosensitizers with better performance. For example, gold nanoparticles of 5–10 nm size have been loaded onto g-C_3N_4 nanosheets through a photodeposition process to enable ROS production under 670 nm laser irradiation in an oxygen-free environment.[214]

Several kinds of nanoparticles with catalytic activity, such as MnO_2 nanoparticles, platinum nanozymes, and gold nanoclusters are also frequently used to decorate photosensitizers to relieve tumor hypoxia through *in situ* production of oxygen.[218,274–277]

3.4.5. SiRNA. SiRNA is a kind of double-stranded RNA of about 20–27 base pairs in length. Similar to small molecule inhibitors, siRNA is also an important tool to modulate intracellular processes, which functions in the degradation of messenger RNA of the target genes.[278] Compared with chemical drugs, the advantage of siRNA is that it is very convenient to design and synthesize different siRNA sequences to downregulate the expression of various genes.[279] Therefore, siRNA is a powerful tool to modulate proteins without specific chemical inhibitors.[280] In the fabrication of novel nanocomposite photosensitizers, siRNA is frequently used to modulate proteins and signaling pathways to enhance the tumor inhibition of PDT. For example, siRNA targeting MutT homolog-1 (MTH1), an enzyme participating in the hydrolyzation of oxidized nucleotides, has been successfully applied in PDT to overcome tumor resistance to the therapy through the repair of ROS-induced DNA damage.[38]

Since siRNA is unstable and sensitive to RNase both *in vitro* and *in vivo*, highly efficient delivery of siRNA is challenging.[257,280] Various organic and inorganic nanoparticles have been utilized in the loading and intracellular delivery of siRNA. For example, liposomes have been shown to be ideal carriers of both siRNA and photosensitizers.[279,281,282] When incorporated into liposomes, both the stability and cellular uptake of siRNA are increased, making it possible to modulate the tumor resistance of PDT with high efficiency. Although siRNA has been successfully loaded into liposomes with different charges, the cellular uptake and biocompatibility of different formulations are quite different.[280] Other organic nanoparticles, such as those based on polymers, dendrimers, and polysaccharides, are also suitable for the loading and delivery of both siRNA and photosensitizers for highly efficient PDT of cancer. Meanwhile, inorganic nanoparticles, such as silica nanoparticles, metal oxide nanoparticles, gold nanoparticles, carbon-based nanoparticles, and BP, are also ideal carriers for siRNA in the preparation of multifunctional nanocomposite photosensitizers. Based on the knowledge about signaling pathways and critical regulators involved in tumor resistance to PDT (discussed in Section 6), it is speculated that the knock-down of critical genes involved in photosensitizer excretion, ROS degradation, cellular damage repair or pro-survival signaling pathways with siRNA will be a promising strategy for overcoming the internal barriers of PDT.

3.4.6. Proteins. Proteins with certain biochemical properties are also applied in construction of nanocomposite photosensitizers.[49,91,109,112] As mentioned above, ligands or antibodies of tumor or tissue specific surface markers are widely used in targeted delivery of photosensitizers. Besides, conjugation of photosensitizers with hemoglobin, an effective oxygen carrier, has been shown to relieve the limitation of ROS production by tumor hypoxia.[283] Similarly, several enzymes, such as catalase, can also be incorporated into photosensitizers to catalyze the production of oxygen with H_2O_2 in tumor tissues as substrate to relief tumor hypoxia.[284] Since the normal structure and biochemical activity is important for these proteins to function in nanocomposites, mild conditions are required in the preparation of these photosensitizers.

In summary, the application of nanomaterials, as carriers or as photosensitizers, represents an important progress in the development of PDT. Through the construction of multifunctional nanocomposite photosensitizers with various strategies and components, the drawbacks of traditional photosensitizers (poor photo-stability, lack of tumor specificity, dark toxicity, imperfect pharmacokinetics, *etc.*) can be effectively overcome. To further improve the tumor inhibition of PDT, a promising strategy is to modulate various critical proteins, signaling pathways, and the microenvironment with co-delivered components, which will be discussed in detail in the following sections. Nevertheless, further investigation is still needed to confirm the biocompatibility of the nanoparticles and their degradation products, and their long-term impacts on human health.

4. Photosensitizers and excitation strategies for deep PDT

The light sources for photosensitizer excitation are critical in the clinical application of PDT. Due to light absorption by biological molecules, such as proteins, lipids, DNA, and RNA, light penetration into human tissues is relatively poor, except for light with a wavelength in the first (650–950 nm) and second NIR bio-windows (1000–1350 nm).[285] Phototherapy usually uses light in this range to minimize the absorption of light by tissues. However, traditional photosensitizers usually exhibit an excellent photodynamic response to light with a relatively short wavelength and a high photon energy. However, the short wavelength results in the limited penetration depth of light in tumor tissues during light-induced therapy. Photosensitizers activated by light of long wavelengths, especially in two bio-windows, are urgently needed to address this issue. Additionally, novel PDT strategies with photon upconversion,[286–291] two-photon excitation,[56,292–294] X-ray excitation,[295,296] or internal self-luminescence[297–299] of photosensitizers have been designed to treat tumors in deep tissues.[55]

4.1. NIR light excitation

NIR light refers to the light of a shorter wavelength in the infrared spectrum, especially between 700 and 2500 nm.[285] Compared with UV or visible light, NIR light exhibits enhanced tissue penetration and reduced damage to tissues and cells. NIR light has been widely investigated to stimulate several photosensitizers, including NIR-absorbing organic dyes and inorganic nanoparticles.[1]

NIR light has been applied in PDT to stimulate organic dyes, including boron dipyrromethene (BODIPY) derivatives, cyanine dyes, and phthalocyanine derivatives.[300] BODIPY consists of a group of organoboron compounds composed of dipyrromethene complexes with a disubstituted boron center. The structural diversity, high fluorescence intensity, and low toxicity of BODIPY make it appealing for medical and biological purposes. BODIPY with NIR light-stimulated ROS production has been prepared for cancer PDT through the addition of a substituent with appropriate oxidation potential.[301] For

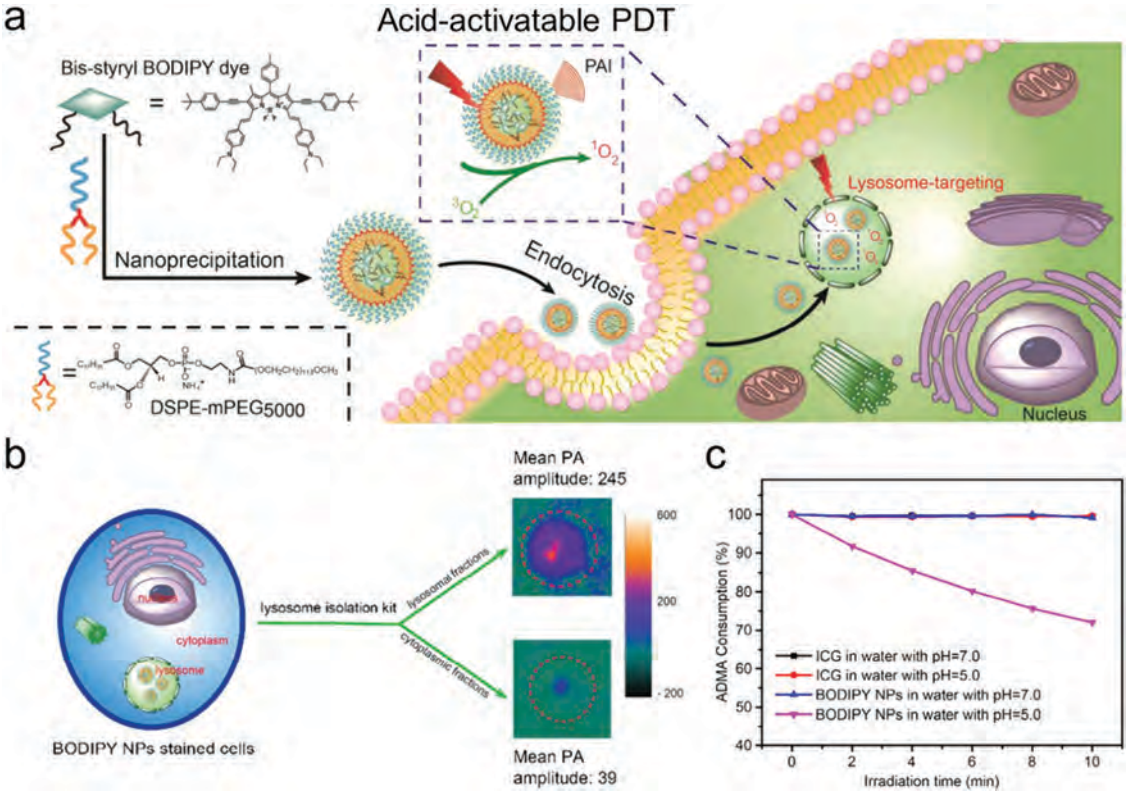

Fig. 11 Fabrication of BODIPY nanoparticles for lysosomal PA imaging and pH-activatable PDT under NIR light. (a) Schematic illustration of the preparation and function of the nanoparticles. (b) PA imaging of lysosomal and cytoplasmic fractions. (c) The absorbance of ADMA at 259 nm after irradiation using a 730 nm laser for indicated times. ADMA, 2,2′-(anthracene-9,10-diylbis(methylene))dimalonic acid. Reproduced with permission.[89] Copyright, 2016, American Chemical Society.

example, Liu *et al.* prepared BODIPY-based NIR light-responsive micelles with a galactose-targeted amphiphilic copolymer of a polypeptide as nanocarriers. Complete suppression of hepatoma tumor cells expressing galactose receptors, following the stimulation of NIR light with an extremely low energy density, was achieved with these nanocomposites.[302] Hu *et al.* reported the fabrication of lysosome-targeting NIR-absorptive BODIPY nanoparticles for acid-activated PDT of the tumor (Fig. 11). Encapsulation of BODIPY with amphiphilic DSPE-mPEG5000 gives rise to the formation of nanoparticles suitable for tumor targeting photoacoustic imaging and PDT. Interestingly, the modification of BODIPY with the acid-sensitive dimethylaminophenyl group enabled the selective accumulation of the nanoparticles in acidic lysosomes and provided acid-activated PDT (Fig. 10b and c).[89]

Cyanine dyes are composed of two aromatic nitrogen-containing heterocyclic structures connected with a polymethine linker. Cyanine dyes are widely used in fluorescence labeling and analysis due to their high extinction coefficients and spectral properties in the NIR region.[1] However, low ROS generation efficiency and weak fluorescence intensity are the limitations in using NIR cyanine dyes for PDT. Lu *et al.* prepared a novel multifunctional nanoagent, AuNRs@SiO_2-IR795, to enhance the fluorescence emission and ROS production of the cyanine dye IR795. Since the LSPR band of AuNRs overlaps with the absorption or fluorescence emission band of the IR795 dye, both fluorescence intensity and ROS generation of the nanocomposites were enhanced significantly. More efficient inhibition of cancer cells was observed in response to NIR irradiation-stimulated synergistic PDT/PTT. The enhanced fluorescence intensity also enabled fluorescence imaging in tumor cells.[303]

Several inorganic nanoparticles have also been used as NIR light-responsive photosensitizers for PDT. Gold nanomaterials, as one of the most studied nanomaterials, have been extensively investigated for their promising potential in imaging and biomedical applications. The optical properties of gold nanomaterials can be fine-tuned by modulating their morphology, shapes, and structures to prepare nanoplatforms that are responsive to NIR light stimulation. Following the exposure of gold NRs to a very low light-emitting diode/laser dose of single-photon NIR (915 nm, <130 mW cm^{-2}) light, the production of singlet oxygen was detected (Fig. 6b). Further investigations of singlet oxygen production and cellular responses confirmed the PDT-mediated cytotoxicity in response to NIR light excitation (Fig. 6c and d). In a mouse model of B16F0 melanoma, efficient PDT-mediated destruction of tumors was observed. It was found that 915 nm light-sensitized gold NR-mediated PDT exhibited better therapeutic effects on B16F0 melanoma than doxorubicin or PTT (Fig. 6f).[81] NIR light is also utilized in deep PDT

with several other inorganic nanoparticles, such as carbon-based nanomaterials,[98] BP nanosheets,[140] and quantum dots.[143,304]

4.2. Upconversion luminescence

Photon upconversion is defined as a process in which two or more low-energy photons are absorbed sequentially, resulting in the emission of photons with a relatively high energy.[305–307] The absorption generally occurs in the infrared spectrum, while the emission occurs in the visible or UV spectrum, ideal for various exciting photosensitizers in deep sites.[54] Materials with such photon upconversion properties are usually composed of host lattices of ceramic materials doped with lanthanide or actinide ions, such as Yb^{3+}, Er^{3+}, and Tm^{3+}.[54] Upconversion luminescence from these nanoparticles is widely used in bio-imaging and bio-sensing of deep tissues.[273,308,309]

When applied in PDT, UCNPs might function both as photosensitizer carriers and as agents that convert NIR light to higher-energy light for efficient activation of photosensitizers. The application of upconversion luminescence as a light source in PDT enables the efficient excitation of photosensitizers in deep-seated tumors. For example, the biological photosensitizer KillerRed should be activated by visible light, which largely limits its application in PDT. However, with the covalent conjugation of KillerRed with UCNPs, NIR light-stimulated ROS production was achieved from this nanocomposite. Approximately 70% PDT efficacy was observed at 1 cm tissue depth with this strategy, significantly enhancing the PDT-mediated tumor-killing effect of KillerRed.[310]

With the proper design of the nanocomposite to overcome the drawbacks of traditional PDT strategies, the anti-tumor efficiency of upconversion luminescence-stimulated PDT can be further improved. For example, the hypoxic microenvironment of tumor tissues hampers the production of ROS in a type II photodynamic reaction. Gu *et al.* synthesized mesoporous silica nanospheres with fine CaF_2:Yb,Er upconversion nanocrystals embedded in their pores through a thermal decomposition method to solve this problem. A thin MnO_2 layer was then coated onto the nanospheres (Fig. 12a). Finally, the photosensitizer Ce6 was loaded into the nanospheres (Fig. 12b). With NIR light stimulation, red light was produced through the upconversion process to activate Ce6 *via* resonance energy transfer. Meanwhile, the hypoxic tumor microenvironment was resolved by the *in situ* generation of O_2 from endogenous H_2O_2 by catalyzing MnO_2 (Fig. 12c and d). Efficient PDT-mediated cytotoxicity was observed even in hypoxic conditions with the application of this nanocomposite (Fig. 12e and f). The hypoxic microenvironment of deep tumor tissues was effectively resolved following the administration of these nanospheres (Fig. 12g). The enhanced tissue penetration depth and *in situ* O_2 production ensured the therapeutic effects of PDT (Fig. 12h).[311] In another similar work, Ding *et al.* prepared photosensitizer-loaded and PEG-modified $MnFe_2O_4$-decorated large-pore mesoporous silica-coated UCNPs for NIR light-induced and O_2 self-sufficient PDT. The UCNPs convert the light into higher-energy light for the activation of the photosensitizer to generate ROS following stimulation with NIR light. Meanwhile, the sub-10 nm $MnFe_2O_4$ nanoparticles act as a Fenton catalyst to generate O_2 *in situ* to overcome tumor hypoxia. Overall, better anti-tumor effects were achieved with this nanocomposite.[312]

4.3. Two-photon absorption

Two-photon absorption refers to the nonlinear absorption of two relatively low-energy photons, followed by the emission of relatively high-energy photons.[313,314] Two-photon excitation is also an attractive strategy to improve the tissue penetration depth for bio-imaging and phototherapy because of the high tissue-penetration ability of low-energy photons.[315,316] The use of a relatively low-energy light source in PDT also reduced the photo-bleaching capacity of photosensitizers. Interestingly, the nonlinearity of photon absorption in two-photon excitation enables precise spatial control of ROS production in tissues, leading to enhanced therapeutic effects and reduced damage to surrounding tissues. Nanomaterials are widely used in two-photon excitation-based PDT. Generally, nanomaterials might be used as two-photon absorption materials to activate the co-delivered photosensitizers through high-energy photon emission. Meanwhile, nanomaterials might also function as carriers for the delivery and tumor-specific targeting of two-photon absorption dyes and photosensitizers.[56]

For example, two-photon absorption of several semiconductor quantum dots was successfully implemented in the PDT of deep-seated tumors. The high-emission quantum yield, broad-absorption spectra, excellent photostability, and highly adjustable optical properties make semiconductor quantum dots ideal candidates for two-photon emission-mediated PDT for cancer as a group of nanomaterials widely investigated in tumor theranostics.[317,318] Semiconductor quantum dots might be directly used as photosensitizers for ROS production. However, investigations with CdSe quantum dots showed a very low $^1O_2$ quantum yield. Therefore, it is more promising to use quantum dots to transfer energy to co-delivered photosensitizers for the efficient production of ROS.[318] Dayal and Burda covalently modified CdSe quantum dots with the photosensitizer silicon phthalocyanine. In this nanocomposite, the maximum emission of the CdSe quantum dots was achieved to match the absorption of silicon phthalocyanine for more efficient energy transfer. Upon stimulation with a low-energy 1100 nm laser, two-photon absorption of the CdSe quantum dots and the following fluorescence resonance energy transfer to silicon phthalocyanine were observed, resulting in the efficient production of ROS.[317] Skripka *et al.* reported highly efficient energy transfer between two-photon excited quantum dots and non-covalently loaded photosensitizers. The photosensitizer Ce6 was loaded onto lipid-coated CdSe/ZnS quantum dots through hydrophobic interactions. When stimulated with a 1030 nm laser beam, the quantum dots were activated through two-photon absorption. The energy was then transferred to Ce6 with an efficiency of about 80%, indicating high potential for use in two-photon absorption-mediated PDT.[319]

Given the potentially toxic effects of heavy metal ions from the quantum dots mentioned above, quantum dots with better

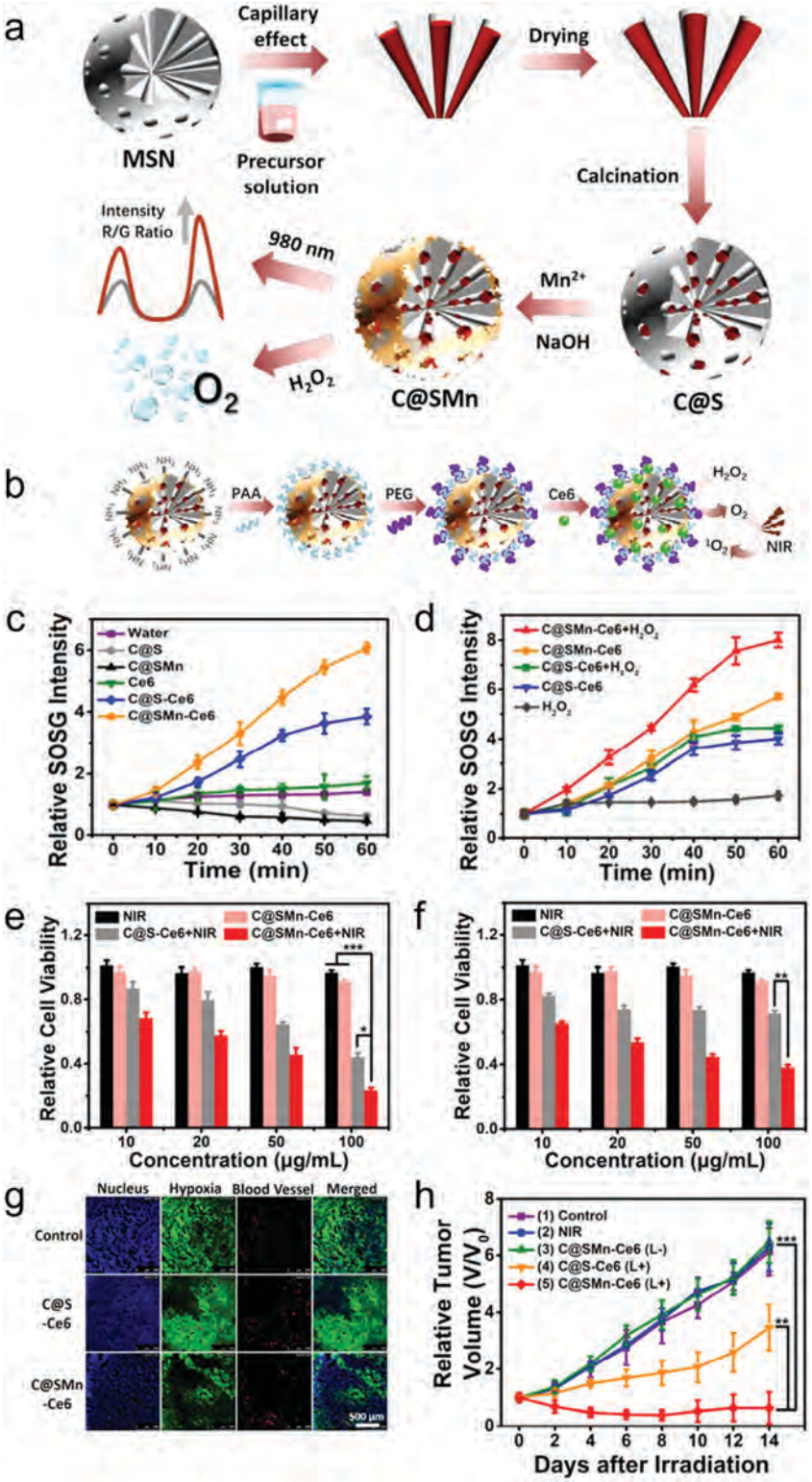

Fig. 12 UCNPs for enhanced NIR-triggered PDT. (a) Schematic illustration of the synthesis of the UCNPs. (b) Surface modification and Ce6 loading procedures. (c) Singlet oxygen generation under 980 nm laser irradiation. (d) Singlet oxygen generation in the absence or presence of H_2O_2. (e) *In vitro* PDT treatment of breast cancer cells in the normoxic atmosphere. (f) *In vitro* PDT treatment of breast cancer cells in the hypoxic atmosphere. (g) Hypoxia-staining immunofluorescence images of tumor tissues. (h) Tumor growth curves following indicated treatments. Reproduced with permission.[311] Copyright, 2018, American Chemical Society.

biocompatibility were also investigated as two-photon absorption materials for PDT. Fowley *et al.* reported the two-photon absorption of carbon quantum dots for deep PDT. Singlet oxygen was produced through energy transfer following exposure to an 800 nm laser with the conjugation of the photosensitizer PpIX to carbon quantum dots. Efficient cancer inhibition was achieved with this conjugate *in vitro* and *in vivo*.[320] Nitrogen-doped graphene quantum dots are also suitable for deep two-photon absorption-stimulated PDT when coupled with suitable photosensitizers.[321]

Noble metal-based nanomaterials are also ideal candidates for the construction of nanocomposites for two-photon absorption-stimulated PDT due to their unique optical properties. Li *et al.* fabricated nano-sized photosensitizers with improved two-photon PDT efficacy by combining conjugated polymers and gold NRs (Fig. 13). The photosensitizer

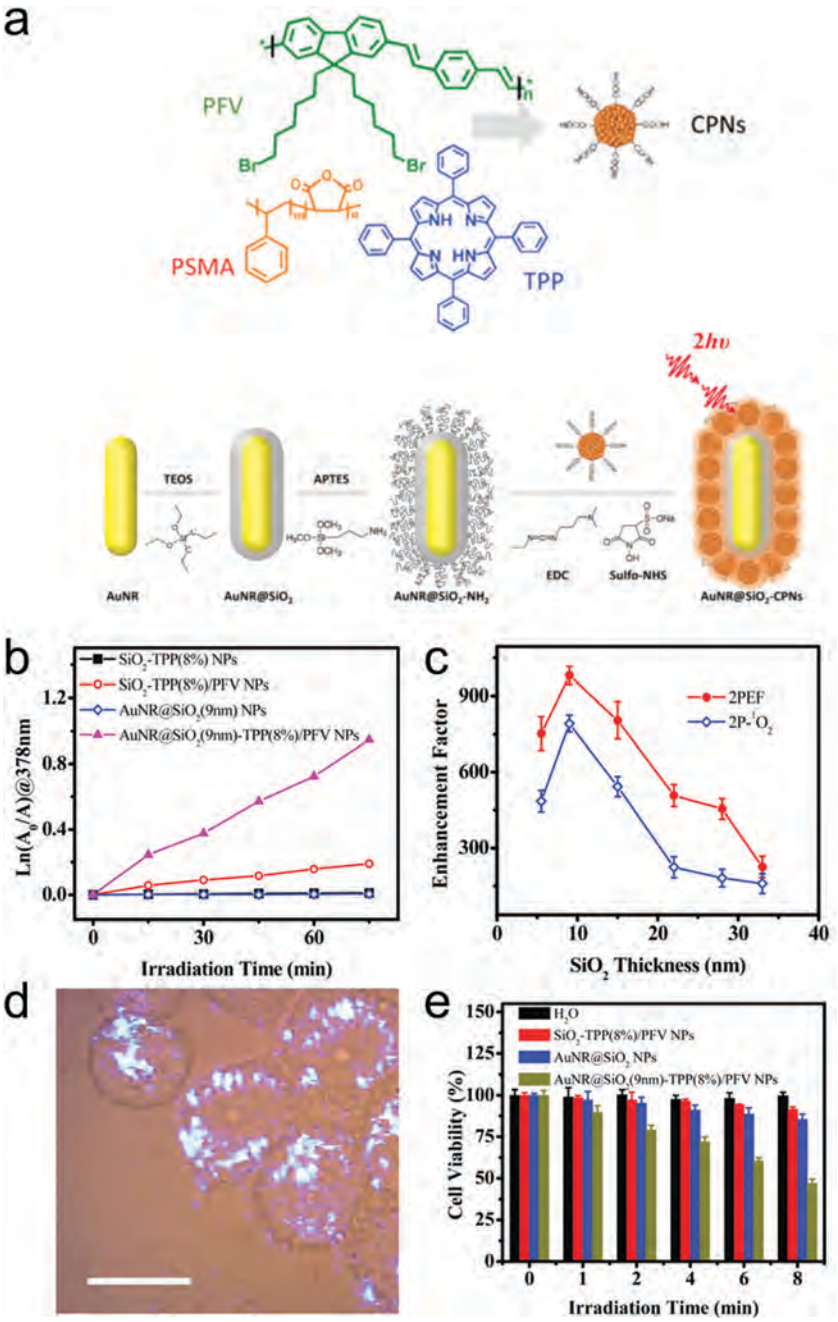

Fig. 13 Two-photon excitation-induced PDT with conjugated polymers and gold NRs. (a) Schematic illustration of the preparation of conjugated polymers and silica-coated gold NRs. (b) Singlet oxygen generation of the nanoparticles under two-photon excitation evaluated by photo-induced oxidation of ABDA. (c) Impact of SiO_2 thickness on the singlet oxygen production of the nanoparticles. (d) Two-photon images of HeLa cells treated as indicated. (e) The viability of HeLa cells treated as indicated, followed by irradiation using a femtosecond laser. Reproduced with permission.[322] Copyright, 2019, The Royal Society of Chemistry.

tetraphenylporphyrin was encapsulated into the conjugated polymers, which were then covalently linked to silica-coated gold NRs (Fig. 13a). The two-photon optical property of tetraphenylporphyrin was enhanced by both the conjugated polymers and the gold NRs. Two-photon-induced singlet oxygen production of tetraphenylporphyrin was thus significantly enhanced up to 792-fold, enabling dramatically enhanced cytotoxicity to cancer cells (Fig. 13b–e).[322]

4.4. X-Rays

X-Rays have a much better tissue penetration depth compared with most other light sources.[323,324] Several nanomaterial-based X-ray-activated photosensitizers have been developed for the PDT of deep-seated tumors by making use of this property.[325–328] Lan *et al.* reported X-ray-activated PDT with metal–organic layer-based materials for cancer treatment. The heavy Hf atoms absorb the energy of X-rays in the materials and then transfer it to $Ir[bpy(ppy)_2]^+$ or $[Ru(bpy)_3]^{2+}$ moieties for ROS generation and tumor inhibition.[329] The excellent tissue penetration ability of X-rays largely improved the range of PDT application in cancer treatment.[330] Besides, X-ray-induced PDT (X-PDT) exhibited stronger tumor cell killing efficacy than radiotherapy alone through the combination of PDT and radiotherapy (Fig. 14). PDT mainly damages the cell membrane to induce necrosis, while radiotherapy mainly targets DNA to induce apoptosis (Fig. 14d and e). As a result, both the short-term viability and long-term clonogenicity of cancer cells were inhibited by X-PDT. This is a promising strategy to kill radio-resistant cancer cells even in deep tissues (Fig. 14f).[331]

4.5. Self-luminescence

Traditionally, an external light source is necessary to stimulate the production of ROS in PDT. Therefore, the tissue penetration ability of the light used is usually a limitation of the therapeutic effect. However, the application of self-illuminating materials effectively overcomes this limitation. The photosensitizers, with proper formulation, can be activated *in situ* by the self-luminescence of co-delivered self-illuminating materials with the emission of chemoluminescence, bioluminescence or Cerenkov luminescence, resulting in the efficient production of ROS for PDT in deep tissue sites.[55,297,332]

4.5.1. Luminol-based self-luminescence. Luminol is a widely used chemoluminescent donor with self-luminescence emission at around 425 nm. Both H_2O_2 and horseradish peroxidase (HRP) are required for this reaction.[333,334] Luminol induces intracellular chemoluminescence, suitable for the excitation of photosensitizers. Laptev *et al.* designed a self-luminescent PDT system by combining luminol and bioconjugates composed of transferrin and haematoporphyrin to inhibit erythroleukemic cells.[335] Zhang *et al.* fabricated a tumor-specific self-illuminating PDT system by integrating luminol, HRP, and the photosensitizer m-THPC onto semiconducting polymer dots. Folic acid was used to target these nanomaterials to tumor cells. HRP catalyzed the chemoluminescence of luminol with the consumption of highly enriched H_2O_2 in tumors. m-THPC was then activated by chemoluminescence, leading to ROS production and the killing of tumor cells. On-site imaging of tumor cells was also carried out with these nanocomposites.[336] The chemoluminescence of luminol

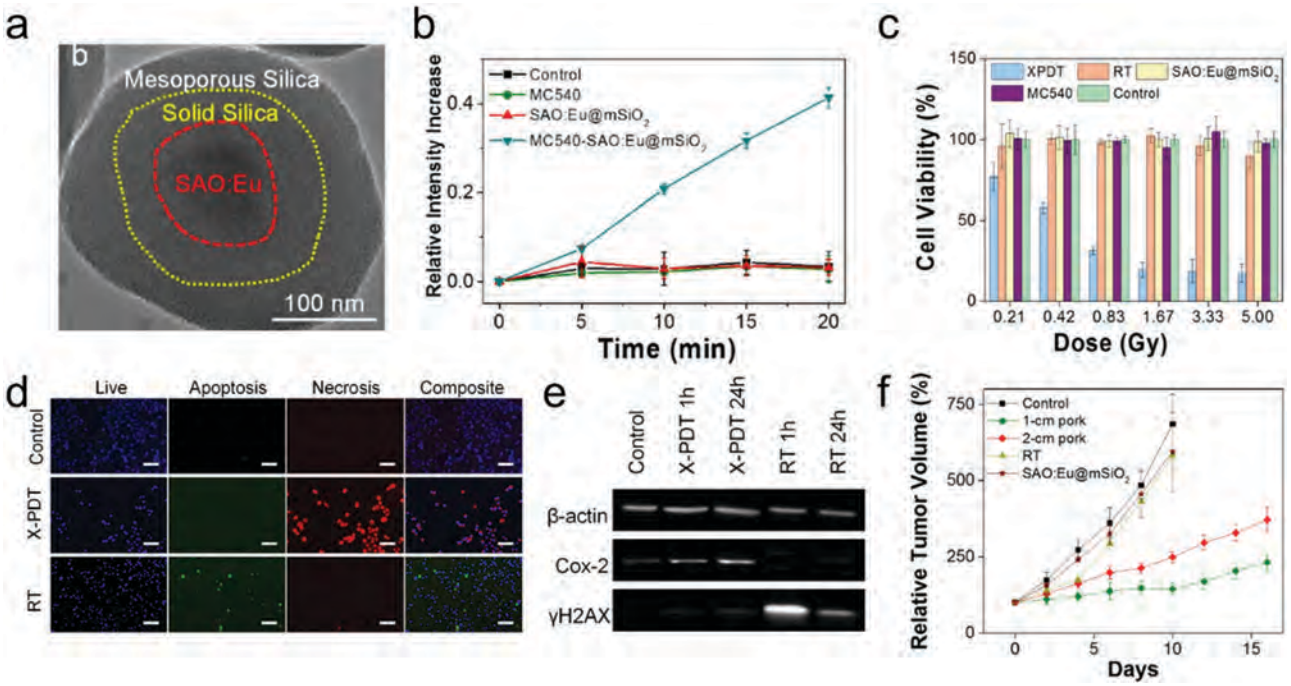

Fig. 14 X-PDT for cancer treatment. (a) TEM images of $SAO:Eu@mSiO_2$ nanoparticles. (b) Singlet oxygen generation following X-ray irradiation. (c) Cell viability after X-PDT treatment. (d) Apoptosis and necrosis of cancer cells after X-PDT. (e) Impact of X-PDT on DNA and membrane lipids indicated by the western blot of marker proteins. (f) Tumor growth curves after X-PDT over thick tissues. Reproduced with permission.[331] Copyright, 2016, Ivyspring International Publisher.

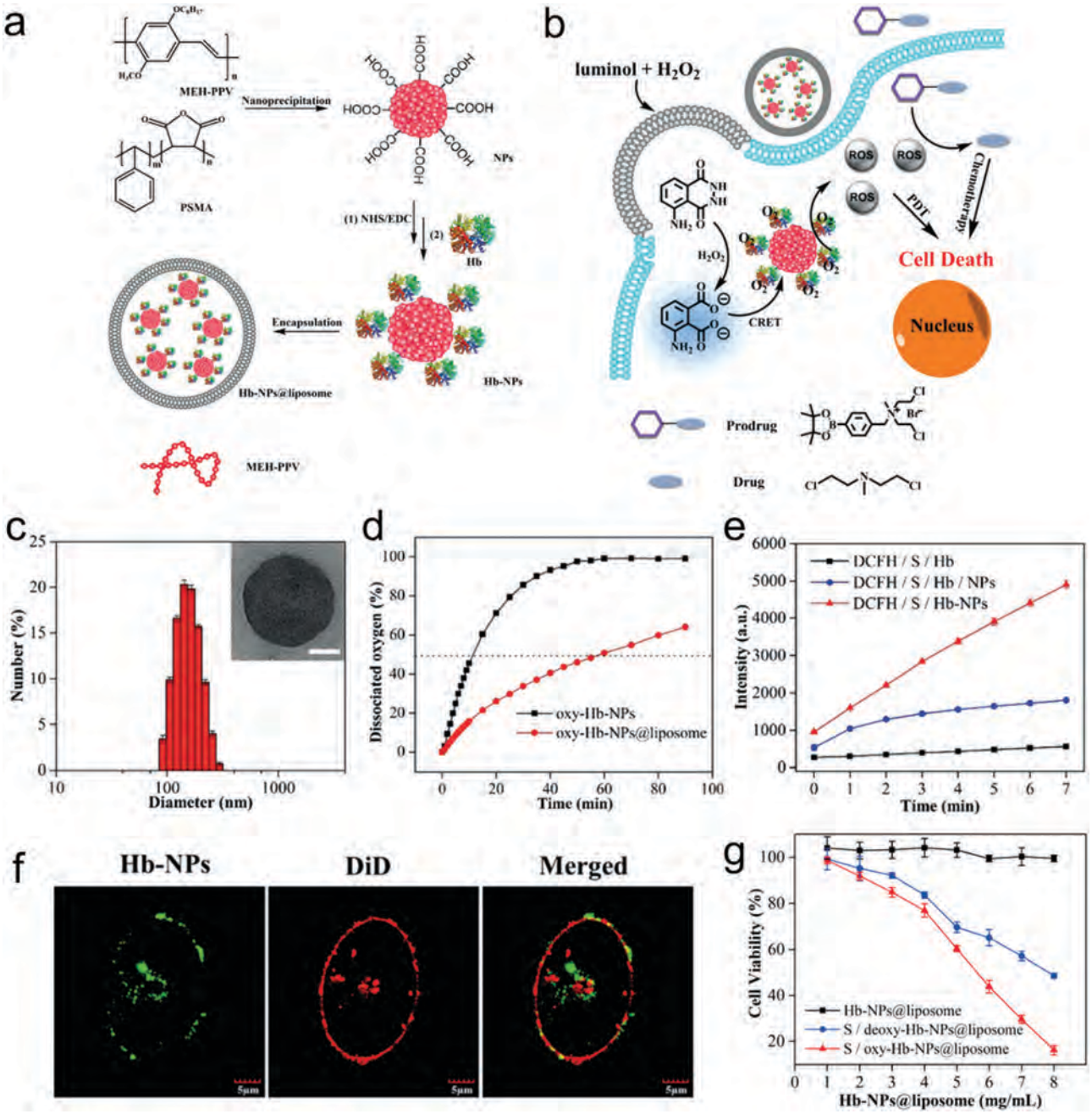

Fig. 15 Luminol-based self-luminescent nanoparticles for PDT. (a) Schematic illustration of the synthesis of Hb-NP liposomes. (b) Schematic illustration of the self-luminescing and oxygen-supplying nanocomposites for PDT. (c) Size distribution and TEM image of Hb-NP liposomes. (d) Oxygen dissociation of the oxygen-carrying nanoparticles. (e) ROS yield of the self-luminescent nanoparticles. (f) Nanoparticle uptake by HeLa cells. The cell membrane is stained with DiD. (g) Viability of HeLa cells treated with self-luminescent nanoparticles. Reproduced with permission.[339] Copyright, 2019, Wiley-VCH.

was also used to activate *meso*-tetraphenyl porphyrin or Ce6 for *in vivo* imaging and PDT.[337,338] Jiang *et al.* fabricated a self-luminescent and oxygen-supplying nano-platform with luminol to enhance the therapeutic efficacy in hypoxic tumors (Fig. 15). Upon cellular uptake, luminol was activated by hemoglobin; chemoluminescence was then absorbed by conjugated polymer MEH-PPV nanoparticles through chemoluminescence resonance energy transfer (Fig. 15a and b). Finally, ROS was produced with oxygen supplied by hemoglobin (Fig. 15d and e). Effective cytotoxicity was observed when these nanoparticles were taken up by HeLa cancer cells (Fig. 15g).[339]

4.5.2. Luciferase-based self-luminescence. Bioluminescence is defined as light emission from enzyme-catalyzed reactions, widely applied in bio-imaging and analysis.[340–344] Luciferase from *Renilla reniformis* is widely used as a light source for bioluminescence-mediated PDT. Coelenterazine is a substrate for *Renilla* luciferase. Hsu *et al.* immobilized *Renilla* luciferase with quantum dots-655 for use in bioluminescence

resonance energy transfer (BRET)-mediated PDT. The incorporation of coelenterazine resulted in self-illumination at 655 nm by the conjugate, leading to the activation of the co-delivered photosensitizer. Efficient cancer cell killing was observed with this nanocomposite.[345]

Luciferase from a firefly was also used in bioluminescence-mediated PDT (Fig. 16). When conjugated with PLGA nanoparticles carrying the photosensitizer RB, firefly luciferase effectively catalyzed the bioluminescence reaction with luciferin as the substrate (Fig. 16a and b). RB was then activated by BRET, leading to the efficient production of ROS and the killing of cancer cells (Fig. 16d–f).[346]

In summary, various light sources with better tissue penetrability have been developed to overcome the limitation to PDT efficiency by tissue depth. Among these light sources, dramatically improved tissue penetrability may be achieved by using X-ray or self-luminescence excited photosensitizers. These strategies may pave the way for the clinical application of PDT in the treatment of deep-seated tumors. However, the quantum yields of several strategies, especially photon up-conversion, may still be a limitation to clinical applications. Meanwhile, when self-luminescence is used as the light source, strategies are still needed to reduce the risk of non-specificity to normal tissues and organs.

5. Nanocomposites for the modulation of PDT induced anti-tumor effects

Several pathways are involved in PDT-induced anti-tumor effects (Table 3). Tumor cells might be directly killed through ROS-induced cell death pathways, such as apoptosis, necrosis, or autophagy-mediated cell death.[347] Meanwhile, ROS-induced damage to the vascular system is also involved in the anti-tumor effects of PDT.[348–350] More interestingly, there are strong relationships between PDT and the immune system. PDT-induced anti-tumor immune response might function in the inhibition of circulating tumor cells and metastatic tumors (Fig. 17).[351–354]

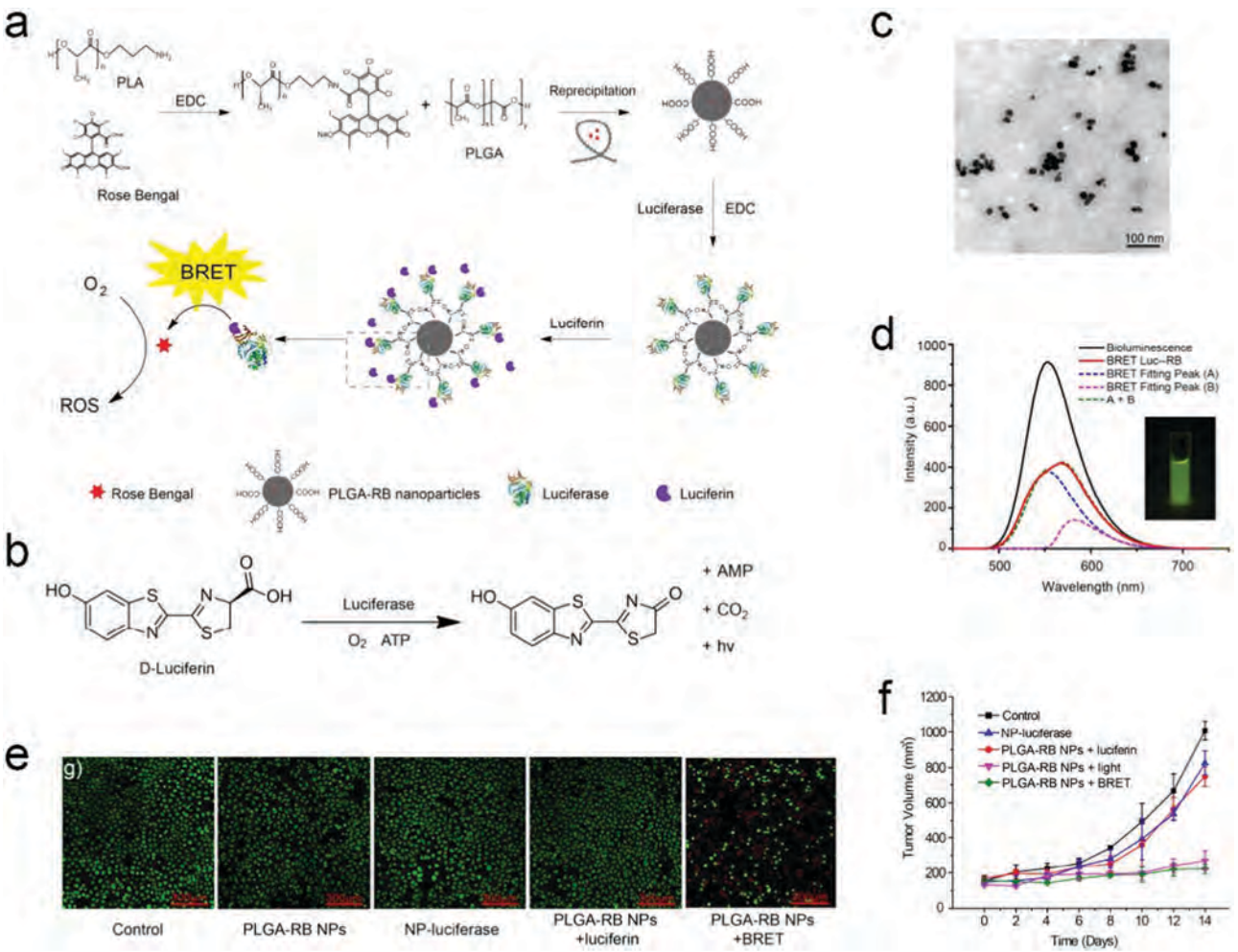

Fig. 16 Luciferase-based self-luminescent nanoparticles for PDT. (a) Schematic illustration of the fabrication of self-luminescent PLGA-RB nanocomposites for PDT. (b) Photon emission reaction catalyzed by firefly luciferase. (c) TEM image of the nanoparticles. (d) The bioluminescence spectra without and with BRET. (e) Viability of MCF-7 cells after BRET-PDT treatment. (f) Tumor growth curves after BRET-PDT treatment. Reproduced with permission.[346] Copyright, 2017, American Chemical Society.

Table 3 Mechanisms of PDT mediated tumor inhibition

Process	Characteristics	Key regulators	Impacts	Ref.
Apoptosis	Cell blebbing, shrinkage, nuclear fragmentation, chromatin condensation, chromosomal DNA fragmentation, and global mRNA decay	Mitochondria, cytochrome *C*, Bcl-2, Bcl-xL, Bid	Main process for PDT-induced cancer cell death	28, 29, 360, 361, 373 and 375
Necrosis	Cytoplasmic granulation, organelle and/or cellular swelling and breakdown, and release of cellular contents and pro-inflammatory molecules	TNF, RIPK1, PARP-1	Main process for PDT-induced cancer cell death and induction of inflammatory reaction, important for long-term anti-tumor effects	371–375
Autophagy	Accumulation of autophagosomes	PI3K, AKT, mTOR, LC3	Induction of cancer cell death and suppression of tumor formation, possibly promoting tumor cell survival in PDT	29, 374, 378 and 379
Vascular damage	Damage to vascular endothelial cells, destruction of tight junctions, exposure of basement membranes, aggregation of platelets, leukocyte adhesion, and vascular leakage or shutdown	VEGF, VEGFR, HIF-1α	Persistent shortage of nutrients and oxygen in tumor tissues and inhibition of tumor growth, possibly promoting resistance to therapy	26 and 27
Immune response	Activated by PDT, highly related to the mode of cancer cell death	Damage-associated molecular patterns (DAMPs), innate immune cells, cytokines, dendritic cells, and T lymphocytes	Long-term inhibition of tumor growth, recurrence, and metastasis	44, 351, 354, 508 and 509

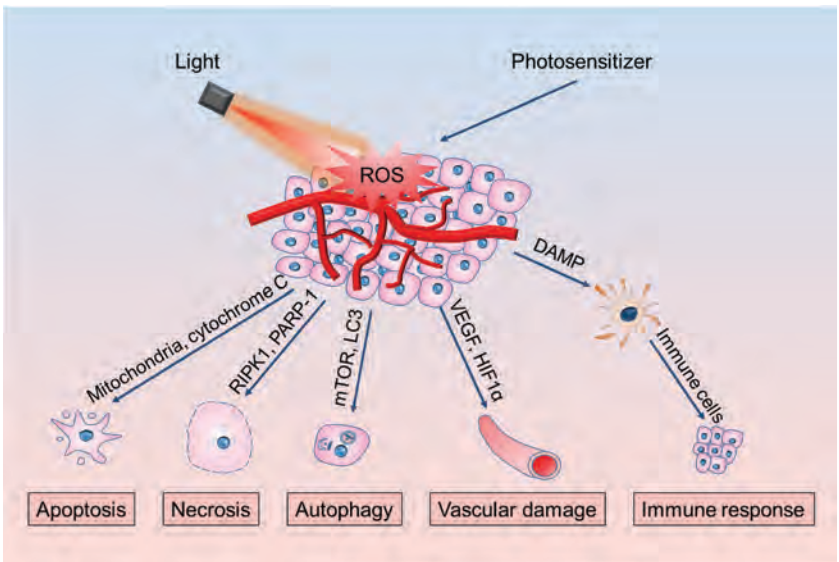

Fig. 17 Targets for the modulation of PDT induced anti-tumor effects with nanocomposites. During exposure to light, the photosensitizers absorb the energy to catalyze ROS formation in tumor tissues. ROS might kill tumor cells directly by inducing apoptosis, necrosis, or autophagy-mediated cell death. Meanwhile, damage and shutdown of microvessels also contribute to the anti-tumor effect of PDT. Furthermore, the acute inflammatory response recruits leukocytes, including dendritic cells and neutrophils, to stimulate the host immune system, resulting in the long-term inhibition of tumor metastasis and recurrence. Potential targets for the modulation of these processes are listed [RIPK1: receptor-interacting protein kinase 1; PARP-1: poly(ADP-ribose) polymerase-1; mTOR: mammalian target of rapamycin; LC3: microtubule-associated protein 1A/1B-light chain 3; VEGF: vascular endothelial growth factor; HIF1α: hypoxia-induced factor 1α].

Recently, various novel nanocomposites and combined therapy platforms have been designed to modulate these processes to promote the tumor inhibition of PDT. Most of these nanocomposites are fabricated through the combination of photosensitizers with bioactive reagents, such as agonists, antagonists, siRNA, proteins, and immunomodulators. It is critical to maintain the activity of these reagents during the fabrication of the nanocomposite photosensitizers and the therapy processes.

5.1. Nanocomposites for the modulation of apoptosis

Apoptosis is defined as the programmed cell death tightly regulated by a series of signaling pathways.[355–357] It is characterized by several morphological changes, including cell blebbing, shrinkage, nuclear fragmentation, chromatin condensation, chromosomal DNA fragmentation, and global mRNA decay.[358] Two subtypes of apoptosis have been defined: extrinsic apoptosis and intrinsic apoptosis. Extrinsic apoptosis is regulated by membrane receptors, including death receptors and tumor necrosis factor (TNF) receptors, while intrinsic apoptosis is mainly triggered by mitochondrial outer membrane permeabilization and the release of mitochondrial proteins, especially cytochrome *C*.[359] Apoptosis is induced by different stresses, including ROS-mediated oxidative stress in PDT.[28,29,360–362] In normal conditions, the cellular antioxidant system maintained a balance between ROS production and consumption. When challenged by overwhelming ROS produced by photodynamic reactions, oxidative damage of cellular components is induced. As mentioned above, the peroxidation of membrane lipids and damage to proteins and DNA are induced by excessive ROS. These events result in structural and functional damage to cancer cells, finally leading to apoptosis.[359]

PDT-induced apoptosis of cancer cells was first investigated in mouse lymphoma L5178Y cells sensitized with the photosensitizer chloroaluminum phthalocyanine. DNA fragmentation and chromatin condensation of cancer cells were detected in response to the therapy. The PDT-induced apoptosis of L5178Y cells was rapid, which occurred along with DNA degradation as early as 30 minutes after therapy.[363] PDT-induced apoptosis was also observed in mouse MS-2 fibrosarcoma with liposome-administered ZnPc as a photosensitizer. Following light exposure, dramatic ultra-structural changes characteristic of apoptosis were observed under an electron microscope, including the early occurrence of chromatin condensation and margination, the disappearance of nuclear pores, karyopyknosis, karyorrhexis, cell surface protuberance formation, and cell fragmentation.[364]

Complex molecular mechanisms are involved in the apoptosis induced by PDT. Several pathways might be involved in this process, depending on the type and subcellular localization of the photosensitizers, the genetic background of the cancer cells, the dosage of light exposure, and the involvement of other stimulations. Critical proteins and processes in these pathways are important targets for the modulation of PDT induced cancer cell apoptosis with nanocomposite photosensitizers. For example, mitochondrial cytochrome *C* plays a crucial role in the regulation of cell apoptosis. When the mitochondria of cancer cells were damaged by ROS during PDT, the immediate loss of mitochondrial membrane potential and the release of cytochrome *C* into the cytosol occurred.[360] The leakage of cytochrome *C* into the cytosol resulted in the inhibition of cellular respiration.[365] Caspase-3 like proteases were then rapidly activated, resulting in the apoptosis of cancer cells.[360]

The anti-apoptotic protein Bcl-2 is also a target for PDT to induce cell apoptosis. Bcl-2 protein was cleaved or photochemically cross-linked following PDT with the mitochondrial and ER-localized photosensitizer Pc4.[74] In further research, it was revealed that caspase-mediated cleavage is not required for PDT-induced photodamage of Bcl-2. The photodamage of Bcl-2 protein was a direct result of the photodynamic action without the involvement of protease or other enzymatic activity. The deletion of the N-terminus of Bcl-2 protein does not affect the PDT-induced photodamage to the protein. The C-terminus transmembrane domain, required for the membrane localization of Bcl-2 protein, is needed for PDT-induced photodamage. Besides, the alpha-helices 5 and 6 are very crucial for photodamage of the protein. It is speculated that the cross-linking of Bcl-2 protein is mediated by the interaction of these two helices with other protein domains. This process is vital for the induction of apoptosis by PDT.[366]

Bcl-xL, a protein with size, sequence, sub-cellular localization, and physiological function similar to Bcl-2, is also damaged by PDT. It is probably involved in the regulation of PDT-induced cell apoptosis. Interestingly, Bcl-xL protein localized in the mitochondria is more sensitive to PDT-induced photodamage than Bcl-xL in the cytosol.[367]

Lysosome-localized photosensitizers induce apoptosis through an alternative pathway. Lysosomes were damaged, resulting in the release of lysosomal proteases following ROS production in PDT. The Bid protein in the cytosol was cleaved by proteases to form a pro-apoptotic fragment referred to as tBid, which interacted with the mitochondria to initiate cell apoptosis.[368] This pathway is required for the apoptosis induced by lysosome-localized photosensitizers, but not for the apoptosis induced by mitochondria or ER-localized photosensitizers.[369]

PDT also causes rapid activation of phospholipase C and phospholipase A2, leading to downstream events, such as the breakdown of membrane phosphoinositides and the release of Ca^{2+} from the intracellular pools. These processes also participate in the initiation of PDT-induced apoptosis of cancer cells.[363]

Considering the involvement of these proteins and pathways in PDT induced cancer cell apoptosis, modulation of their activity may maximize the tumor inhibition efficiency of the therapy. For example, Liu *et al.* designed a mitochondria-targeting nanocomposite photosensitizer with a UCNP core and a silica shell for photosensitizer incorporation. Mitochondria-targeting of this nanocomposite was achieved through modification with (3-carboxypropyl)triphenylphosphonium bromide (TPP). Following NIR irradiation, *in situ* production of ROS led to serious damage to the mitochondria, resulting in the release of cytochrome *C* and the apoptosis of tumor cells.[370]

5.2. Nanocomposites for the modulation of necrosis

Necrosis is defined as cell injury that leads to the premature death of cells by autolysis.[371,372] Morphologically, necrosis is characterized by cytoplasmic granulation and organelle and/or cellular swelling and breakdown, followed by the release of cellular contents and pro-inflammatory molecules.[373–375] Inflammatory reactions are induced by these processes. Recent research revealed multiple signaling pathways in the regulation

of necrosis though it was initially considered as accidental cell death following exposure to physicochemical stimulations.[372] TNF is a classical extracellular inducer of necrosis through the activation of RIPK1. Meanwhile, intracellular oxidative stress also induces necrosis through the activation of PARP-1 and RIPK1.[30]

PDT also induces necrosis. Following the exposure of cancer cells to an increased PDT dose, a dramatic increase in the ROS level results in immediate damage to cellular metabolism, leading to a shift from apoptotic cell death to necrotic cell death. Subcellular localization of the photosensitizer is a key determinant of the type of death of cancer cells exposed to PDT.[376] Targeted delivery of photosensitizers to the plasma membrane usually leads to more dramatic necrosis following the therapy, probably due to the rapid destruction of plasma membrane integrity, failure in the maintenance of ion fluxes, and depletion of ATP in the cytosol.[31] Oxygen levels might also affect the choice of cell death pathways following PDT with the same photosensitizer, probably due to the different efficiencies and types of ROS produced in normoxic and hypoxic conditions.[377] It is also suggested that the ROS damage essential enzymes and other components of the apoptosis pathway, resulting in the failure of apoptosis induction and transition to necrosis.[376]

Therefore, modulation of PDT induced necrosis may also be an effective strategy to promote tumor inhibition. This can be achieved through membrane targeting of photosensitizers, activation of the necrosis pathway, or inhibition of the apoptosis pathway. Nanocomposite photosensitizers loaded with corresponding functional components (target ligands, small molecule drugs, siRNA, *etc.*) may be used to investigate this issue. Considering the difference of necrosis and apoptosis in the induction of immune responses, the impacts of this combined strategy to PDT induced anti-tumor immunity may also be attractive.

5.3. Nanocomposites for the modulation of autophagy-mediated cancer cell death

Autophagy involves a self-digesting process of cells, characterized by the accumulation of autophagosomes. Autophagy is mainly regulated by the PI3K-Akt-mTOR pathway.[378–380] It maintains cellular homeostasis through the degradation of unnecessary or dysfunctional proteins and organelles.[381] The role of autophagy is complex in cancer cells. Autophagy might have a role in suppressing tumor formation through the inhibition of necrosis and inflammation-induced genetic instability. However, autophagy-mediated recycling of nutrients and energy might also promote tumor cell survival under stressed conditions.[382,383] Autophagy is activated in response to several stress conditions, including anti-cancer therapies. Therefore, it is speculated that autophagy might have a role in resistance to cancer therapeutics, such as radiotherapy, chemotherapy, and immunotherapy.[384,385] Interestingly, autophagy is also involved in the maintenance of cancer stem cells; however, its exact function is still controversial.[386] Targeting autophagy is a potential strategy to tackle drug resistance and promote the effects of cancer therapy.[387,388]

Autophagy is also induced in cancer cells following PDT.[32] Several stress sensors in cancer cells are activated to initiate the autophagy process to collect and digest damaged proteins and organelles to recycle nutrients and energy. Superoxide is the major ROS regulating autophagy after exposure to ROS produced in PDT.[389] The oxidative stress induced by PDT promoted the formation of ubiquitin aggregates, which were recognized and degraded by autophagy. Inhibition of this process led to increased photo-oxidative stress and cell death.[390] PpIX-mediated PDT induced autophagy in colorectal cancer stem-like cells. Suppression of PDT-induced autophagy gave rise to increased apoptosis and decreased colonosphere formation and tumorigenicity, indicating the potential to sensitize cancer stem cells to PDT through autophagy inhibition.[391] In the human osteosarcoma cell line MG-63, aloe emodin-mediated PDT induced autophagy through the ROS-c-Jun amino-terminal kinase (JNK) signaling pathway. The inhibition of autophagy with 3-methyladenine or chloroquine also resulted in enhanced apoptosis.[392] Inhibition of autophagy sensitized the tumor cells to Photofrin-mediated PDT.[393]

Autophagy might also function as a pro-death pathway. Inhibition of apoptosis induces autophagic cell death through the activation of receptor–interacting protein and JNK.[394,395] In methyl pyropheophenylchlorin-mediated PDT, the protein kinase R-like ER kinase signaling-mediated ER stress pathway induced autophagy to kill breast cancer cells.[396] In GQD-mediated PDT, the cytotoxic effect on U251 human glioma cells was also mediated by cell death through both apoptosis and autophagy. Autophagy inhibition through the knock-down of LC3B reduced the cytotoxicity of GQD, indicating the pro-death effect of autophagy in GQD-mediated PDT.[397] Generally, the autophagy induced by moderate PDT mainly protects cells, while the autophagy induced by prolonged or over-primed PDT promotes cell death.

Modulation of PDT induced autophagy in tumor cells with nanocomposites is also applied in enhancing the therapeutic efficiency. For example, Wang *et al.* loaded the photosensitizer phthalocyanine and the autophagy promoter rapamycin together into self-assembled dendrimer nanoparticles for the modulation of PDT induced autophagy. When these nanoparticles were taken up by tumor cells, rapamycin was released after light irradiation to stimulate autophagy. Efficient tumor inhibition was achieved with this strategy.[244] Recently, Deng *et al.* integrated 3-bromopyruvate into Ce6-loaded nanoparticles to modulate PDT induced autophagy. Stimulation of PDT induced autophagy with this nanocomposite promoted the apoptosis of cancer cells, contributing to tumor inhibition of the therapy.[398]

5.4. Nanocomposites for the modulation of vascular damage

The highly proliferative nature of tumor cells requires a massive supply of nutrients and oxygen, making angiogenesis a critical step for the progression of solid tumors.[399–401] The low oxygen concentration in tumor tissues induces the expression

of several growth factors through HIF-1, leading to tumor angiogenesis. However, this pathological angiogenesis usually leads to the formation of tortuous and disorganized leaky vascular structures, allowing nanoparticles to penetrate and accumulate in tumor tissues.[402]

Cells of both the tumor vasculature and parenchyma can be the targets of ROS produced in PDT. The preference is determined by photosensitizer distribution, which is affected by the pharmacokinetic properties of the photosensitizers and the interval between photosensitizer administration and light illumination.[26,27] Tumor vasculature is the main target of photo-induced damage with shorter photosensitizer–light intervals. In contrast, longer photosensitizer–light intervals give rise to photodamage mainly in tumor cells.

In addition to the passive targeting mechanism, tumor vasculature can also be actively targeted when using surface markers of tumor endothelial cells. For example, the ED-B domain of fibronectin, VEGFR-2, and neuropilin-1 are ideal tumor endothelial markers for active targeting of photosensitizers to tumor vessels.[403] Photodynamic reaction-induced damage to vascular endothelial cells destroys tight junctions and exposes the basement membranes,[403] resulting in platelet aggregation, leukocyte adhesion, vascular leakage, and finally vascular shutdown. Tumor growth will be primarily restricted by a persistent shortage of nutrients and oxygen.

With the combination of vascular targeting and tumor cell-targeting PDT reactions, more effective tumor growth inhibition can be achieved. For instance, Bechet *et al.* reported a tumor vasculature targeting PDT strategy for the treatment of brain tumors. Both photosensitizer and magnetic resonance imaging (MRI) contrast agents were used to prepare multifunctional nanocomposites. Vasculature targeting of the nanocomposites was achieved through surface modification with a neuropilin-1 peptide.[404] An efficient interstitial PDT was observed using this nanoplatform for brain tumors guided by real-time MRI. Jang *et al.* designed an anti-angiogenic PDT strategy for tumor treatment. The photosensitizer Ce6 was loaded into microbubbles for ultrasound-triggered local delivery. Meanwhile, an anti-angiogenic siRNA was delivered with nanoparticles protected by two biocompatible polymers to inhibit angiogenesis. The tumor inhibition efficiency of PDT was improved with this strategy.[405] Wei *et al.* prepared carrier-free nanocomposites through the combination of the photosensitizer Ce6 and the anti-angiogenic drug sorafenib for the PDT/PTT of cancer. Upon light stimulation, sorafenib was released to inhibit angiogenesis and cut off the supply of oxygen and nutrients, contributing to tumor inhibition of the therapy.[406]

5.5. Nanocomposites for the modulation of immune responses

The immune system is essential for the body to fight against and clear external (such as viruses, bacteria, fungi, parasites, and other foreign substances) and internal (such as mutant cells, dead cells, and cell debris) threats to maintain the healthy structure and normal function of the body. Evasion from the recognition and killing of the immune system is the first step for spontaneously malignant cells to become cancerous.[407–409] In patients with tumors, the immune system is largely dysfunctional. Normalization or stimulation of the immune system is a promising strategy for cancer treatment.[410,411] Traditional tumor therapy usually suppresses the immune system, which is harmful to the long-term survival of patients. Interestingly, PDT has a much more different impact on the immune system. Apart from the destruction of tumor cells and vasculature, PDT can modulate the immune system and initiate immune responses against tumor cells, providing long-term protection for the patients from recurrence and metastasis of tumors.[33]

The cell death mode in the therapy is closely related to the extent of PDT-induced anti-tumor immunity. As mentioned previously, PDT-induced cell death might involve apoptosis, necrosis, and autophagy-mediated modes. This is unique in current tumor therapies. Research in other systems has shown that distinctive immune gene expression patterns in viable and dying cells are detected in apoptosis or necrosis induced by different agents, eliciting different host immune responses.[24] Some investigations have indicated that apoptotic tumor cells are better immune stimulators than necrotic tumor cells.[412] However, several other reports have shown that tumor therapy mainly inducing necrosis of cancer cells is more efficient in stimulating the host immune system than those that mainly lead to apoptotic cell death.[413,414] During PDT-induced necrosis, the damage to the plasma membrane leads to the exposure of cytosolic constituents to extracellular spaces, resulting in a strong inflammatory response. The host leukocytes are attracted to the tumor by these constituents. Meanwhile, increased tumor-specific antigen presentation also contributes to enhanced immune responses.[33]

PDT can stimulate innate immune responses against pathogenic substances with phagocytes, complement cascade, and natural killer cells. PDT induces an acute inflammatory response, leading to the release of cytokines, activation of complement, and recruitment and activation of innate immune cells.[415,416] PDT-induced destruction of tumor cells gives rise to the presentation of DAMPs on the cell surface or in the extracellular matrix.[417] These signals are recognized and neutralized by the innate immune phagocytes, leading to the elimination of tumor cellular debris.[418]

PDT might also activate adaptive immune responses. Dendritic cells are activated following PDT-induced cancer cell death. Dendritic cells recognize DAMPs and differentiate into mature cells as potent antigen-presenting cells. After migration into the lymph nodes, the mature dendritic cells present tumor-associated antigens to naive T cells, which differentiate to become cytotoxic tumor-specific T lymphocytes to attack and destroy the remaining tumor cells.[418,419]

Moreover, apoptotic and necrotic tumor cells in PDT might also function as tumor vaccines to provide long-term protection for the host.[420] Interestingly, different protection effects between apoptotic and necrotic cells have been identified. In several tumor models (colon carcinoma cells CT26 and CT26-HA, renal cortical adenocarcinoma [RENCA], and melanoma

cell B16), apoptotic cancer cells prevented tumor outgrowth efficiently for more than 30 days, while necrotic cancer cells exhibited very weak or no protection. In terms of the mechanism, injection of apoptotic cells induced a strong $CD4^+$ and $CD8^+$ T-cell response accompanied by the presence of dendritic cells, while the injection of necrotic cells stimulated a strong local macrophage response.[412] The use of PDT-based tumor vaccine to protect hosts from several types of tumors has been thoroughly investigated with different photosensitizers. In a report of the PDT-based tumor vaccine, 5-5-(4-*N*,*N*-diacetoxylphenyl-10,15,20-tetraphenylporphyrin) was applied as a photosensitizer to induce cell death of LA795 murine lung cells. The tumor cell lysates and cell surface antigens obtained from acid-eluted adherent cells were used as a tumor vaccine to study the mechanisms involved. Injection of the tumor vaccine gave rise to increased $CD4^+/CD8^+$ ratios, NK cell percentages, serum IFN-γ and IL-2 levels, and lymphocyte aggregation at the edge of tumors. More importantly, significant inhibition of lung tumor growth was achieved with this tumor vaccine.[421] ROS-induced ER stress leads to the dysregulation of ''eat me'' and ''don't eat me'' signals during the PDT-based tumor vaccine preparation. It is suggested that this dysregulation promotes the uptake of PDT-killed tumor cells by dendritic cells, enhancing the phenotypic maturation and functional stimulation of dendritic cells.[422]

Considering the extensive interplay between PDT and the immune system, various combined PDT/immunotherapy strategies have been investigated for tumor treatment.[49] Modulation of PDT induced anti-tumor immunity has been investigated with nanocomposites based on various nanomaterials, including 2D materials, metal-based nanoparticles, and organic nanoparticles.[423–425] The tumor inhibition efficiency of PDT may be enhanced through the relief of the immunosuppressive environment in tumor tissues with these strategies.[426,427] For example, Li *et al.* prepared pro-nanostimulants with SPNs for cancer immunotherapy. An immunostimulant was conjugated with SPNs through a singlet oxygen cleavable linker. Following NIR laser irradiation, singlet oxygen is generated to kill tumor cells and produce tumor-associated antigens. At the same time, the immunostimulant was released from the nanoparticles to trigger a synergistic antitumor immune response.[428] Yang *et al.* reported a combined PDT strategy with pH-responsive nanovesicles to induce immunogenic cell death. The indoleamine 2,3-dioxygenase inhibitor indoximod (IND) was also co-delivered to promote the development of $CD8^+$ T cells. The tumor inhibition efficiency of PDT was thus improved.[429] Zeng *et al.* designed activatable nanoenzymes with SPNs to modulate tumor immunometabolism. To achieve this goal, kynureninase was conjugated with SPNs through a singlet oxygen cleavable linker. When irradiated by NIR light, singlet oxygen was generated for PDT mediated immunogenic cell death of cancer. Meanwhile, kynureninase was released to catalyze the degradation of the immunosuppressive kynurenine, contributing to systemic antitumor T cell immunity. Both primary and distant tumors were inhibited by this strategy.[5] Yu *et al.* prepared a nanocomposite with pheophorbide A as the photosensitizer for PDT. An anti-PD-L1 peptide was co-delivered to relieve the immunosuppressive environment. After PDT, immunogenic cell death was induced, followed by enhanced activation of cytotoxic T cells and secretion of cytokines. Inhibition of both tumor growth and metastasis was achieved with this strategy.[430]

In summary, an investigation of the mechanisms involved in PDT mediated tumor inhibition provides a series of targets for the modulation of these processes to enhance the therapeutic efficiency. Small molecule drugs and siRNA targeting critical proteins involved in these pathways are ideal candidates for the preparation of nanocomposites to regulate these processes. More efficient induction of tumor cell death can be achieved with these strategies. Moreover, PDT induced immune responses may also be altered by these strategies. Recent developments have revealed the extraordinary potential of PDT associated anti-tumor immunity in long-term inhibition of tumor growth and metastasis. It is promising to further investigate the application of these combined therapy strategies in the treatment of various solid tumors, especially those with poor responsiveness to traditional immunotherapy.

6. Nanocomposites for the relief of tumor resistance to PDT

Although PDT induces several anti-tumor pathways, tumors might also trigger multiple mechanisms to antagonize the effect of PDT (Fig. 18 and Table 4), leading to tumor recurrence after therapy.[39,431–433] Investigations into the mechanisms involved in tumor resistance to PDT will shed light on the design of combined therapeutic strategies to achieve better tumor inhibition effects. Recently, a variety of nanocomposite photosensitizers have been designed to relieve tumor resistance to PDT.

6.1. Inhibition of photosensitizer excretion

PDT mainly induces cancer cell death locally due to the very short diffusion range of ROS.[2] Therefore, intracellular accumulation of photosensitizers is critical to ensure cytotoxic effects on tumor cells. However, photosensitizer excretion hampered the retention of photosensitizers in tumor cells, leading to resistance to PDT.

Some proteins might function as transporters to transport conventional photosensitizers out of tumor cells. Notably, several proteins critical for multidrug resistance of tumor cells, such as P-gp and ABCG2, are involved in resistance to PDT through the excretion of photosensitizers.[41] For example, both P-gp and ABCG2 are involved in the efflux of the photosensitizer benzoporphyrin derivative (BPD) in breast cancer cells. Overexpression of P-gp and ABCG2 inhibited the accumulation of BPD in tumor cells and enhanced resistance to PDT. Covalent conjugation of BPD with a phospholipid inhibited the efflux of BPD by these two proteins. The nanoliposomal formulation of phospholipid-conjugated BPD maintained the

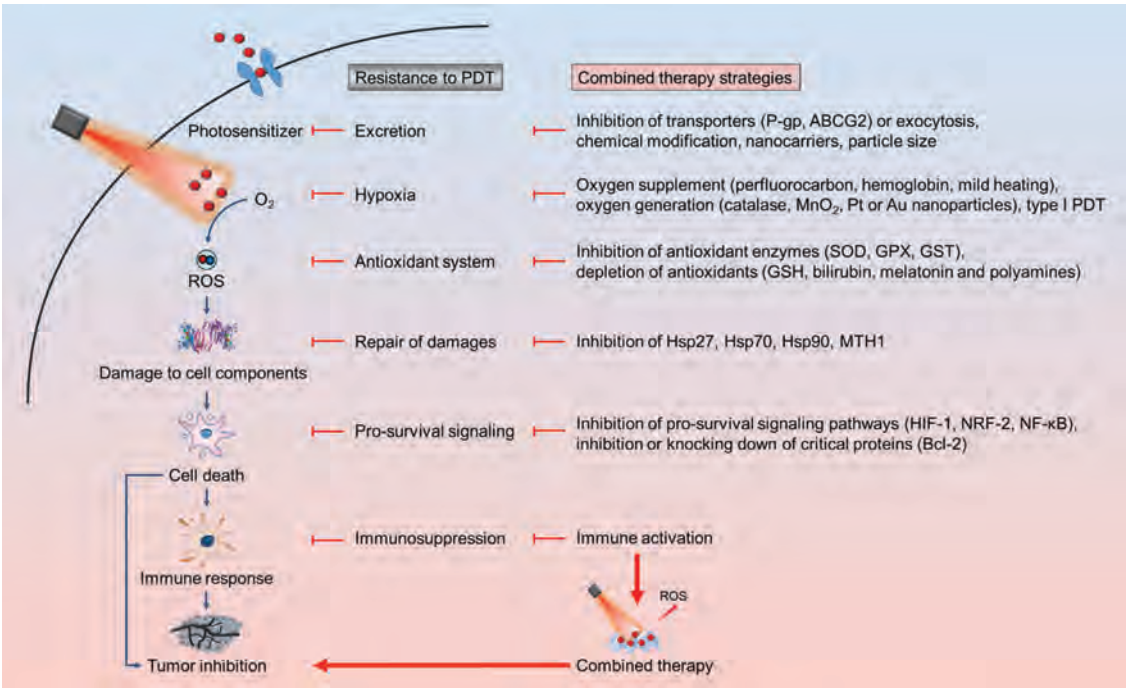

Fig. 18 Summary of combined therapy strategies to relieve tumor resistance to PDT.

BPD concentration in breast cancer cells for 24 hours and ensured effective PDT.[434] The photosensitizer pheophorbide a has also been shown to be a substrate for ABCG2. ABCG2 can transport several other photosensitizers with a structure similar to pheophorbide a, resulting in reduced intracellular accumulation of these photosensitizers in ABCG2-overexpressing tumor cells. Stronger resistance to PDT was found to be mediated by these photosensitizers in ABCG2-overexpressing cells through this process.[40] ABCG2 can be inhibited by tyrosine kinase inhibitors, such as imatinib mesylate (Gleevec), which might thus be used in combination with PDT to promote the accumulation of pheophorbide a in tumor cells to promote tumor inhibition.[271] In another similar research, ABCG2 was also shown to be involved in the efflux of HPPH in cancer cells (Fig. 19). Several modulators of ABCG2 promoted the accumulation of HPPH in both cell culture and the tumor model (Fig. 19c and d). Pretreatment with the ABCG2 modulator imatinib mesylate led to an increased PDT effect of HPPH both *in vitro* and *in vivo*.[270]

The therapeutic efficacy of nanomedicine might also be affected by the excretion of nanoparticles. Upon endocytosis, nanoparticles are encapsulated by early endosomes. Some nanoparticles might be recycled back to the plasma membrane. The others might be delivered to late endosomes and then lysosomes.[435] Exocytosis of some lysosomes might also lead to the excretion of undigested nanoparticles.[436] Among a series of excretion processes, lysosomal exocytosis is considered the most important one for the excretion of nanoparticles.[437] The rate of exocytosis is affected by cell type, subcellular localization, surface modification, particle size, and concentration of nanoparticles. The inhibition of excretion promotes the cellular retention of nanoparticles and enhances the therapeutic efficacy of PDT. For example, Zhang *et al.* prepared a photosensitizer-loaded supramolecular nanogel for PDT. The pH-sensitive nanogel aggregated in acidic endosomes/lysosomes after endocytosis to disturb the exocytosis of tumor cells. The tumor retention of the photosensitizers was significantly improved, resulting in enhanced tumor inhibition following PDT.[43] Nevertheless, the mechanisms of nanoparticle excretion are yet to be fully revealed. Much effort is needed to investigate the impact of nanoparticle excretion on PDT and to modulate this process to promote the accumulation of photosensitizers in tumor cells.

6.2. Relief of hypoxia

The hypoxic tumor microenvironment results in resistance to type II PDT. PDT-induced oxygen consumption and damage to tumor microvasculature further increase this problem.[438] Several strategies have been designed to promote the tumor inhibition efficacy of PDT in hypoxic conditions. Generally, an increase of oxygen supply, utilization of oxygen-independent PDT reaction, and a combination of PDT with hypoxia-activated or oxygen-independent therapies are the main strategies for the optimization of PDT in the hypoxic tumor microenvironment.[46,438]

6.2.1. Replenishment of oxygen. Oxygen replenishment is an effective strategy to enhance PDT effects in hypoxic tumor tissues. O_2 carriers, such as hemoglobin or perfluorocarbons, are widely used in combination with photosensitizers to treat hypoxic tumors. Hemoglobin carries O_2 in red blood cells. Four O_2 molecules can be delivered by each hemoglobin molecule into tumor tissues to meet the need of PDT reactions through proper incorporation of hemoglobin into photosensitizer formulations.[283] Perfluorocarbons are a group of chemicals

Table 4 Combined therapy strategies to overcome cancer resistance to PDT

Photosensitizer	Carrier	Cargo/inhibitor	Mechanism	Cancer	Ref.
BPD	Nanoliposomes	Phospholipid-conjugated BPD	Evading P-glycoprotein and ABCG2 mediated efflux	Breast cancer	434
HPPH	—	Imatinib mesylate	Inhibition of the photosensitizer transporter ABCG2	Fibrosarcoma	270
TPPS	Nanogel	—	Aggregation in acidic endosomes/lysosomes for retardation of exocytosis	Lung cancer	43
IR780	Perfluorocarbon nanoparticles	—	Replenishment of oxygen with perfluorocarbon	Colon cancer	441
RB	Bis(pyrene) nanoaggregates	Hemoglobin	Replenishment of oxygen with hemoglobin	Breast cancer	510
Ce6	PEG shelled liposomes	DiR	Increase of intra-tumor blood flow and relief of tumor hypoxia through mild photothermal heating	Breast cancer	442
BP quantum dots	MOFs	Catalase	Generation of oxygen catalyzed by catalase with consumption of H_2O_2 in tumor tissues	Cervical cancer	446
Ce6	HAS–MnO_2–Ce6 nanoparticles	MnO_2	Generation of oxygen catalyzed by MnO_2 with consumption of H_2O_2 in tumor tissues	Bladder cancer	274
Ce6	3-D dendritic mesoporous silica nanospheres	Pt nanoparticles	Generation of oxygen catalyzed by Pt nanoparticles with consumption of H_2O_2 in tumor tissues	Lung cancer	276
TBP	Titanium-based MOFs	—	Type I PDT	Colon cancer	448
Hypericin	—	2-Methoxyestradiol	Inhibition of SOD-2	Breast cancer	34
Ce6	MnO_2 nanosheets	—	Decrease in intracellular GSH by MnO_2	Breast cancer	455
Porphyrin	Cu^{2+}-metalated nano-MOF	—	Direct adsorption of GSH by Cu^{2+}-metalated nano-MOF	Breast cancer	456
Ce6	α-Cyclodextrin–Ce6–NO nanoparticles	—	Depletion of GSH by both the nanoparticle and NO, relief of hypoxia through NO triggered blood vessel relaxation	Breast cancer	457
Porphyrin	Porphyrin-based telodendrimer	17AAG	Inhibition of HSP90	Prostate cancer	459
Ce6	MSN	siRNA targeting MTH1	Downregulation of MTH1	Colon cancer	38
ZnPc	UCNPs	ABT737	Inhibition of the anti-apoptotic protein Bcl-2	Lung cancer	39
SPNs	—	Kynureninase	Degradation of the immunosuppressive kynurenine	Melanoma	5

with extraordinarily high O_2 solubility. This unique characteristic of perfluorocarbons can be used for O_2 replenishment combined with several kinds of photosensitizers to improve tumor therapy outcomes.[439] In transitional cell carcinoma spheroids, perfluorodecalin was used in combination with the photosensitizer hypericin for PDT. A dramatic enhancement of ROS-induced tumor cell apoptosis was observed with enhanced oxygenation of the spheroids by perfluorodecalin.[440] Perfluorocarbon nanodroplets were also used to load photosensitizers to produce an oxygen self-enriching PDT system. Significantly enhanced cytotoxicity and tumor-inhibition efficacy were achieved with a single-dose intravenous injection of these nanodroplets due to the high oxygen capacity and long singlet oxygen lifetime in perfluorocarbon.[441]

An improvement in blood flow is also useful for increasing O_2 concentrations in hypoxic tumors. Pretreatment of the tumor with mild photothermal-mediated heating is widely used to increase the blood flow of tumors. A mild increase in the local temperature is sufficient to increase the tumor blood flow and O_2 concentration within the tumor. Following mild photothermal-mediated tumor heating, enhanced photodynamic inhibition of hypoxic tumors and reduced photo-toxicity to the skin were achieved.[442]

Oxygen might also be generated in tumors with H_2O_2 as a substrate. A high level of H_2O_2 exists in tumor tissues due to the altered metabolism processes of tumor cells. An increased H_2O_2 concentration is related to altered DNA integrity, cell proliferation, apoptosis resistance, and cancer metastasis. A decrease in the H_2O_2 level reduces the malignancy of tumors.[443] Meanwhile, H_2O_2 can be transformed into O_2 and H_2O with catalase enzyme as a catalyst. By incorporating a catalase into photosensitizer formulations, *in situ* O_2 generation is achieved for a photodynamic reaction with the consumption of H_2O_2. An enhanced PDT effect and decreased malignancy of tumors give rise to a better tumor therapeutic effect.[284,444,445] A delicate design of the formulation is required to maintain the activity of catalase during the whole process. Nanoparticles are ideal carriers for catalase. Recently, Liu *et al.* prepared a hybrid nano-platform with MOFs for the PDT of hypoxic tumors (Fig. 20). BP quantum dots were loaded into the inner layer of MOFs with a stepwise *in situ* growth method to function as a photosensitizer, while catalase was encapsulated into the outer layer of MOFs to increase the O_2 concentration in the hypoxic region of the tumor by converting H_2O_2 into O_2 (Fig. 20a and b). *In vitro* experiments have confirmed the dramatically enhanced singlet oxygen production in hypoxic conditions in the

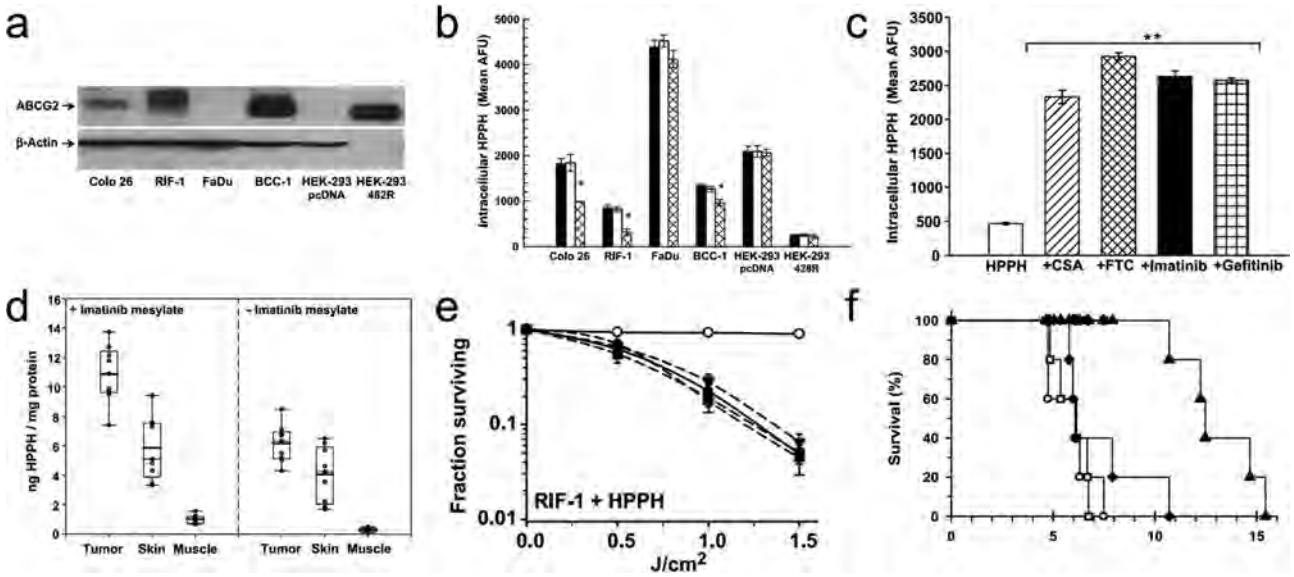

Fig. 19 Inhibition of the photosensitizer transporter ABCG2 enhances the tumor inhibition effect of PDT. (a) ABCG2 protein expression in cells. (b) Temperature-dependent efflux of the photosensitizer. In each cell, the left column indicates the uptake of the photosensitizer HPPH. The central column indicates intracellular HPPH after efflux in the HPPH-free medium at 4 °C, while the right column indicates intracellular HPPH after efflux at 37 °C. (c) Modulators promote the accumulation of the photosensitizer in cells. (d) Treatment with imatinib mesylate increases HPPH levels in tumors. (e) Modulators of ABCG2 enhance the PDT cytotoxicity. (f) Imatinib mesylate enhances the PDT efficiency of HPPH. Reproduced with permission.[270] Copyright, 2007, American Association for Cancer Research.

presence of H_2O_2 (Fig. 20c). The hypoxic microenvironment of tumor tissues was mostly resolved by this nanocomposite (Fig. 20d). The PDT-mediated tumor cell killing efficacy was 8.7-fold higher than that without catalase, leading to proper inhibition of tumor *in vivo* (Fig. 20e).[446]

Similar to catalase, a series of nanomaterials (MnO_2 nanoparticles, platinum nanozymes, and gold nanoclusters) have also been successfully used to generate O_2 *in situ* for efficient PDT in hypoxic tumors.[274–277] As inorganic substances, the preparation and preservation of these nanomaterials are more convenient than catalase, facilitating their incorporation into nanocomposite photosensitizers.

6.2.2. Type I PDT. A type I PDT reaction is O_2-independent, which is different from the widely used type II PDT reaction. In a type I PDT reaction, electron transfer from photosensitizers to surrounding molecules leads to the production of superoxide anions, hydrogen peroxide, and hydroxyl radicals (Fig. 1).[2,54] The implementation of a type I photodynamic reaction for the treatment of hypoxic tumors has been carefully investigated.[447–449] In a recent report, a nanoscale MOF composed of Ti-oxo chain secondary building units and photosensitizing 5,10,15,20-tetra(*p*-benzoato)porphyrin (TBP) ligands was prepared for the PDT of hypoxic tumors. Both type II and type I photodynamic reactions were induced with light stimulation, resulting in the generation of singlet oxygen, superoxide, hydrogen peroxide, and hydroxyl radicals. A much more enhanced anti-tumor effect was achieved with the efficient production of the above four distinct cytotoxic ROS.[448]

6.3. Inhibition of antioxidant systems

The anti-tumor effects of PDT depend on the production of ROS by photosensitizers in response to light stimulation. ROS is also produced in biochemical reactions in cells under normal conditions. Normal cells fight against metabolic ROS mainly through the antioxidant system, which is composed of enzymatic and non-enzymatic components.[450–452]

The antioxidant enzymes include SOD, catalase, GPX, and GST.[452] SODs catalyze the dismutation of superoxide anion in different subcellular compartments, depending on the subcellular localization of the enzyme isoforms. SOD1 functions in the cytoplasm and nucleus, while SOD2 and SOD3 function in the mitochondria and extracellular space, respectively. Catalase converts H_2O_2 into water and oxygen in peroxisomes. GPX is involved in the catalysis of lipid hydroperoxide and H_2O_2 in the mitochondria, cytoplasm, and nucleus. Selenium is required for the enzyme activity of GPXs. GST catalyzes the conjugation of reduced GSH to xenobiotic electrophilic substrates.[451,452]

The non-enzymatic antioxidants include GSH, metal-binding proteins, bilirubin, melatonin, and polyamines.[452] GSH is the most important among them. It might interact with ROS or electrophiles directly. Meanwhile, GSH is also an essential cofactor for enzymes like GPX to maintain their normal antioxidant activity.[359] The antioxidant system is involved in the detoxification of endogenous and exogenous ROS to maintain the survival of normal cells.[451,452]

However, tumor cells can also implement these mechanisms to antagonize the oxidative stress induced by ROS produced in PDT. High levels of intracellular and pericellular ROS are often observed in cancer cells.[451,453] Accordingly, an enhanced detoxification system of ROS is also evolved in cancer cells, which might also be involved in resistance to PDT.[454] Inhibition of critical antioxidant enzymes and non-enzyme antioxidants promotes ROS accumulation, enhancing the therapeutic efficacy of PDT.

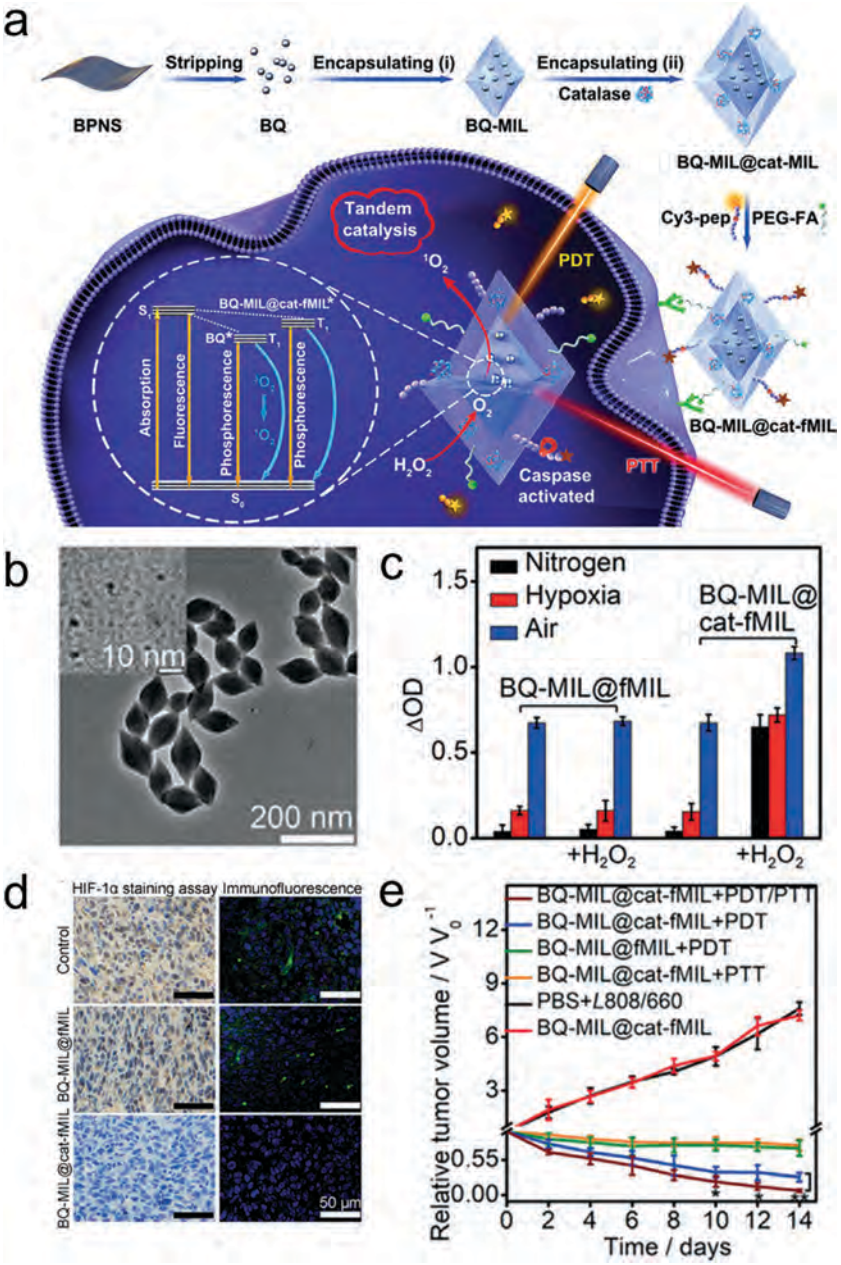

Fig. 20 Replenishment of oxygen with catalase for enhanced PDT efficacy in hypoxic tumors. (a) Schematic illustration of the incorporation of BPQD and catalase in MOF layers for achieving an enhanced therapeutic effect against hypoxic tumor cells. (b) TEM image of the nanocomposite. Inset: TEM image of BPQD. (c) Production of singlet oxygen in the presence or absence of H_2O_2. (d) HIF-1α in tumor tissues following the indicated treatment. (e) Tumor growth curves following therapy. Reproduced with permission.[446] Copyright, 2019, Wiley-VCH.

For example, it is well established that PDT induces the expression of SOD-2 in breast cancer cells, resulting in a decrease in intracellular ROS levels. Inhibition of the SOD-2 activity with 2-methoxyestradiol enhances the cytotoxicity of PDT to breast cancer cells.[34] A combination of the photosensitizer with the SOD inhibitor also sensitized lung adenocarcinoma cells to PDT.[35] Besides, inhibition of catalase also effectively enhanced the tumor inhibitory effect of PDT.[272]

GSH is also enriched in cancer cells and participates in resistance to PDT through the consumption of ROS. Fan *et al.* prepared a Ce6–MnO_2 nanosystem to enhance PDT efficiency. When taken up by cancer cells, the reduction of MnO_2 nanosheets by GSH resulted in a decrease in intracellular GSH levels and the release of Ce6 to produce ROS. Enhanced tumor inhibition was achieved with this nanosystem.[455] Zhang *et al.* prepared a Cu^{2+}-metalated nano-MOF to overcome GSH-mediated PDT resistance. When taken up by breast cancer cells, direct adsorption of GSH by this MOF-2 effectively decreased GSH levels in cells, resulting in increased ROS levels and cancer cell apoptosis following light stimulation.[456] Deng *et al.* prepared a GSH-sensitive nitric oxide (NO) nanogenerator through the conjugation of *S*-nitrosothiol, α-cyclodextrin, Ce6, and PEG

for efficient PDT. The reaction of GSH with this nanoagent led to the depletion of intracellular GSH and NO production. Blood vessel relaxation by NO resolved hypoxia of tumor tissues. Furthermore, the reaction between NO and ROS resulted in the production of reactive nitrogen species, which was more efficient in the induction of tumor cell death. Enhanced tumor inhibition was observed with these multifunctional nanoagents.[457]

6.4. Inhibition of damage repair

As mentioned earlier, the cytotoxic effect of PDT relies on ROS-mediated damage to proteins, nucleic acids, and phospholipids in cancer cells.[347] However, cancer cells might also repair the damage caused by ROS through various mechanisms, leading to resistance to PDT. The inhibition of these processes might also enhance the therapeutic efficacy of PDT.

For example, heat shock protein family members (including Hsp27, Hsp70, and Hsp90) are deeply involved in cellular protein homeostasis. Therefore, they also play critical roles in PDT-induced cellular events.[36,37,458] ROS-induced damage to protein conformation and function is an integral part of cytotoxicity. As molecular chaperones, heat shock proteins promote the conformation recovery of proteins and remove misfolded proteins. Also, heat shock proteins antagonize the cytotoxicity of PDT to cancer cells through the regulation of anti-apoptotic pathways, autophagy, angiogenesis, and immune responses. Accordingly, the inhibition of the heat shock protein activity enhances the anti-tumor efficacy of PDT.[36,37,458,459] Lin *et al.* prepared a porphyrin-based nanoplatform for the tumor-specific delivery of the Hsp90 inhibitor 17AAG. When irradiated with NIR light, both heat and ROS could be generated for dual-modal PTT/PDT. Meanwhile, the inhibition of Hsp90 by 17AAG sensitized the tumor cells to the therapy, resulting in enhanced therapeutic efficacy.[459]

ROS produced in PDT also damages nucleic acids through oxidation, resulting in mispairing and mutation of DNA and apoptosis of cells.[76,77] However, enzymes, such as MTH1, are used by cancer cells to repair this damage. MTH1 is involved in the hydrolyzation of oxidized nucleotides, contributing to resistance to ROS-induced damage in PDT. Fan *et al.* prepared a nanosystem for enhanced PDT efficacy through the down-regulation of MTH1. In this nanosystem, both Ce6 and siRNA-targeting MTH1 were loaded onto mesoporous silica nanoparticles. When irradiated with light, ROS was produced by Ce6 for PDT. Meanwhile, the expression of MTH1 was effectively down-regulated by siRNA released from the nanoparticles. The sensitivity of cancer cells to ROS increased, leading to enhanced tumor inhibition.[38]

6.5. Inhibition of pro-survival signaling pathways

PDT inhibits tumors through the induction of apoptosis, necrosis, or autophagic cell death. However, pro-survival signaling pathways, such as HIF-1, nuclear factor E2-related factor 2 (NRF2), and nuclear factor κB (NF-κB), might also be activated to help cancer cells adjust their internal physiological activities for the survival of cancer cells.[460] Inhibition of these pro-survival signaling pathways can effectively promote the therapeutic efficacy of PDT.

For instance, Bcl-2 is a pro-survival protein activated by several signaling pathways to inhibit the apoptosis induced by various stimuli. The overexpression of Bcl-2 protein in various tumors contributes to tumor cell survival and resistance to tumor therapies, including PDT.[461] Liu *et al.* prepared a novel pH-sensitive upconversion nano-photosensitizer containing ZnPc and the Bcl-2 inhibitor ABT737 to overcome tumor resistance to PDT through Bcl-2. When this nanosystem was taken up by tumor cells and bonded to lysosomes, the acidic conditions triggered the release of ABT737. Inhibition of the Bcl-2-mediated pro-survival pathway sensitized tumor cells to ROS-induced apoptosis, resulting in enhanced therapeutic efficacy both *in vitro* and *in vivo*.[39]

In summary, several physiological processes participate in tumor resistance to PDT. The tumor inhibition efficiency of PDT can be effectively improved through the modulation of these processes. Considering the diverse mechanisms involved in tumor resistance to PDT, it will be important to determine which process contributes the most to PDT resistance of a certain type of tumor. It will be beneficial to examine the gene expression profile (expression of transporters, antioxidant enzymes, pro-survival proteins, heat shock proteins, *etc.*) and microenvironment (oxygen and GSH levels, blood supply, status of immune cells, *etc.*) of the tumor before designing photosensitizer formulation and therapeutic strategy. Therefore, the combination of PDT with precision medicine will be promising in the future.

7. Photosensitizers and strategies to reduce PDT induced severe pain

A relatively less concerned but essential question in PDT research is pain management during the therapy. Treatment-associated pain limits the widespread application of PDT as a clinically approved therapy for superficial malignancies. Clinical trials indicate that PDT is significantly more likely to result in severe pain than surgery.[50] The pain experienced by patients sometimes is severe and unbearable during PDT treatment, which causes the interruption or termination of the PDT process.[51,52] Several strategies have been implemented to reduce PDT-associated severe pain, such as nerve block, cold analgesia, and subcutaneous infiltration anesthesia (Fig. 21).[51]

Meanwhile, it has been reported that the choice of photosensitizers and light sources might determine the pain scores of PDT.[462] For example, ALA, as a precursor of porphyrin approved for the treatment of actinic keratosis and basal cell carcinoma, leads to more pain than methyl aminolevulinate.[463] PDT with sunlight leads to less pain than traditional light sources.[464] A TiO_2–nanoparticle–gold–nanocluster–graphene heterogeneous nanocomposite was prepared to improve the sunlight efficacy in PDT. The efficient use of simulated sunlight was achieved with this nanocomposite. The production of intracellular ROS, depletion of GSH, dysfunction of

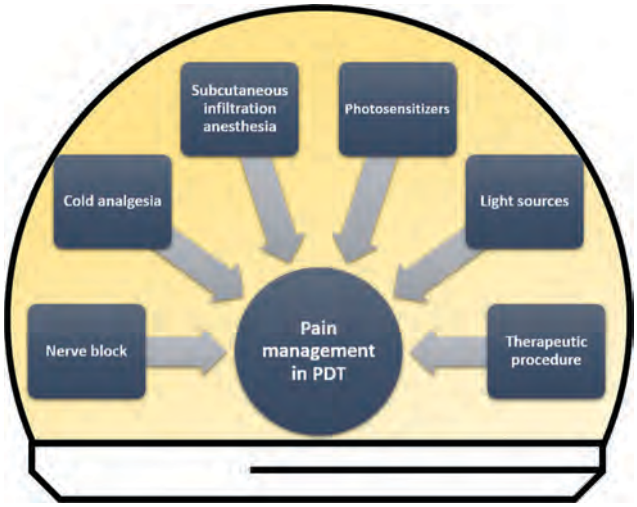

Fig. 21 Strategies to reduce PDT induced severe pain.

mitochondria, and efficient cancer cell killing were observed in melanoma cells. Both intravenous and intra-tumoral administration of the nanocomposite led to the proper inhibition of tumor growth following PDT with simulated sunlight.[465] Low-irradiance PDT using a portable inorganic light-emitting diode also resulted in less pain with comparative 1-year clearance rates for treating non-melanoma skin cancer compared with conventional PDT in clinical trials.[466]

Therapeutic procedure optimization is also useful in relieving PDT-associated pain. A two-step irradiation scheme was investigated in patients with superficial basal cell carcinomas for the effect of PDT with ALA as the photosensitizer. The tumors were first irradiated with low irradiation until 90% of the PpIX was photo-bleached and then with high-intensity irradiation until the prescribed fluence was delivered. No severe pain was reported with this procedure. More importantly, a similar therapeutic effect was achieved compared with traditional continuous treatment.[467] Further research confirmed the effect of this PDT protocol in minimizing pain and maintaining excellent clinical outcomes in superficial lesions.[468] Reduced side effects were also observed in low fluence rate PDT of bladder tumor without hampering the therapeutic efficacy.[469]

Nevertheless, further investigations for pain management in PDT are still required, especially for nanomaterial-based therapeutic strategies. In fact, more detailed investigations of PDT associated pain management are carried out with traditional photosensitizers. However, the physicochemical properties, ROS generation, *in vivo* distribution, and pharmacokinetics of nanophotosensitizers are quite different from those of traditional photosensitizers. Therefore, it is probable that different pain management strategies are required for PDT with nanophotosensitizers. Meanwhile, PDT with high fluence rates promote the necrosis of cancer cells, while low fluence rates induce apoptotic cell death.[469] It is essential to clarify whether and how PDT-induced anti-tumor immunity is affected by pain management strategies, considering the impact of cancer cell death pathways on PDT-induced long-term anti-tumor immunity.

8. Discussion and perspectives

In summary, various strategies have been developed to overcome the barriers in the clinical application of PDT in tumor treatment. Most of the aforementioned strategies are based on nanomaterials. Recent developments in nanomaterial-based PDT platforms largely broaden the choice of photosensitizers and strategies for precise targeting and theranostics of tumors. Nanomaterials are ideal carriers for efficient loading and targeted delivery of traditional photosensitizers. Some nanomaterials can also function as photosensitizers to catalyze the production of ROS following light stimulation. Significantly, nanomaterials are ideal building blocks for the construction of multifunctional nanocomposites through conjugation with various polymers, targeting ligands, small molecule drugs, other nanoparticles, siRNA, proteins, *etc.* The physical, chemical, and biochemical properties of the resulting nanocomposite photosensitizers are therefore highly programmable, making it possible to modulate physiological processes both in tumors and in the human body to optimize PDT efficiency. Various barriers in the clinical application of PDT can be overcome using these novel photosensitizers and therapy strategies. For example, the application of photosensitizers and corresponding light sources with better tissue penetrability effectively overcomes the limitations caused by tissue depth. Inspired by the mechanisms involved in PDT induced anti-tumor pathways, nanocomposite photosensitizers have been designed to modulate these processes to maximize the tumor inhibition efficiency of PDT. Meanwhile, various processes participate in tumor resistance to PDT. Knowledge about these events inspires the design of novel nanocomposites to relieve tumor resistance to PDT to enhance tumor control efficacy. Development of novel photosensitizers and optimization of the therapy procedures may also reduce the severe pain induced by PDT. All these efforts will pave the way for the clinical application of PDT. Nevertheless, several aspects should be further investigated in future research to promote the clinical application of these photosensitizers and therapeutic strategies in PDT.

Targeted delivery of nanomaterials into tumor tissues is critical for achieving more favorable therapeutic outcomes with lower side effects. Both passive and active targeting strategies have been applied for tumor-specific delivery of nanomaterials in PDT. Passive tumor targeting of nanomaterials relies on the EPR effect, which has been widely applied in nanomedicine research in rodent tumor models.[470] However, several recent investigations argue that the EPR effect might not work well in humans.[88,471] Therefore, it is vitally important to develop more reliable and efficient tumor targeting strategies for clinical research into nanomaterial-based PDT. A series of active tumor targeting strategies have been developed.[472] Tumor cell-specific surface markers are widely used for precise targeting of nanomaterials into tumor tissues. Moieties recognizing tumor cell-specific surface markers enable precise tumor targeting and treatment.[471] Antibodies are also excellent for surface modification of nanomaterials to enhance tumor-targeting efficacy.[260,261,473] The recent development of single-domain

antibodies, which have a smaller size and higher specificity, provides new tools for the tumor-specific delivery of nanomaterials.[474] Aptamers, oligonucleotides specifically binding to certain target molecules, are also widely investigated for functionalization and tumor-specific targeting of nanomaterials for PDT. Targeted delivery of various nanomaterials, such as gold NRs,[475] fullerenes,[476] MoS_2 nanoplates,[477] silica nanocomposites,[478] NMOF,[479] and UCNPs[262] with tumor-specific aptamers, has been successfully applied in the PDT of several types of cancer. With extremely high diversity, antibodies and aptamers render it possible to target numerous cell surface markers simultaneously, making the discovery and validation of novel markers more urgent for different cancer types and cancer cell subtypes. Development of models that can more effectively simulate the gene expression profile, microenvironment and anatomical structure of tumors in patients is also desired for investigation of the tumor targeting efficiency of these photosensitizers.

The tumor microenvironment has significant impacts on the efficacy of tumor therapeutic strategies, including PDT. First, it provides a powerful tool for targeted delivery and controlled release of nanomaterials, photosensitizers, imaging agents, and drugs into tumors. Compared to normal tissues, lower levels of pH and oxygen and higher levels of GSH, H_2O_2, and metabolites are found in tumor tissues.[480] Nanocomposites responsive to acids,[481–483] H_2O_2,[480] hypoxia,[484–486] and GSH[487–490] have been designed to enhance the tumor-targeting ability and therapeutic efficiency of PDT using these characteristics. Imaging agents accumulated in tumors in response to the tumor microenvironment also enable more effective tumor theranostics combined with PDT.[491,492] Second, modulation of the tumor microenvironment might enhance the cytotoxicity of PDT to cancer cells. For example, the conversion of H_2O_2 into oxygen and water with certain catalysts relieves hypoxia-mediated inhibition to ROS production in type II PDT.[493] Depletion of GSH can also protect the ROS produced in PDT for more efficient tumor inhibition.[494] Third, the modulation of the tumor microenvironment also relieves the resistance of the tumor to chemotherapy and immunotherapy.[495] For example, the hypoxic microenvironment is essential for drug resistance and immune-suppression of tumors. Replenishment of oxygen in tumor tissues down-regulated the expression of HIF-1α and P-gp and sensitized the tumor to DOX-mediated chemotherapy, enabling efficient combined PDT/chemotherapy.[496] Therefore, the development of novel strategies to construct tumor microenvironment-responsive nanocomposites for imaging-guided PDT and combined therapy will mostly promote the specificity, efficiency, and safety of the tumor treatment.

Another critical issue that should be considered is the retention of nanomaterials by normal tissues and organs, especially the liver. This process primarily affects the circulation of nanoparticles in the bloodstream and diminishes the accumulation of nanomaterials and co-delivered photosensitizers in the tumor. It might also result in increased toxicity and side effects to normal tissues. However, the details of this process are yet to be fully elucidated. Recently, Jiang *et al.* investigated the GSH-mediated biotransformation of nanomaterials in the liver using a well-designed thiol-activatable ICG-GS-Au25 fluorescent nanoprobe. The results indicated that the high local concentrations of GSH and cysteine in the liver sinusoids transformed the surface chemistry of nanoparticles, resulting in decreased affinity to serum proteins, and dramatically changed blood retention, tumor targeting, and renal excretion.[42] The mononuclear phagocyte system is also crucial for the processing of nanoparticles *in vivo*.[497,498] Further investigation of the mechanisms involved in the uptake and processing of nanomaterials by normal tissues and tumors might also inspire the design of nanocomposites for enhanced tumor targeting efficacy and reduced side effects.

The biocompatibility of nanomaterials is also extremely important for their clinical application. However, current research on the biocompatibility of nanomaterials is mostly incomplete. The absence of standardized procedures for the study of *in vivo* bio-distribution, pharmacokinetics, and short-term and long-term impacts on the body of nanomaterials is considered the major bottleneck for the clinical translation of these agents.[54] Generally, organic nanomaterials, such as liposomes, micelles, and dendrimers, are more biocompatible and easily degraded or eliminated from the body. Noble metal-based nanomaterials, such as gold and silver nanoparticles, also exhibit favorable biocompatibility in cell culture.[499] However, their excellent stability *in vitro* and *in vivo* gives rise to long-term impacts on cells and the human body. Concentration-dependent cytotoxicity and induction of apoptosis of gold nanoparticles were also observed.[500] Besides, gold nanoparticles entered the nucleus of cells upon exposure for 24 h.[501] Meanwhile, silver nanoparticles have been shown to affect the embryonic development of zebrafish embryos in long-term treatment.[502] Therefore, the effects of long-term treatment of highly stable nanomaterials, such as noble metal nanoparticles, on DNA replication, cell division, and embryonic development should be investigated further. Besides, several nanomaterials used in PDT contain heavy metal ions, the dosage and potential side effects of which should also be noticed. Although generally considered biocompatible, carbon-based nanoparticles were also found to cause complex impacts on cells and embryos in certain conditions.[503–505] It is quite important to achieve a balance between the therapeutic efficacy and the potential risks for each case in the clinical practice. Therefore, more information about the uptake, circulation, retention, degradation, and elimination of nanomaterials, both *in vitro* and *in vivo*, is required to promote the clinical application of nanomaterial-based PDT in cancer treatment.

It is now widely recognized that a combination of PDT with other therapies is a favorable cancer treatment strategy considering the unique advantages and apparent limitations of PDT. Several critical drawbacks of PDT, such as limited penetration depth and dependence of oxygen, can be partially or largely overcome through combined therapy. As mentioned above, a combination of PDT with ionizing radiation significantly improves the tissue penetration of PDT.[506] Mild PTT was

also used to improve O_2 supply in hypoxic tumor tissues for enhanced PDT efficacy.[442] More interestingly, PDT-induced anti-tumor immunity makes it promising to combine PDT with tumor immunotherapy for long-term control of tumors *in situ* and metastasis.[418] Knowledge about the anti-tumor mechanisms of PDT and the responses of normal and tumor tissues to PDT is essential for the design of novel combined therapy strategies. Therefore, further investigations of these processes, especially the complicated interaction between PDT and the immune system, are still desired.

Conflicts of interest

There are no conflicts to declare.

Acknowledgements

This work was supported by the State Key Research Development Program of China (Grant No. 2019YFB2203503), the National Natural Science Fund (Grant No. 61875138, 61961136001, and U1801254), the Science and Technology Innovation Commission of Shenzhen (KQTD20150324162703 85, JCYJ20170811093453105, JCYJ20180307164612205, GJHZ20180928160209731 and KQJSCX20180321164801762), the Innovation Team Project of the Department of Education of Guangdong Province (No. 2018KCXTD026), the Science and Technology Innovation Leading Talents Program of Guangdong Province (No. 2019TX05C343), the College Teacher Characteristic Innovation Research Project of Foshan (No. 2020SWYY01), and the CRI Project (No. 2018R1A3B1052702, JSK) of the National Research Foundation of Korea. The authors also acknowledge the support from the Instrumental Analysis Center of Shenzhen University (Xili Campus).

References

1 K. Deng, C. Li, S. Huang, B. Xing, D. Jin, Q. Zeng, Z. Hou and J. Lin, *Small*, 2017, **13**, 1702299, DOI: 10.1002/smll.201702299.
2 R. Vankayala and K. C. Hwang, *Adv. Mater.*, 2018, **30**, e1706320, DOI: 10.1002/adma.201706320.
3 Z. Q. Meng, X. F. Zhou, J. Xu, X. Han, Z. L. Dong, H. R. Wang, Y. J. Zhang, J. L. She, L. G. Xu, C. Wang and Z. Liu, *Adv. Mater.*, 2019, **31**, 12, DOI: 10.1002/adma.201900927.
4 A. Gao, B. F. Chen, J. Gao, F. Q. Zhou, M. Saeed, B. Hou, Y. P. Li and H. J. Yu, *Nano Lett.*, 2020, **20**, 353–362, DOI: 10.1021/acs.nanolett.9b04012.
5 Z. L. Zeng, C. Zhang, J. C. Li, D. Cui, Y. Y. Jiang and K. Y. Pu, *Adv. Mater.*, 2021, **33**, 9, DOI: 10.1002/adma.202007247.
6 H. Stepp and R. Waidelich, *Aktuelle Urol.*, 2007, **38**, 455–464, DOI: 10.1055/s-2007-980149.
7 D. Jocham, H. Stepp and R. Waidelich, *Eur. Urol.*, 2008, **53**, 1138–1150, DOI: 10.1016/j.eururo.2007.11.048.
8 G. Bozzini, P. Colin, N. Betrouni, P. Nevoux, A. Ouzzane, P. Puech, A. Villers and S. Mordon, *Photodiagn. Photodyn. Ther.*, 2012, **9**, 261–273, DOI: 10.1016/j.pdpdt.2012.01.005.
9 J. Garcia-Zuazaga, K. D. Cooper and E. D. Baron, *Expert Rev. Anticancer Ther.*, 2005, **5**, 791–800, DOI: 10.1586/14737140.5.5.791.
10 A. Sieron, A. Kawczyk-Krupka, M. Adamek, W. Cebula, W. Zieleznik, K. Niepsuj, G. Niepsuj, A. Pietrusa, M. Szygula, T. Biniszkiewicz, S. Mazur, J. Malyszek, A. Romanczyk, A. Ledwon, A. Frankiewicz, A. Zybura, E. Koczy and B. Birkner, *Photodiagn. Photodyn. Ther.*, 2006, **3**, 132–133, DOI: 10.1016/j.pdpdt.2006.03.009.
11 S. Karrer, R. M. Szeimies, W. G. Philipp-Dormston, P. A. Gerber, W. Prager, E. Datz, F. Zeman, K. Muller and M. Koller, *Acta Derm.-Venereol.*, 2021, **101**, 9, DOI: 10.2340/00015555-3717.
12 P. Rundle, *Biomedicines*, 2017, **5**, 7, DOI: 10.3390/biomedicines5040069.
13 H. Chen, J. Yang, L. Sun, H. R. Zhang, Y. S. Guo, J. Qu, W. Y. Jiang, W. Chen, J. Ji, Y. W. Yang and B. L. Wang, *Small*, 2019, **15**, 13, DOI: 10.1002/smll.201903880.
14 Y. Ye, J. He, Y. Qiao, Y. C. Qi, H. B. Zhang, H. A. Santos, D. N. Zhong, W. L. Li, S. Y. Hua, W. Wang, A. Grzybowski, K. Yao and M. Zhou, *Theranostics*, 2020, **10**, 8541–8557, DOI: 10.7150/thno.46895.
15 T. Kimura, S. Takatsuki, S. Miyoshi, M. Takahashi, E. Ogawa, Y. Katsumata, T. Nishiyama, N. Nishiyama, Y. Tanimoto, Y. Aizawa, T. Arai and K. Fukuda, *EP Europace*, 2015, **17**, 1309–1315, DOI: 10.1093/europace/euu335.
16 T. Kimura, S. Takatsuki, S. Miyoshi, M. Takahashi, E. Ogawa, K. Nakajima, S. Kashimura, Y. Katsumata, T. Nishiyama, N. Nishiyama, Y. Tanimoto, Y. Aizawa, T. Arai and K. Fukuda, *EP Europace*, 2016, **18**, 294–300, DOI: 10.1093/europace/euv016.
17 T. Kimura, S. Takatsuki, S. Miyoshi, K. Fukumoto, M. Takahashi, E. Ogawa, A. Ito, T. Arai, S. Ogawa and K. Fukuda, *Circ.: Arrhythmia Electrophysiol.*, 2013, **6**, 1025–1031, DOI: 10.1161/circep.113.000810.
18 K. Wang, B. X. Yu and J. L. Pathak, *J. Cancer*, 2021, **12**, 1154–1160, DOI: 10.7150/jca.51537.
19 L. D. Dias and V. S. Bagnato, *Laser Phys. Lett.*, 2020, **17**, 9, DOI: 10.1088/1612-202X/ab95a9.
20 V. A. Svyatchenko, S. D. Nikonov, A. P. Mayorov, M. L. Gelfond and V. B. Loktev, *Photodiagn. Photodyn. Ther.*, 2021, **33**, 5, DOI: 10.1016/j.pdpdt.2020.102112.
21 H. Gursoy, C. Ozcakir-Tomruk, J. Tanalp and S. Yilmaz, *Clin. Oral Invest.*, 2013, **17**, 1113–1125, DOI: 10.1007/s00784-012-0845-7.
22 F. Javed and G. E. Romanos, *Photomed. Laser Surg.*, 2013, **31**, 512–518, DOI: 10.1089/pho.2012.3329.
23 S. M. Lashkari, H. Kariminezhad, H. Amani, P. Mataji and M. Rahimnejad, *Photodiagn. Photodyn. Ther.*, 2019, **25**, 336–343, DOI: 10.1016/j.pdpdt.2019.01.021.
24 W. J. Magner and T. B. Tomasi, *Mol. Immunol.*, 2005, **42**, 1033–1042, DOI: 10.1016/j.molimm.2004.09.030.
25 M. Sivasubramanian, Y. C. Chuang and L. W. Lo, *Molecules*, 2019, **24**, 520, DOI: 10.3390/molecules24030520.

26 U. Schmidt-Erfurth, U. Schlotzer-Schrehard, C. Cursiefen, S. Michels, A. Beckendorf and G. O. H. Naumann, *Invest. Ophthalmol. Visual Sci.*, 2003, **44**, 4473–4480, DOI: 10.1167/iovs.02-1115.
27 V. H. Fingar, *J. Clin. Laser Med. Surg.*, 1996, **14**, 323–328, DOI: 10.1089/clm.1996.14.323.
28 K. Plaetzer, T. Kiesslich, C. B. Oberdanner and B. Krammer, *Curr. Pharm. Des.*, 2005, **11**, 1151–1165, DOI: 10.2174/1381612053507648.
29 D. Kessel, M. G. H. Vicente and J. J. Reiners, Jr., *Lasers Surg. Med.*, 2006, **38**, 482–488, DOI: 10.1002/lsm.20334.
30 E. Buytaert, M. Dewaele and P. Agostinis, *Biochim. Biophys. Acta*, 2007, **1776**, 86–107, DOI: 10.1016/j.bbcan.2007.07.001.
31 Y. J. Hsieh, C. C. Wu, C. J. Chang and J. S. Yu, *J. Cell. Physiol.*, 2003, **194**, 363–375, DOI: 10.1002/jcp.10273.
32 D. Kessel and N. L. Oleinick, *Methods Enzymol.*, 2009, **453**, 1–16, DOI: 10.1016/S0076-6879(08)04001-9.
33 A. P. Castano, P. Mroz and M. R. Hamblin, *Nat. Rev. Cancer*, 2006, **6**, 535–545, DOI: 10.1038/nrc1894.
34 P. Kimakova, P. Solar, B. Feckova, V. Sackova, Z. Solarova, L. Ilkovicova and M. Kello, *Biomed. Pharmacother.*, 2017, **85**, 749–755, DOI: 10.1016/j.biopha.2016.11.093.
35 H. T. Soares, J. R. Campos, L. C. Gomes-da-Silva, F. A. Schaberle, J. M. Dabrowski and L. G. Arnaut, *ChemBioChem*, 2016, **17**, 836–842, DOI: 10.1002/cbic.201500573.
36 M. E. Rodriguez, I. S. Cogno, L. S. Milla Sanabria, Y. S. Moran and V. A. Rivarola, *Photochem. Photobiol. Sci.*, 2016, **15**, 1090–1102, DOI: 10.1039/c6pp00097e.
37 D. Helbig, J. C. Simon and U. Paasch, *Int. J. Hyperthermia*, 2011, **27**, 802–810, DOI: 10.3109/02656736.2011.569966.
38 H. Fan, L. Zhang, X. Hu, Z. Zhao, H. Bai, X. Fu, G. Yan, L.-H. Liang, X.-B. Zhang and W. Tan, *Chem. Commun.*, 2018, **54**, 4310–4313, DOI: 10.1039/c8cc01841c.
39 X. Liu, Z. Fan, L. Zhang, Z. Jin, D. Yan, Y. Zhang, X. Li, L. Tu, B. Xue, Y. Chang, H. Zhang and X. Kong, *Biomaterials*, 2017, **144**, 73–83, DOI: 10.1016/j.biomaterials.2017.08.010.
40 R. W. Robey, K. Steadman, O. Polgar and S. E. Bates, *Cancer Biol. Ther.*, 2005, **4**, 187–194, DOI: 10.4161/cbt.4.2.1440.
41 Z. Huang, Y.-C. Hsu, L.-B. Li, L.-W. Wang, X.-D. Song, C. M. N. Yow, X. Lei, A. I. Musani, R.-C. Luo and B. J. Day, *J. Innovative Opt. Health Sci.*, 2015, **8**, 1530002, DOI: 10.1142/s1793545815300025.
42 X. Jiang, B. Du and J. Zheng, *Nat. Nanotechnol.*, 2019, **14**, 874–882, DOI: 10.1038/s41565-019-0499-6.
43 X. Zhang, X. Chen, Y. Guo, H.-R. Jia, Y.-W. Jiang and F.-G. Wu, *Nanoscale Horiz.*, 2020, **5**, 481–487, DOI: 10.1039/c9nh00643e.
44 D. Nowis, T. Stoklosa, M. Legat, T. Issat, M. Jakobisiak and J. Golab, *Photodiagn. Photodyn. Ther.*, 2005, **2**, 283–298, DOI: 10.1016/s1572-1000(05)00098-0.
45 J. Liu, P. Du, H. Mao, L. Zhang, H. Ju and J. Lei, *Biomaterials*, 2018, **172**, 83–91, DOI: 10.1016/j.biomaterials.2018.04.051.
46 J. Dang, H. He, D. Chen and L. Yin, *Biomater. Sci.*, 2017, **5**, 1500–1511, DOI: 10.1039/c7bm00392g.
47 H. R. Wang, Y. F. Guo, C. Wang, X. Jiang, H. H. Liu, A. Yuan, J. Yan, Y. Q. Hu and J. H. Wu, *Biomaterials*, 2021, **269**, 13, DOI: 10.1016/j.biomaterials.2020.120621.
48 T. Su, F. R. Cheng, Y. J. Pu, J. Cao, S. B. Lin, G. Z. Zhu and B. He, *Chem. Eng. J.*, 2021, **411**, 12, DOI: 10.1016/j.cej.2021.128561.
49 H. Wang, J. Li, Z. W. Wang, Y. Q. Wang, X. X. Xu, X. Gong, J. Y. Wang, Z. W. Zhang and Y. P. Li, *Biomaterials*, 2021, **269**, 15, DOI: 10.1016/j.biomaterials.2020.120609.
50 A. J. Dixon, S. J. Anderson, M. P. Dixon and J. B. Dixon, *J. Plast. Reconstr. Aesthet. Surg.*, 2015, **68**, e28–e32, DOI: 10.1016/j.bjps.2013.02.002.
51 C. Fink, A. Enk and P. Gholam, *J. Dtsch. Dermatol. Ges.*, 2015, **13**, 15–22, DOI: 10.1111/ddg.12546.
52 A. Kasche, S. Luderschmidt, J. Ring and R. Hein, *J. Drugs Dermatol.*, 2006, **5**, 353–356.
53 U. Chilakamarthi and L. Giribabu, *Chem. Rec.*, 2017, **17**, 775–802, DOI: 10.1002/tcr.201600121.
54 S. S. Lucky, K. C. Soo and Y. Zhang, *Chem. Rev.*, 2015, **115**, 1990–2042, DOI: 10.1021/cr5004198.
55 W. Fan, P. Huang and X. Chen, *Chem. Soc. Rev.*, 2016, **45**, 6488–6519, DOI: 10.1039/c6cs00616g.
56 Y. Shen, A. J. Shuhendler, D. Ye, J. J. Xu and H. Y. Chen, *Chem. Soc. Rev.*, 2016, **45**, 6725–6741, DOI: 10.1039/c6cs00442c.
57 Q. Guan, Y. A. Li, W. Y. Li and Y. B. Dong, *Chem. – Asian J.*, 2018, **13**, 3122–3149, DOI: 10.1002/asia.201801221.
58 S. Wang, Z. Y. Liu, Y. Tong, Y. Q. Zhai, X. J. Zhao, X. M. Yue, Y. Q. Qiao, Y. H. Liu, Y. M. Yin, R. M. Xi, W. Zhao and M. Meng, *J. Controlled Release*, 2021, **330**, 483–492, DOI: 10.1016/j.jconrel.2020.12.048.
59 P. Garcia Calavia, G. Bruce, L. Perez-Garcia and D. A. Russell, *Photochem. Photobiol. Sci.*, 2018, **17**, 1534–1552, DOI: 10.1039/c8pp00271a.
60 A. Bucharskaya, G. Maslyakova, G. Terentyuk, A. Yakunin, Y. Avetisyan, O. Bibikova, E. Tuchina, B. Khlebtsov, N. Khlebtsov and V. Tuchin, *Int. J. Mol. Sci.*, 2016, **17**, 1295, DOI: 10.3390/ijms17081295.
61 H. Wang, X. Yang, W. Shao, S. Chen, J. Xie, X. Zhang, J. Wang and Y. Xie, *J. Am. Chem. Soc.*, 2015, **137**, 11376–11382, DOI: 10.1021/jacs.5b06025.
62 Z. H. Zhou, J. Zhao, Z. H. Di, B. Liu, Z. H. Li, X. M. Wu and L. L. Li, *Nanoscale*, 2021, **13**, 131–137, DOI: 10.1039/d0nr07681c.
63 X. Q. Yi, J. J. Hu, J. Dai, X. D. Lou, Z. J. Zhao, F. Xia and B. Tang, *ACS Nano*, 2021, **15**, 3026–3037, DOI: 10.1021/acsnano.0c09407.
64 P. Kalluru, R. Vankayala, C. S. Chiang and K. C. Hwang, *Biomaterials*, 2016, **95**, 1–10, DOI: 10.1016/j.biomaterials.2016.04.006.
65 X. Q. Wang, W. J. Wang, M. Y. Peng and X. Z. Zhang, *Biomaterials*, 2021, **266**, 15, DOI: 10.1016/j.biomaterials.2020.120474.
66 L. Benov, *Med. Princ. Pract.*, 2015, **24**(Suppl 1), 14–28, DOI: 10.1159/000362416.
67 A. W. Girotti, *J. Photochem. Photobiol., B*, 2001, **63**, 103–113, DOI: 10.1016/s1011-1344(01)00207-x.
68 F. Gueraud, M. Atalay, N. Bresgen, A. Cipak, P. M. Eckl, L. Huc, I. Jouanin, W. Siems and K. Uchida, *Free Radical Res.*, 2010, **44**, 1098–1124, DOI: 10.3109/10715762.2010.498477.

69 A. W. Girotti and T. Kriska, *Antioxid. Redox Signaling*, 2004, **6**, 301–310, DOI: 10.1089/152308604322899369.
70 B. Epe, *Photochem. Photobiol. Sci.*, 2012, **11**, 98–106, DOI: 10.1039/c1pp05190c.
71 L. Benov, J. Craik and I. Batinic-Haberle, *Amino Acids*, 2012, **42**, 117–128, DOI: 10.1007/s00726-010-0640-1.
72 M. J. Davies, *Photochem. Photobiol. Sci.*, 2004, **3**, 17–25, DOI: 10.1039/b307576c.
73 J. E. Plowman, S. Deb-Choudhury, A. J. Grosvenor and J. M. Dyer, *Photochem. Photobiol. Sci.*, 2013, **12**, 1960–1967, DOI: 10.1039/c3pp50182e.
74 L. Y. Xue, S. M. Chiu and N. L. Oleinick, *Oncogene*, 2001, **20**, 3420–3427, DOI: 10.1038/sj.onc.1204441.
75 D. I. Pattison, A. S. Rahmanto and M. J. Davies, *Photochem. Photobiol. Sci.*, 2012, **11**, 38–53, DOI: 10.1039/c1pp05164d.
76 S. Rangasamy, H. Ju, S. Um, D. C. Oh and J. M. Song, *J. Med. Chem.*, 2015, **58**, 6864–6874, DOI: 10.1021/acs.jmedchem.5b01095.
77 J. R. Sparrow, J. Zhou and B. Cai, *Invest. Ophthalmol. Visual Sci.*, 2003, **44**, 2245–2251, DOI: 10.1167/iovs.02-0746.
78 A. E. O'Connor, W. M. Gallagher and A. T. Byrne, *Photochem. Photobiol.*, 2009, **85**, 1053–1074, DOI: 10.1111/j.1751-1097.2009.00585.x.
79 C. Chen, J. Wang, X. Li, X. Liu and X. Han, *Comb. Chem. High Throughput Screening*, 2017, **20**, 414–422, DOI: 10.2174/1386207320666170113123132.
80 X. W. Wang, X. Y. Zhong and L. Cheng, *Coord. Chem. Rev.*, 2021, **430**, 29, DOI: 10.1016/j.ccr.2020.213662.
81 R. Vankayala, Y. K. Huang, P. Kalluru, C. S. Chiang and K. C. Hwang, *Small*, 2014, **10**, 1612–1622, DOI: 10.1002/smll.201302719.
82 E. A. Rozhkova, I. Ulasov, B. Lai, N. M. Dimitrijevic, M. S. Lesniak and T. Rajh, *Nano Lett.*, 2009, **9**, 3337–3342, DOI: 10.1021/nl901610f.
83 K. Albert and H. Y. Hsu, *Molecules*, 2016, **21**, 1585, DOI: 10.3390/molecules21111585.
84 K. Lu, C. He and W. Lin, *J. Am. Chem. Soc.*, 2014, **136**, 16712–16715, DOI: 10.1021/ja508679h.
85 R. Tang, L. M. Habimana-Griffin, D. D. Lane, C. Egbulefu and S. Achilefu, *Nanomedicine*, 2017, **12**, 1101–1105, DOI: 10.2217/nnm-2017-0077.
86 D. Peer, J. M. Karp, S. Hong, O. C. Farokhzad, R. Margalit and R. Langer, *Nat. Nanotechnol.*, 2007, **2**, 751–760, DOI: 10.1038/nnano.2007.387.
87 H. Shi, R. Gu, W. Xu, H. Huang, L. Xue, W. Wang, Y. Zhang, W. Si and X. Dong, *ACS Appl. Mater. Interfaces*, 2019, **11**, 44970–44977, DOI: 10.1021/acsami.9b17716.
88 Y. Nakamura, A. Mochida, P. L. Choyke and H. Kobayashi, *Bioconjugate Chem.*, 2016, **27**, 2225–2238, DOI: 10.1021/acs.bioconjchem.6b00437.
89 W. Hu, H. Ma, B. Hou, H. Zhao, Y. Ji, R. Jiang, X. Hu, X. Lu, L. Zhang, Y. Tang, Q. Fan and W. Huang, *ACS Appl. Mater. Interfaces*, 2016, **8**, 12039–12047, DOI: 10.1021/acsami.6b02721.
90 W. S. Kuo, H. H. Chen, S. Y. Chen, C. Y. Chang, P. C. Chen, Y. I. Hou, Y. T. Shao, H. F. Kao, C. L. L. Hsu, Y. C. Chen, S. J. Chen, S. R. Wu and J. Y. Wang, *Biomaterials*, 2017, **120**, 185–194, DOI: 10.1016/j.biomaterials.2016.12.022.
91 C. Wang, X. H. Zhao, H. Y. Jiang, J. X. Wang, W. X. Zhong, K. Xue and C. L. Zhu, *Nanoscale*, 2021, **13**, 1195–1205, DOI: 10.1039/d0nr07342c.
92 Q. Liu, J. W. Tian, Y. Tian, Q. C. Sun, D. Sun, F. F. Wang, H. J. Xu, G. L. Ying, J. G. Wang, A. K. Yetisen and N. Jiang, *ACS Nano*, 2021, **15**, 515–525, DOI: 10.1021/acsnano.0c05317.
93 A. Maleki, H. Kettiger, A. Schoubben, J. M. Rosenholm, V. Ambrogi and M. Hamidi, *J. Controlled Release*, 2017, **262**, 329–347, DOI: 10.1016/j.jconrel.2017.07.047.
94 Z. J. Wang, Y. Y. He, C. G. Huang, J. S. Huang, Y. C. Huang, J. Y. An, Y. Gu and L. J. Jiang, *Photochem. Photobiol.*, 1999, **70**, 773–780, DOI: 10.1562/0031-8655(1999)070<0773:ptdapt>2.3.co;2.
95 S. H. Voon, L. V. Kiew, H. B. Lee, S. H. Lim, M. I. Noordin, A. Kamkaew, K. Burgess and L. Y. Chung, *Small*, 2014, **10**, 4993–5013, DOI: 10.1002/smll.201401416.
96 L. Y. Guo, S. Z. Yan, Q. Li, Q. Xu, X. Lin, S. S. Qi, S. Q. Yu and S. L. Chen, *RSC Adv.*, 2017, **7**, 42073–42082, DOI: 10.1039/c7ra04748g.
97 J. U. Menon, P. Jadeja, P. Tambe, K. Vu, B. Yuan and K. T. Nguyen, *Theranostics*, 2013, **3**, 152–166, DOI: 10.7150/thno.5327.
98 X. L. Wu, H. Yang, X. M. Chen, J. X. Gao, Y. Duan, D. H. Wei, J. C. Zhang, K. Ge, X. J. Liang, Y. Y. Huang, S. Z. Feng, R. L. Zhang, X. Chen and J. Chang, *Biomaterials*, 2021, **269**, 11, DOI: 10.1016/j.biomaterials.2021.120654.
99 L. Yan, A. Amirshaghaghi, D. Huang, J. Miller, J. M. Stein, T. M. Busch, Z. Cheng and A. Tsourkas, *Adv. Funct. Mater.*, 2018, **28**, 1707030, DOI: 10.1002/adfm.201707030.
100 S. R. Xiong, G. S. Xiong, Z. H. Li, Q. Jiang, J. Yin, T. Yin and H. Zheng, *Nanotechnology*, 2021, **32**, 11, DOI: 10.1088/1361-6528/abd816.
101 Y. Wang, Q. Zhao, N. Han, L. Bai, J. Li, J. Liu, E. Che, L. Hu, Q. Zhang, T. Jiang and S. Wang, *Nanomedicine*, 2015, **11**, 313–327, DOI: 10.1016/j.nano.2014.09.014.
102 C. A. McCarthy, R. J. Ahern, R. Dontireddy, K. B. Ryan and A. M. Crean, *Expert Opin. Drug Delivery*, 2016, **13**, 93–108, DOI: 10.1517/17425247.2016.1100165.
103 J. Peng, L. Zhao, X. Zhu, Y. Sun, W. Feng, Y. Gao, L. Wang and F. Li, *Biomaterials*, 2013, **34**, 7905–7912, DOI: 10.1016/j.biomaterials.2013.07.027.
104 S. Bayir, A. Barras, R. Boukherroub, S. Szunerits, L. Raehm, S. Richeter and J. O. Durand, *Photochem. Photobiol. Sci.*, 2018, **17**, 1651–1674, DOI: 10.1039/c8pp00143j.
105 C. Huang, Z. Zhang, Q. Guo, L. Zhang, F. Fan, Y. Qin, H. Wang, S. Zhou, W. Ou-Yang, H. Sun, X. Leng, X. Pang, D. Kong, L. Zhang and D. Zhu, *Adv. Healthcare Mater.*, 2019, **8**, e1900840, DOI: 10.1002/adhm.201900840.
106 S. Rajkumar and M. Prabaharan, *Curr. Top. Med. Chem.*, 2017, **17**, 1858–1871, DOI: 10.2174/1568026617666161122120537.
107 O. Penon, M. J. Marin, D. B. Amabilino, D. A. Russell and L. Perez-Garcia, *J. Colloid Interface Sci.*, 2016, **462**, 154–165, DOI: 10.1016/j.jcis.2015.09.060.

108 Z. Li, C. Wang, L. Cheng, H. Gong, S. Yin, Q. Gong, Y. Li and Z. Liu, *Biomaterials*, 2013, **34**, 9160–9170, DOI: 10.1016/j.biomaterials.2013.08.041.
109 Z. F. Wen, F. Y. Liu, G. X. Liu, Q. Y. Sun, Y. H. Zhang, M. Muhammad, Y. Q. Xu, H. J. Li and S. G. Sun, *J. Colloid Interface Sci.*, 2021, **590**, 290–300, DOI: 10.1016/j.jcis.2021.01.052.
110 Y. Y. Yang, X. Liu, W. Ma, Q. Xu, G. Chen, Y. F. Wang, H. H. Xiao, N. Li, X. J. Liang, M. Yu and Z. Q. Yu, *Biomaterials*, 2021, **265**, 15, DOI: 10.1016/j.biomaterials.2020.120456.
111 C. F. van Nostrum, *Adv. Drug Delivery Rev.*, 2004, **56**, 9–16, DOI: 10.1016/j.addr.2003.07.013.
112 Z. W. Su, Z. C. Xiao, J. S. Huang, Y. Wang, Y. C. An, H. Xiao, Y. Peng, P. F. Pang, S. S. Han, K. S. Zhu and X. T. Shuai, *ACS Appl. Mater. Interfaces*, 2021, **13**, 12845–12856, DOI: 10.1021/acsami.0c20422.
113 H. C. Tsai, C. H. Tsai, S. Y. Lin, C. R. Jhang, Y. S. Chiang and G. H. Hsiue, *Biomaterials*, 2012, **33**, 1827–1837, DOI: 10.1016/j.biomaterials.2011.11.014.
114 R. R. Kudarha and K. K. Sawant, *Mater. Sci. Eng., C*, 2017, **81**, 607–626, DOI: 10.1016/j.msec.2017.08.004.
115 D. Hu, Z. Sheng, G. Gao, F. Siu, C. Liu, Q. Wan, P. Gong, H. Zheng, Y. Ma and L. Cai, *Biomaterials*, 2016, **93**, 10–19, DOI: 10.1016/j.biomaterials.2016.03.037.
116 K. Butzbach, F. A. Rasse-Suriani, M. M. Gonzalez, F. M. Cabrerizo and B. Epe, *Photochem. Photobiol.*, 2016, **92**, 611–619, DOI: 10.1111/php.12602.
117 X. Zhuang, X. Ma, X. Xue, Q. Jiang, L. Song, L. Dai, C. Zhang, S. Jin, K. Yang, B. Ding, P. C. Wang and X. J. Liang, *ACS Nano*, 2016, **10**, 3486–3495, DOI: 10.1021/acsnano.5b07671.
118 K. R. Kim, D. Bang and D. R. Ahn, *Biomater. Sci.*, 2016, **4**, 605–609, DOI: 10.1039/c5bm00467e.
119 X. H. Huang, I. H. El-Sayed, W. Qian and M. A. El-Sayed, *J. Am. Chem. Soc.*, 2006, **128**, 2115–2120, DOI: 10.1021/ja057254a.
120 E. B. Dickerson, E. C. Dreaden, X. H. Huang, I. H. El-Sayed, H. H. Chu, S. Pushpanketh, J. F. McDonald and M. A. El-Sayed, *Cancer Lett.*, 2008, **269**, 57–66, DOI: 10.1016/j.canlet.2008.04.026.
121 L. R. Hirsch, R. J. Stafford, J. A. Bankson, S. R. Sershen, B. Rivera, R. E. Price, J. D. Hazle, N. J. Halas and J. L. West, *Proc. Natl. Acad. Sci. U. S. A.*, 2003, **100**, 13549–13554, DOI: 10.1073/pnas.2232479100.
122 J. Krajczewski, K. Rucinska, H. E. Townley and A. Kudelski, *Photodiagn. Photodyn. Ther.*, 2019, **26**, 162–178, DOI: 10.1016/j.pdpdt.2019.03.016.
123 Y. J. Liu and K. Z. Wang, *Eur. J. Inorg. Chem.*, 2008, 5214–5219, DOI: 10.1002/ejic.200800699.
124 S. K. Bhunia, A. Saha, A. R. Maity, S. C. Ray and N. R. Jana, *Sci. Rep.*, 2013, **3**, 7, DOI: 10.1038/srep01473.
125 A. J. Gormley, N. Larson, S. Sadekar, R. Robinson, A. Ray and H. Ghandehari, *Nano Today*, 2012, **7**, 158–167, DOI: 10.1016/j.nantod.2012.04.002.
126 Z. Krpetic, P. Nativo, V. See, I. A. Prior, M. Brust and M. Volk, *Nano Lett.*, 2010, **10**, 4549–4554, DOI: 10.1021/nl103142t.
127 P. K. Jain, X. H. Huang, I. H. El-Sayed and M. A. El-Sayed, *Acc. Chem. Res.*, 2008, **41**, 1578–1586, DOI: 10.1021/ar7002804.
128 P. Ghosh, G. Han, M. De, C. K. Kim and V. M. Rotello, *Adv. Drug Delivery Rev.*, 2008, **60**, 1307–1315, DOI: 10.1016/j.addr.2008.03.016.
129 T. Zhao, X. Shen, L. Li, Z. Guan, N. Gao, P. Yuan, S. Q. Yao, Q. H. Xu and G. Q. Xu, *Nanoscale*, 2012, **4**, 7712–7719, DOI: 10.1039/c2nr32196c.
130 P. Vijayaraghavan, C.-H. Liu, R. Vankayala, C.-S. Chiang and K. C. Hwang, *Adv. Mater.*, 2014, **26**, 6689–6695, DOI: 10.1002/adma.201400703.
131 R. Vankayala, C.-C. Lin, P. Kalluru, C.-S. Chiang and K. C. Hwang, *Biomaterials*, 2014, **35**, 5527–5538, DOI: 10.1016/j.biomaterials.2014.03.065.
132 J. Lv, X. Zhang, N. Li, B. Wang and S. He, *RSC Adv.*, 2015, **5**, 81897–81904, DOI: 10.1039/c5ra15362j.
133 M. Misawa and J. Takahashi, *Nanomed. Nanotechnol. Biol. Med.*, 2011, **7**, 604–614, DOI: 10.1016/j.nano.2011.01.014.
134 A. El-Hussein, I. Mfouo-Tynga, M. Abdel-Harith and H. Abrahamse, *J. Photochem. Photobiol., B*, 2015, **153**, 67–75, DOI: 10.1016/j.jphotobiol.2015.08.028.
135 A. Fujishima and K. Honda, *Nature*, 1972, **238**, 37–38, DOI: 10.1038/238037a0.
136 S. Yamaguchi, H. Kobayashi, T. Narita, K. Kanehira, S. Sonezaki, Y. Kubota, S. Terasaka and Y. Iwasaki, *Photochem. Photobiol.*, 2010, **86**, 964–971, DOI: 10.1111/j.1751-1097.2010.00742.x.
137 R. X. Cai, Y. Kubota, T. Shuin, H. Sakai, K. Hashimoto and A. Fujishima, *Cancer Res.*, 1992, **52**, 2346–2348, DOI: 10.1007/s11033-010-0136-9.
138 J. Xu, Y. Sun, J. J. Huang, C. M. Chen, G. Y. Liu, Y. Jiang, Y. M. Zhao and Z. Y. Jiang, *Bioelectrochemistry*, 2007, **71**, 217–222, DOI: 10.1016/j.bioelechem.2007.06.001.
139 J. W. Seo, H. Chung, M. Y. Kim, J. Lee, I. H. Choi and J. Cheon, *Small*, 2007, **3**, 850–853, DOI: 10.1002/smll.200600488.
140 A. Ancona, B. Dumontel, N. Garino, B. Demarco, D. Chatzitheodoridou, W. Fazzini, H. Engelke and V. Cauda, *Nanomaterials*, 2018, **8**, 15, DOI: 10.3390/nano8030143.
141 A. Nadhman, S. Nazir, M. I. Khan, S. Arooj, M. Bakhtiar, G. Shahnaz and M. Yasinzai, *Free Radical Biol. Med.*, 2014, **77**, 230–238, DOI: 10.1016/j.freeradbiomed.2014.09.005.
142 C. Constantin, M. Neagu, R. M. Ion, M. Gherghiceanu and C. Stavaru, *Nanomedicine*, 2010, **5**, 307–317, DOI: 10.2217/nnm.09.111.
143 Y. Li, H. Dong, Y. Li and D. Shi, *Int. J. Nanomed.*, 2015, **10**, 2451–2459, DOI: 10.2147/IJN.S68600.
144 J. Ge, M. Lan, B. Zhou, W. Liu, L. Guo, H. Wang, Q. Jia, G. Niu, X. Huang, H. Zhou, X. Meng, P. Wang, C. S. Lee, W. Zhang and X. Han, *Nat. Commun.*, 2014, **5**, 4596, DOI: 10.1038/ncomms5596.
145 H. W. Kroto, J. R. Heath, S. C. Obrien, R. F. Curl and R. E. Smalley, *Nature*, 1985, **318**, 162–163, DOI: 10.1038/318162a0.

146 Y. Y. Huang, S. K. Sharma, R. Yin, T. Agrawal, L. Y. Chiang and M. R. Hamblin, *J. Biomed. Nanotechnol.*, 2014, **10**, 1918–1936, DOI: 10.1166/jbn.2014.1963.
147 Q. Li, C. Huang, L. Liu, R. Hu and J. Qu, *Cytometry, Part A*, 2018, **93**, 997–1003, DOI: 10.1002/cyto.a.23596.
148 H. Zhang, Q. Bao, D. Tang, L. Zhao and K. Loh, *Appl. Phys. Lett.*, 2009, **95**, 141103, DOI: 10.1063/1.3244206.
149 H. Zhang, D. Tang, R. J. Knize, L. Zhao, Q. Bao and K. P. Loh, *Appl. Phys. Lett.*, 2010, **96**, 111112, DOI: 10.1063/1.3367743.
150 H. Zhang, D. Tang, L. Zhao, Q. Bao and K. P. Loh, *Opt. Commun.*, 2010, **283**, 3334–3338, DOI: 10.1016/j.optcom.2010.04.064.
151 H. Zhang, D. Y. Tang, L. M. Zhao, Q. L. Bao, K. P. Loh, B. Lin and S. C. Tjin, *Laser Phys. Lett.*, 2010, **7**, 591–596, DOI: 10.1002/lapl.201010025.
152 J. Zhao, Y. Wang, S. Ruan, P. Yan, H. Zhang, Y. H. Tsang, J. Yang and G. Huang, *J. Opt. Soc. Am. B*, 2014, **31**, 716, DOI: 10.1364/josab.31.000716.
153 W. Huang, C. Xing, Y. Wang, Z. Li, L. Wu, D. Ma, X. Dai, Y. Xiang, J. Li, D. Fan and H. Zhang, *Nanoscale*, 2018, **10**, 2404–2412, DOI: 10.1039/c7nr09046c.
154 Z. Huang, W. Han, H. Tang, L. Ren, D. S. Chander, X. Qi and H. Zhang, *2D Mater.*, 2015, **2**, 035011, DOI: 10.1088/2053-1583/2/3/035011.
155 Y. Wang, H. Mu, X. Li, J. Yuan, J. Chen, S. Xiao, Q. Bao, Y. Gao and J. He, *Appl. Phys. Lett.*, 2016, **108**, 221901, DOI: 10.1063/1.4953072.
156 H. Ding, X. Shu, Y. Jin, T. Fan and H. Zhang, *Nanoscale*, 2019, **11**, 5839–5860, DOI: 10.1039/c8nr09736d.
157 B. Zhang, T. Fan, N. Xie, G. Nie and H. Zhang, *Adv. Sci.*, 2019, **6**, 1901787, DOI: 10.1002/advs.201901787.
158 H. Wang, L. Miao, Y. Jiang, S. Lu, Z. Li, P. Li, C. Zhao, H. Zhang and S. Wen, *Phys. Status Solidi B*, 2015, **252**, 2159–2166, DOI: 10.1002/pssb.201552172.
159 Z. T. Wang, Y. Chen, C. J. Zhao, H. Zhang and S. C. Wen, *IEEE Photonics J.*, 2012, **4**, 869–876, DOI: 10.1109/jphot.2012.2199102.
160 Q. Bao, H. Zhang, B. Wang, Z. Ni, C. H. Y. X. Lim, Y. Wang, D. Y. Tang and K. P. Loh, *Nat. Photonics*, 2011, **5**, 411–415, DOI: 10.1038/nphoton.2011.102.
161 J. Shi, Z. Li, D. K. Sang, Y. Xiang, J. Li, S. Zhang and H. Zhang, *J. Mater. Chem. C*, 2018, **6**, 1291–1306, DOI: 10.1039/c7tc05460b.
162 Y. Song, Z. Liang, H. Zhang, Q. Zhang, L. Zhao, D. Shen and D. Tang, *IEEE Photonics J.*, 2017, **9**, 1–8, DOI: 10.1109/jphot.2017.2734163.
163 Q. Bao, H. Zhang, Y. Wang, Z. Ni, Y. Yan, Z. X. Shen, K. P. Loh and D. Y. Tang, *Adv. Funct. Mater.*, 2009, **19**, 3077–3083, DOI: 10.1002/adfm.200901007.
164 L. Miao, Y. Jiang, S. Lu, B. Shi, C. Zhao, H. Zhang and S. Wen, *Photonics Res.*, 2015, **3**, 214–219, DOI: 10.1364/prj.3.000214.
165 Q. Feng, Y. Chen, C. Zhao, Y. Li, J. Wen and H. Zhang, *Opt. Eng.*, 2013, **52**, 044201, DOI: 10.1117/1.oe.52.4.044201.
166 Y. F. Song, H. Zhang, L. M. Zhao, D. Y. Shen and D. Y. Tang, *Opt. Express*, 2016, **24**, 1814–1822, DOI: 10.1364/OE.24.001814.
167 D. Du, K. Wang, Y. Wen, Y. Li and Y. Y. Li, *ACS Appl. Mater. Interfaces*, 2016, **8**, 3287–3294, DOI: 10.1021/acsami.5b11154.
168 X. Yu, D. Gao, L. Gao, J. Lai, C. Zhang, Y. Zhao, L. Zhong, B. Jia, F. Wang, X. Chen and Z. Liu, *ACS Nano*, 2017, **11**, 10147–10158, DOI: 10.1021/acsnano.7b04736.
169 S. Y. Choi, S. H. Baek, S. J. Chang, Y. Song, R. Rafique, K. T. Lee and T. J. Park, *Biosens. Bioelectron.*, 2017, **93**, 267–273, DOI: 10.1016/j.bios.2016.08.094.
170 W. S. Kuo, H. H. Chen, S. Y. Chen, C. Y. Chang, P. C. Chen, Y. I. Hou, Y. T. Shao, H. F. Kao, C. L. Lilian Hsu, Y. C. Chen, S. J. Chen, S. R. Wu and J. Y. Wang, *Biomaterials*, 2017, **120**, 185–194, DOI: 10.1016/j.biomaterials.2016.12.022.
171 D. Zhang, L. Wen, R. Huang, H. Wang, X. Hu and D. Xing, *Biomaterials*, 2018, **153**, 14–26, DOI: 10.1016/j.biomaterials.2017.10.034.
172 Q. Li, L. Hong, H. Li and C. Liu, *Biosens. Bioelectron.*, 2017, **89**, 477–482, DOI: 10.1016/j.bios.2016.03.072.
173 Z. Hu, C. Wang, F. Zhao, X. Xu, S. Wang, L. Yu, D. Zhang and Y. Huang, *Nanoscale*, 2017, **9**, 8825–8833, DOI: 10.1039/c7nr02922e.
174 H. Mu, S. Lin, Z. Wang, S. Xiao, P. Li, Y. Chen, H. Zhang, H. Bao, S. P. Lau, C. Pan, D. Fan and Q. Bao, *Adv. Opt. Mater.*, 2015, **3**, 1447–1453, DOI: 10.1002/adom.201500336.
175 Z. Chu, J. Liu, Z. Guo and H. Zhang, *Opt. Mater. Express*, 2016, **6**, 2374–2379, DOI: 10.1364/ome.6.002374.
176 Y. Wang, G. Huang, H. Mu, S. Lin, J. Chen, S. Xiao, Q. Bao and J. He, *Appl. Phys. Lett.*, 2015, **107**, 091905, DOI: 10.1063/1.4930077.
177 T. Fan, Z. Xie, W. Huang, Z. Li and H. Zhang, *Nanotechnology*, 2019, **30**, 114002, DOI: 10.1088/1361-6528/aafc0f.
178 W. Huang, Z. Xie, T. Fan, J. Li, Y. Wang, L. Wu, D. Ma, Z. Li, Y. Ge, Z. N. Huang, X. Dai, Y. Xiang, J. Li, X. Zhu and H. Zhang, *J. Mater. Chem. C*, 2018, **6**, 9582–9593, DOI: 10.1039/c8tc03284j.
179 K. Chen, Y. Wang, J. Liu, J. Kang, Y. Ge, W. Huang, Z. Lin, Z. Guo, Y. Zhang and H. Zhang, *Nanoscale*, 2019, **11**, 16852–16859, DOI: 10.1039/c9nr06488e.
180 X. Liang, X. Ye, C. Wang, C. Xing, Q. Miao, Z. Xie, X. Chen, X. Zhang, H. Zhang and L. Mei, *J. Controlled Release*, 2019, **296**, 150–161, DOI: 10.1016/j.jconrel.2019.01.027.
181 J. Shao, H. Xie, H. Huang, Z. Li, Z. Sun, Y. Xu, Q. Xiao, X. F. Yu, Y. Zhao, H. Zhang, H. Wang and P. K. Chu, *Nat. Commun.*, 2016, **7**, 12967, DOI: 10.1038/ncomms12967.
182 W. Chen, J. Ouyang, H. Liu, M. Chen, K. Zeng, J. Sheng, Z. Liu, Y. Han, L. Wang, J. Li, L. Deng, Y. N. Liu and S. Guo, *Adv. Mater.*, 2017, **29**, 1603864, DOI: 10.1002/adma.201603864.
183 Y. Li, Z. Liu, Y. Hou, G. Yang, X. Fei, H. Zhao, Y. Guo, C. Su, Z. Wang, H. Zhong, Z. Zhuang and Z. Guo, *ACS Appl. Mater. Interfaces*, 2017, **9**, 25098–25106, DOI: 10.1021/acsami.7b05824.
184 T. Guo, Y. Wu, Y. Lin, X. Xu, H. Lian, G. Huang, J. Z. Liu, X. Wu and H. H. Yang, *Small*, 2018, **14**, 1702815, DOI: 10.1002/smll.201702815.
185 T. Zhang, Y. Wan, H. Xie, Y. Mu, P. Du, D. Wang, X. Wu, H. Ji and L. Wan, *J. Am. Chem. Soc.*, 2018, **140**, 7561–7567, DOI: 10.1021/jacs.8b02156.

186 T. Ahmed, S. Balendhran, M. N. Karim, E. L. H. Mayes, M. R. Field, R. Ramanathan, M. Singh, V. Bansal, S. Sriram, M. Bhaskaran and S. Walia, *npj 2D Mater. Appl.*, 2017, **1**, 7, DOI: 10.1038/s41699-017-0023-5.

187 Z. J. Li, H. Xu, J. D. Shao, C. Jiang, F. Zhang, J. Lin, H. Zhang, J. Q. Li and P. Huang, *Appl. Mater. Today*, 2019, **15**, 297–304, DOI: 10.1016/j.apmt.2019.02.002.

188 J. Liu, Y. Yang, W. Zhu, X. Yi, Z. Dong, X. Xu, M. Chen, K. Yang, G. Lu, L. Jiang and Z. Liu, *Biomaterials*, 2016, **97**, 1–9, DOI: 10.1016/j.biomaterials.2016.04.034.

189 Y. Wang, W. Wu, J. Liu, P. N. Manghnani, F. Hu, D. Ma, C. Teh, B. Wang and B. Liu, *ACS Nano*, 2019, **13**, 6879–6890, DOI: 10.1021/acsnano.9b01665.

190 J. C. Li, J. H. Rao and K. Y. Pu, *Biomaterials*, 2018, **155**, 217–235, DOI: 10.1016/j.biomaterials.2017.11.025.

191 X. Zhen, K. Y. Pu and X. Q. Jiang, *Small*, 2021, **17**, 22, DOI: 10.1002/smll.202004723.

192 Y. Zhang, S. S. He, W. Chen, Y. H. Liu, X. F. Zhang, Q. Q. Miao and K. Y. Pu, *Angew. Chem., Int. Ed.*, 2021, **60**, 5921–5927, DOI: 10.1002/anie.202015116.

193 J. Y. Sun, Q. Zhang, X. M. Dai, P. H. Ling and F. Gao, *Chem. Commun.*, 2021, **57**, 1989–2004, DOI: 10.1039/d0cc07182j.

194 J. C. Li and K. Y. Pu, *Acc. Chem. Res.*, 2020, **53**, 752–762, DOI: 10.1021/acs.accounts.9b00569.

195 J. C. Li, X. Zhen, Y. Lyu, Y. Y. Jiang, J. G. Huang and K. Y. Pu, *ACS Nano*, 2018, **12**, 8520–8530, DOI: 10.1021/acsnano.8b04066.

196 H. J. Zhu, J. C. Li, X. Y. Qi, P. Chen and K. Y. Pu, *Nano Lett.*, 2018, **18**, 586–594, DOI: 10.1021/acs.nanolett.7b04759.

197 D. Cui, J. G. Huang, X. Zhen, J. C. Li, Y. Y. Jiang and K. Y. Pu, *Angew. Chem., Int. Ed.*, 2019, **58**, 5920–5924, DOI: 10.1002/anie.201814730.

198 Y. Y. Jiang, J. C. Li, Z. L. Zeng, C. Xie, Y. Lyu and K. Y. Pu, *Angew. Chem., Int. Ed.*, 2019, **58**, 8161–8165, DOI: 10.1002/anie.201903968.

199 J. C. Li, J. G. Huang, Y. Lyu, J. S. Huang, Y. Y. Jiang, C. Xie and K. Y. Pu, *J. Am. Chem. Soc.*, 2019, **141**, 4073–4079, DOI: 10.1021/jacs.8b13507.

200 K. S. Novoselov, A. K. Geim, S. V. Morozov, D. Jiang, Y. Zhang, S. V. Dubonos, I. V. Grigorieva and A. A. Firsov, *Science*, 2004, **306**, 666–669, DOI: 10.1126/science.1102896.

201 J. Yang, R. J. Xu, J. J. Pei, Y. W. Myint, F. Wang, Z. Wang, S. Zhang, Z. F. Yu and Y. R. Lu, *Light: Sci. Appl.*, 2015, **4**, 7, DOI: 10.1038/lsa.2015.85.

202 S. Zhang, J. Yang, R. J. Xu, F. Wang, W. F. Li, M. Ghufran, Y. W. Zhang, Z. F. Yu, G. Zhang, Q. H. Qin and Y. R. Lu, *ACS Nano*, 2014, **8**, 9590–9596, DOI: 10.1021/nn503893j.

203 Z. N. Guo, H. Zhang, S. B. Lu, Z. T. Wang, S. Y. Tang, J. D. Shao, Z. B. Sun, H. H. Xie, H. Y. Wang, X. F. Yu and P. K. Chu, *Adv. Funct. Mater.*, 2015, **25**, 6996–7002, DOI: 10.1002/adfm.201502902.

204 J. Kang, S. A. Wells, J. D. Wood, J. H. Lee, X. L. Liu, C. R. Ryder, J. Zhu, J. R. Guest, C. A. Husko and M. C. Hersam, *Proc. Natl. Acad. Sci. U. S. A.*, 2016, **113**, 11688–11693, DOI: 10.1073/pnas.1602215113.

205 A. H. Woomer, T. W. Farnsworth, J. Hu, R. A. Wells, C. L. Donley and S. C. Warren, *ACS Nano*, 2015, **9**, 8869–8884, DOI: 10.1021/acsnano.5b02599.

206 P. Ares, F. Aguilar-Galindo, D. Rodriguez-San-Miguel, D. A. Aldave, S. Diaz-Tendero, M. Alcami, F. Martin, J. Gomez-Herrero and F. Zamora, *Adv. Mater.*, 2016, **28**, 6332–6336, DOI: 10.1002/adma.201602128.

207 Y. Huang, Y. H. Pan, R. Yang, L. H. Bao, L. Meng, H. L. Luo, Y. Q. Cai, G. D. Liu, W. J. Zhao, Z. Zhou, L. M. Wu, Z. L. Zhu, M. Huang, L. W. Liu, L. Liu, P. Cheng, K. H. Wu, S. B. Tian, C. Z. Gu, Y. G. Shi, Y. F. Guo, Z. G. Cheng, J. P. Hu, L. Zhao, G. H. Yang, E. Sutter, P. Sutter, Y. L. Wang, W. Ji, X. J. Zhou and H. J. Gao, *Nat. Commun.*, 2020, **11**, 9, DOI: 10.1038/s41467-020-16266-w.

208 K. Yang, L. Z. Feng, X. Z. Shi and Z. Liu, *Chem. Soc. Rev.*, 2013, **42**, 530–547, DOI: 10.1039/c2cs35342c.

209 J. N. Coleman, M. Lotya, A. O'Neill, S. D. Bergin, P. J. King, U. Khan, K. Young, A. Gaucher, S. De, R. J. Smith, I. V. Shvets, S. K. Arora, G. Stanton, H. Y. Kim, K. Lee, G. T. Kim, G. S. Duesberg, T. Hallam, J. J. Boland, J. J. Wang, J. F. Donegan, J. C. Grunlan, G. Moriarty, A. Shmeliov, R. J. Nicholls, J. M. Perkins, E. M. Grieveson, K. Theuwissen, D. W. McComb, P. D. Nellist and V. Nicolosi, *Science*, 2011, **331**, 568–571, DOI: 10.1126/science.1194975.

210 A. Ciesielski and P. Samori, *Chem. Soc. Rev.*, 2014, **43**, 381–398, DOI: 10.1039/c3cs60217f.

211 V. Nicolosi, M. Chhowalla, M. G. Kanatzidis, M. S. Strano and J. N. Coleman, *Science*, 2013, **340**, 1226419, DOI: 10.1126/science.1226419.

212 D. Bitounis, H. Ali-Boucetta, B. H. Hong, D. H. Min and K. Kostarelos, *Adv. Mater.*, 2013, **25**, 2258–2268, DOI: 10.1002/adma.201203700.

213 Z. F. Ma, M. C. Zhang, X. D. Jia, J. Bai, Y. D. Ruan, C. Wang, X. P. Sun and X. Jiang, *Small*, 2016, **12**, 5477–5487, DOI: 10.1002/smll.201601681.

214 J. Y. Dai, J. B. Song, Y. Qiu, J. J. Wei, Z. Z. Hong, L. Li and H. H. Yang, *ACS Appl. Mater. Interfaces*, 2019, **11**, 10589–10596, DOI: 10.1021/acsami.9b01307.

215 S. S. Chou, B. Kaehr, J. Kim, B. M. Foley, M. De, P. E. Hopkins, J. Huang, C. J. Brinker and V. P. Dravid, *Angew. Chem., Int. Ed.*, 2013, **52**, 4160–4164, DOI: 10.1002/anie.201209229.

216 D. K. Ji, Y. Zhang, Y. Zang, J. Li, G. R. Chen, X. P. He and H. Tian, *Adv. Mater.*, 2016, **28**, 9356–9363, DOI: 10.1002/adma.201602748.

217 L. Cheng, X. W. Wang, F. Gong, T. Liu and Z. Liu, *Adv. Mater.*, 2020, **32**, 23, DOI: 10.1002/adma.201902333.

218 J. T. Liu, P. Du, T. R. Liu, B. J. C. Wong, W. P. Wang, H. X. Ju and J. P. Lei, *Biomaterials*, 2019, **192**, 179–188, DOI: 10.1016/j.biomaterials.2018.10.018.

219 J. Ouyang, Y. Y. Deng, W. S. Chen, Q. F. Xu, L. Q. Wang, Z. J. Liu, F. Y. Tang, L. Deng and Y. N. Liu, *J. Mater. Chem. B*, 2018, **6**, 2057–2064, DOI: 10.1039/c8tb00371h.

220 X. Y. Yang, D. Y. Wang, J. W. Zhu, L. Xue, C. J. Ou, W. J. Wang, M. Lu, X. J. Song and X. C. Dong, *Chem. Sci.*, 2019, **10**, 3779–3785, DOI: 10.1039/c8sc04844d.

221 M. Naguib, M. Kurtoglu, V. Presser, J. Lu, J. J. Niu, M. Heon, L. Hultman, Y. Gogotsi and M. W. Barsoum, *Adv. Mater.*, 2011, **23**, 4248–4253, DOI: 10.1002/adma.201102306.

222 H. Chen, T. J. Liu, Z. Q. Su, L. Shang and G. Wei, *Nanoscale Horiz.*, 2018, **3**, 74–89, DOI: 10.1039/c7nh00158d.

223 G. Y. Liu, J. H. Zou, Q. Y. Tang, X. Y. Yang, Y. W. Zhang, Q. Zhang, W. Huang, P. Chen, J. J. Shao and X. C. Dong, *ACS Appl. Mater. Interfaces*, 2017, **9**, 40077–40086, DOI: 10.1021/acsami.7b13421.

224 A. Gazzi, L. Fusco, A. Khan, D. Bedognetti, B. Zavan, F. Vitale, A. Yilmazer and L. G. Delogu, *Front. Bioeng. Biotechnol.*, 2019, **7**, 15, DOI: 10.3389/fbioe.2019.00295.

225 Q. Zhang, W. C. Huang, C. Y. Yang, F. Wang, C. Q. Song, Y. Gao, Y. F. Qiu, M. Yan, B. Yang and C. S. Guo, *Biomater. Sci.*, 2019, **7**, 2729–2739, DOI: 10.1039/c9bm00239a.

226 L. Bai, W. H. Yi, T. Y. Sun, Y. L. Tian, P. Zhang, J. H. Si, X. Hou and J. Hou, *J. Mater. Chem. B*, 2020, **8**, 6402–6417, DOI: 10.1039/d0tb01084g.

227 C. L. Tan, X. H. Cao, X. J. Wu, Q. Y. He, J. Yang, X. Zhang, J. Z. Chen, W. Zhao, S. K. Han, G. H. Nam, M. Sindoro and H. Zhang, *Chem. Rev.*, 2017, **117**, 6225–6331, DOI: 10.1021/acs.chemrev.6b00558.

228 P. R. Somani, S. P. Somani and M. Umeno, *Chem. Phys. Lett.*, 2006, **430**, 56–59, DOI: 10.1016/j.cplett.2006.06.081.

229 Y. M. Shi, C. Hamsen, X. T. Jia, K. K. Kim, A. Reina, M. Hofmann, A. L. Hsu, K. Zhang, H. N. Li, Z. Y. Juang, M. S. Dresselhaus, L. J. Li and J. Kong, *Nano Lett.*, 2010, **10**, 4134–4139, DOI: 10.1021/nl1023707.

230 Y. J. Xu, X. Y. Shi, Y. S. Zhang, H. T. Zhang, Q. L. Zhang, Z. L. Huang, X. F. Xu, J. Guo, H. Zhang, L. T. Sun, Z. M. Zeng, A. L. Pan and K. Zhang, *Nat. Commun.*, 2020, **11**, 8, DOI: 10.1038/s41467-020-14902-z.

231 Y. J. Zhan, Z. Liu, S. Najmaei, P. M. Ajayan and J. Lou, *Small*, 2012, **8**, 966–971, DOI: 10.1002/smll.201102654.

232 D. S. Kong, H. T. Wang, J. J. Cha, M. Pasta, K. J. Koski, J. Yao and Y. Cui, *Nano Lett.*, 2013, **13**, 1341–1347, DOI: 10.1021/nl400258t.

233 C. Chung, Y. K. Kim, D. Shin, S. R. Ryoo, B. H. Hong and D. H. Min, *Acc. Chem. Res.*, 2013, **46**, 2211–2224, DOI: 10.1021/ar300159f.

234 Y. T. Chen, R. Ren, H. H. Pu, J. B. Chang, S. Mao and J. H. Chen, *Biosens. Bioelectron.*, 2017, **89**, 505–510, DOI: 10.1016/j.bios.2016.03.059.

235 S. M. Machado, C. Pacheco-Soares, F. R. Marciano, A. O. Lobo and N. S. da Silva, *Mater. Sci. Eng., C*, 2014, **36**, 180–186, DOI: 10.1016/j.msec.2013.12.004.

236 C. L. Tan and H. Zhang, *Nat. Commun.*, 2015, **6**, 13, DOI: 10.1038/ncomms8873.

237 J. H. Han, S. Lee and J. Cheon, *Chem. Soc. Rev.*, 2013, **42**, 2581–2591, DOI: 10.1039/c2cs35386e.

238 C. Murugan, V. Sharma, R. K. Murugan, G. Malaimegu and A. Sundaramurthy, *J. Controlled Release*, 2019, **299**, 1–20, DOI: 10.1016/j.jconrel.2019.02.015.

239 X. Yang, M. X. Yang, B. Pang, M. Vara and Y. N. Xia, *Chem. Rev.*, 2015, **115**, 10410–10488, DOI: 10.1021/acs.chemrev.5b00193.

240 D. D. Zhang, L. W. Wen, R. Huang, H. H. Wang, X. L. Hu and D. Xing, *Biomaterials*, 2018, **153**, 14–26, DOI: 10.1016/j.biomaterials.2017.10.034.

241 R. Thiruvengadathan, V. Korampally, A. Ghosh, N. Chanda, K. Gangopadhyay and S. Gangopadhyay, *Rep. Prog. Phys.*, 2013, **76**, 54, DOI: 10.1088/0034-4885/76/6/066501.

242 E. De Santis and M. G. Ryadnov, *Chem. Soc. Rev.*, 2015, **44**, 8288–8300, DOI: 10.1039/c5cs00470e.

243 W. Qi, X. Y. Zhang and H. Wang, *Curr. Opin. Colloid Interface Sci.*, 2018, **35**, 36–41, DOI: 10.1016/j.cocis.2018.01.003.

244 T. Wang, J. H. Hu, H. Luo, H. Y. Li, J. H. Zhou, L. Zhou and S. H. Wei, *Small*, 2018, **14**, 13, DOI: 10.1002/smll.201802337.

245 X. K. Cai, Y. T. Luo, B. Liu and H. M. Cheng, *Chem. Soc. Rev.*, 2018, **47**, 6224–6266, DOI: 10.1039/c8cs00254a.

246 B. L. Li, M. I. Setyawati, L. Y. Chen, J. P. Xie, K. Ariga, C. T. Lim, S. Garaj and D. T. Leong, *ACS Appl. Mater. Interfaces*, 2017, **9**, 15286–15296, DOI: 10.1021/acsami.7b02529.

247 Y. W. Wang, J. L. Xie, J. L. Kang, W. Choi, P. Jangili, B. Zhang, N. Xie, G. H. Nie, J. He, H. Zhang, L. P. Liu and J. S. Kim, *Adv. Funct. Mater.*, 2020, **30**, 9, DOI: 10.1002/adfm.202003338.

248 M. Abbas, Q. L. Zou, S. K. Li and X. H. Yan, *Adv. Mater.*, 2017, **29**, 16, DOI: 10.1002/adma.201605021.

249 Y. H. Jia, J. Y. Li, J. C. Chen, P. Hu, L. G. Jiang, X. Y. Chen, M. D. Huang, Z. Chen and P. Xu, *ACS Appl. Mater. Interfaces*, 2018, **10**, 15369–15380, DOI: 10.1021/acsami.7b19058.

250 H. T. Z. Zhu, H. H. Wang, B. B. Shi, L. Q. Shangguan, W. J. Tong, G. C. Yu, Z. W. Mao and F. H. Huang, *Nat. Commun.*, 2019, **10**, 10, DOI: 10.1038/s41467-019-10385-9.

251 S. Thurakkal and X. Y. Zhang, *Adv. Sci.*, 2020, **7**, 28, DOI: 10.1002/advs.201902359.

252 D. An, J. Y. Fu, Z. J. Xie, C. Y. Xing, B. Zhang, B. Wang and M. Qiu, *J. Mater. Chem. B*, 2020, **8**, 7076–7120, DOI: 10.1039/d0tb00824a.

253 F. R. Wu, Y. J. Liu, Y. Wu, D. W. Song, J. W. Qian and B. S. Zhu, *J. Mater. Chem. B*, 2020, **8**, 2128–2138, DOI: 10.1039/c9tb02646k.

254 R. J. Gui, H. Jin, Z. H. Wang and J. H. Li, *Chem. Soc. Rev.*, 2018, **47**, 6795–6823, DOI: 10.1039/c8cs00387d.

255 T. A. Debele, S. Peng and H. C. Tsai, *Int. J. Mol. Sci.*, 2015, **16**, 22094–22136, DOI: 10.3390/ijms160922094.

256 M. Srinivasarao and P. S. Low, *Chem. Rev.*, 2017, **117**, 12133–12164, DOI: 10.1021/acs.chemrev.7b00013.

257 Z. R. Goddard, M. J. Marin, D. A. Russell and M. Searcey, *Chem. Soc. Rev.*, 2020, **49**, 8774–8789, DOI: 10.1039/d0cs01121e.

258 G. De Crozals, R. Bonnet, C. Farre and C. Chaix, *Nano Today*, 2016, **11**, 435–463, DOI: 10.1016/j.nantod.2016.07.002.

259 Q. J. Qiu, C. Li, X. Y. Yan, H. X. Zhang, X. Luo, X. Gao, X. R. Liu, Y. Z. Song and Y. H. Deng, *Biomaterials*, 2021, **269**, 14, DOI: 10.1016/j.biomaterials.2021.120652.

260 O. Penon, M. J. Marin, D. A. Russell and L. Perez-Garcia, *J. Colloid Interface Sci.*, 2017, **496**, 100–110, DOI: 10.1016/j.jcis.2017.02.006.

261 G. Obaid, I. Chambrier, M. J. Cook and D. A. Russell, *Photochem. Photobiol. Sci.*, 2015, **14**, 737–747, DOI: 10.1039/c4pp00312h.

262 H.-C. Lin, W.-T. Li, T. W. Madanayake, C. Tao, Q. Niu, S.-Q. Yan, B.-A. Gao and P. Zhao, *J. Biomater. Appl.*, 2020, **34**, 875–888, DOI: 10.1177/0885328219882152.
263 X. Sun, B. Liu, X. Chen, H. Lin, Y. Peng, Y. Li, H. Zheng, Y. Xu, X. Ou, S. Yan, Z. Wu, S. Deng, L. Zhang and P. Zhao, *J. Mater. Sci.: Mater. Med.*, 2019, **30**, 76, DOI: 10.1007/s10856-019-6278-y.
264 T. R. Daniels, E. Bernabeu, J. A. Rodriguez, S. Patel, M. Kozman, D. A. Chiappetta, E. Holler, J. Y. Ljubimova, G. Helguera and M. L. Penichet, *Biochim. Biophys. Acta, Gen. Subj.*, 2012, **1820**, 291–317, DOI: 10.1016/j.bbagen.2011.07.016.
265 S. Y. Lu and J. Zhang, *J. Med. Chem.*, 2019, **62**, 24–45, DOI: 10.1021/acs.jmedchem.7b01844.
266 K. D. Warner, C. E. Hajdin and K. M. Weeks, *Nat. Rev. Drug Discovery*, 2018, **17**, 547–558, DOI: 10.1038/nrd.2018.93.
267 P. Wu, T. E. Nielsen and M. H. Clausen, *Drug Discovery Today*, 2016, **21**, 5–10, DOI: 10.1016/j.drudis.2015.07.008.
268 H. Jahangirian, K. Kalantari, Z. Izadiyan, R. Rafiee-Moghaddam, K. Shameli and T. J. Webster, *Int. J. Nanomed.*, 2019, **14**, 1633–1657, DOI: 10.2147/ijn.s184723.
269 J. Zhuang, C. H. Kuo, L. Y. Chou, D. Y. Liu, E. Weerapana and C. K. Tsung, *ACS Nano*, 2014, **8**, 2812–2819, DOI: 10.1021/nn406590q.
270 W. Liu, M. R. Baer, M. J. Bowman, P. Pera, X. Zheng, J. Morgan, R. A. Pandey and A. R. Oseroff, *Clin. Cancer Res.*, 2007, **13**, 2463–2470, DOI: 10.1158/1078-0432.CCR-06-1599.
271 P. J. Houghton, G. S. Germain, F. C. Harwood, J. D. Schuetz, C. F. Stewart, E. Buchdunger and P. Traxler, *Cancer Res.*, 2004, **64**, 2333–2337, DOI: 10.1158/0008-5472.CAN-03-3344.
272 S. G. Kimani, J. B. Phillips, J. I. Bruce, A. J. MacRobert and J. P. Golding, *Photochem. Photobiol.*, 2012, **88**, 175–187, DOI: 10.1111/j.1751-1097.2011.01022.x.
273 G. Chen, H. Qju, P. N. Prasad and X. Chen, *Chem. Rev.*, 2014, **114**, 5161–5214, DOI: 10.1021/cr400425h.
274 T. Lin, X. Zhao, S. Zhao, H. Yu, W. Cao, W. Chen, H. Wei and H. Guo, *Theranostics*, 2018, **8**, 990–1004, DOI: 10.7150/thno.22465.
275 C. Ji, Z. Lu, Y. Xu, B. Shen, S. Yu and D. Shi, *J. Biomed. Mater. Res., Part B*, 2018, **106**, 2544–2552, DOI: 10.1002/jbm.b.34071.
276 X. Cai, Y. Luo, Y. Song, D. Liu, H. Yan, H. Li, D. Du, C. Zhu and Y. Lin, *Nanoscale*, 2018, **10**, 22937–22945, DOI: 10.1039/c8nr07679k.
277 C. P. Liu, T. H. Wu, C. Y. Liu, K. C. Chen, Y. X. Chen, G. S. Chen and S. Y. Lin, *Small*, 2017, **13**, 1700278, DOI: 10.1002/smll.201700278.
278 R. L. Setten, J. J. Rossi and S. P. Han, *Nat. Rev. Drug Discovery*, 2019, **18**, 421–446, DOI: 10.1038/s41573-019-0017-4.
279 Y. C. Tseng, S. Mozumdar and L. Huang, *Adv. Drug Delivery Rev.*, 2009, **61**, 721–731, DOI: 10.1016/j.addr.2009.03.003.
280 G. M. Chalbatani, H. Dana, E. Gharagouzloo, S. Grijalvo, R. Eritja, C. D. Logsdon, F. Memari, S. R. Miri, M. R. Rad and V. Marmari, *Int. J. Nanomed.*, 2019, **14**, 3111–3128, DOI: 10.2147/ijn.s200253.
281 Q. Y. Lin, J. Chen, Z. H. Zhang and G. Zheng, *Nanomedicine*, 2014, **9**, 105–120, DOI: 10.2217/nnm.13.192.
282 A. S. L. Derycke and P. A. M. de Witte, *Adv. Drug Delivery Rev.*, 2004, **56**, 17–30, DOI: 10.1016/j.addr.2003.07.014.
283 C. L. Modery-Pawlowski, L. L. Tian, V. Pan and A. Sen Gupta, *Biomacromolecules*, 2013, **14**, 939–948, DOI: 10.1021/bm400074t.
284 D. Hu, Z. Chen, Z. Sheng, D. Gao, F. Yan, T. Ma, H. Zheng and M. Hong, *Nanoscale*, 2018, **10**, 17283–17292, DOI: 10.1039/c8nr05548c.
285 A. M. Smith, M. C. Mancini and S. Nie, *Nat. Nanotechnol.*, 2009, **4**, 710–711, DOI: 10.1038/nnano.2009.326.
286 S. Cui, D. Yin, Y. Chen, Y. Di, H. Chen, Y. Ma, S. Achilefu and Y. Gu, *ACS Nano*, 2013, **7**, 676–688, DOI: 10.1021/nn304872n.
287 Z. Hou, Y. Zhang, K. Deng, Y. Chen, X. Li, X. Deng, Z. Cheng, H. Lian, C. Li and J. Lin, *ACS Nano*, 2015, **9**, 2584–2599, DOI: 10.1021/nn506107c.
288 N. M. Idris, M. K. Gnanasammandhan, J. Zhang, P. C. Ho, R. Mahendran and Y. Zhang, *Nat. Med.*, 2012, **18**, 1580-U1190, DOI: 10.1038/nm.2933.
289 C. Wang, L. Cheng, Y. Liu, X. Wang, X. Ma, Z. Deng, Y. Li and Z. Liu, *Adv. Funct. Mater.*, 2013, **23**, 3077–3086, DOI: 10.1002/adfm.201202992.
290 C. Wang, L. Cheng and Z. Liu, *Theranostics*, 2013, **3**, 317–330, DOI: 10.7150/thno.5284.
291 C. Wang, H. Tao, L. Cheng and Z. Liu, *Biomaterials*, 2011, **32**, 6145–6154, DOI: 10.1016/j.biomaterials.2011.05.007.
292 M. Pawlicki, H. A. Collins, R. G. Denning and H. L. Anderson, *Angew. Chem., Int. Ed.*, 2009, **48**, 3244–3266, DOI: 10.1002/anie.200805257.
293 G. G. Yang, L. Hao, Q. Cao, H. Zhang, J. Yang, L. N. Ji and Z. W. Mao, *ACS Appl. Mater. Interfaces*, 2018, **10**, 28301–28313, DOI: 10.1021/acsami.8b07270.
294 S. Wang, W. Wu, P. Manghnani, S. Xu, Y. Wang, C. C. Goh, L. G. Ng and B. Liu, *ACS Nano*, 2019, **13**, 3095–3105, DOI: 10.1021/acsnano.8b08398.
295 J. P. Scaffidi, M. K. Gregas, B. Lauly, Y. Zhang and T. Vo-Dinh, *ACS Nano*, 2011, **5**, 4679–4687, DOI: 10.1021/nn200511m.
296 L. Larue, A. Ben Mihoub, Z. Youssef, L. Colombeau, S. Acherar, J. C. Andre, P. Arnoux, F. Baros, M. Vermandel and C. Frochot, *Photochem. Photobiol. Sci.*, 2018, **17**, 1612–1650, DOI: 10.1039/c8pp00112j.
297 N. Kotagiri, G. P. Sudlow, W. J. Akers and S. Achilefu, *Nat. Nanotechnol.*, 2015, **10**, 370–379, DOI: 10.1038/nnano.2015.17.
298 C.-Y. Hsu, C.-W. Chen, H.-P. Yu, Y.-F. Lin and P.-S. Lai, *Biomaterials*, 2013, **34**, 1204–1212, DOI: 10.1016/j.biomaterials.2012.08.044.
299 E. H. Moriyama, S. K. Bisland, L. Lilge and B. C. Wilson, *Photochem. Photobiol.*, 2004, **80**, 242–249, DOI: 10.1562/2004-02-20-ra-088.1.
300 A. Yuan, J. Wu, X. Tang, L. Zhao, F. Xu and Y. Hu, *J. Pharm. Sci.*, 2013, **102**, 6–28, DOI: 10.1002/jps.23356.
301 A. Kamkaew, S. H. Lim, H. B. Lee, L. V. Kiew, L. Y. Chung and K. Burgess, *Chem. Soc. Rev.*, 2013, **42**, 77–88, DOI: 10.1039/c2cs35216h.

302 L. Liu, Z. Ruan, T. Li, P. Yuan and L. Yan, *Biomater. Sci.*, 2016, **4**, 1638–1645, DOI: 10.1039/c6bm00581k.
303 M. Lu, N. Kang, C. Chen, L. Yang, Y. Li, M. Hong, X. Luo, L. Ren and X. Wang, *Nanotechnology*, 2017, **28**, 445710, DOI: 10.1088/1361-6528/aa81e1.
304 K. Ghosal and A. Ghosh, *Mater. Sci. Eng., C*, 2019, **96**, 887–903, DOI: 10.1016/j.msec.2018.11.060.
305 M. Pollnau, D. R. Gamelin, S. R. Luthi, H. U. Gudel and M. P. Hehlen, *Phys. Rev. B: Condens. Matter Mater. Phys.*, 2000, **61**, 3337–3346, DOI: 10.1103/PhysRevB.61.3337.
306 F. Wang and X. Liu, *Chem. Soc. Rev.*, 2009, **38**, 976–989, DOI: 10.1039/b809132n.
307 F. Wang, D. Banerjee, Y. Liu, X. Chen and X. Liu, *Analyst*, 2010, **135**, 1839–1854, DOI: 10.1039/c0an00144a.
308 M. Haase and H. Schaefer, *Angew. Chem., Int. Ed.*, 2011, **50**, 5808–5829, DOI: 10.1002/anie.201005159.
309 J. Zhou, Q. Liu, W. Feng, Y. Sun and F. Li, *Chem. Rev.*, 2015, **115**, 395–465, DOI: 10.1021/cr400478f.
310 L. Liang, Y. Lu, R. Zhang, A. Care, T. A. Ortega, S. M. Deyev, Y. Qian and A. V. Zvyagin, *Acta Biomater.*, 2017, **51**, 461–470, DOI: 10.1016/j.actbio.2017.01.004.
311 T. Gu, L. Cheng, F. Gong, J. Xu, X. Li, G. Han and Z. Liu, *ACS Appl. Mater. Interfaces*, 2018, **10**, 15494–15503, DOI: 10.1021/acsami.8b03238.
312 B. Ding, S. Shao, H. Xiao, C. Sun, X. Cai, F. Jiang, X. Zhao, P. Ma and J. Lin, *Nanoscale*, 2019, **11**, 14654–14667, DOI: 10.1039/c9nr04858h.
313 H. F. Wang, T. B. Huff, D. A. Zweifel, W. He, P. S. Low, A. Wei and J. X. Cheng, *Proc. Natl. Acad. Sci. U. S. A.*, 2005, **102**, 15752–15756, DOI: 10.1073/pnas.0504892102.
314 N. J. Durr, T. Larson, D. K. Smith, B. A. Korgel, K. Sokolov and A. Ben-Yakar, *Nano Lett.*, 2007, **7**, 941–945, DOI: 10.1021/nl062962v.
315 J. D. Bhawalkar, N. D. Kumar, C. F. Zhao and P. N. Prasad, *J. Clin. Laser Med. Surg.*, 1997, **15**, 201–204, DOI: 10.1089/clm.1997.15.201.
316 Q. Liu, B. Guo, Z. Rao, B. Zhang and J. R. Gong, *Nano Lett.*, 2013, **13**, 2436–2441, DOI: 10.1021/nl400368v.
317 S. Dayal and C. Burda, *J. Am. Chem. Soc.*, 2008, **130**, 2890–2891, DOI: 10.1021/ja0781285.
318 A. C. Samia, X. Chen and C. Burda, *J. Am. Chem. Soc.*, 2003, **125**, 15736–15737, DOI: 10.1021/ja0386905.
319 A. Skripka, J. Valanciunaite, G. Dauderis, V. Poderys, R. Kubiliute and R. Rotomskis, *J. Biomed. Opt.*, 2013, **18**, 078002, DOI: 10.1117/1.JBO.18.7.078002.
320 C. Fowley, N. Nomikou, A. P. McHale, B. McCaughan and J. F. Callan, *Chem. Commun.*, 2013, **49**, 8934–8936, DOI: 10.1039/c3cc45181j.
321 J. Sun, Q. Xin, Y. Yang, H. Shah, H. Cao, Y. Qi, J. R. Gong and J. Li, *Chem. Commun.*, 2018, **54**, 715–718, DOI: 10.1039/c7cc08820e.
322 S. Li, X. Shen, Q.-H. Xu and Y. Cao, *Nanoscale*, 2019, **11**, 19551–19560, DOI: 10.1039/c9nr05488j.
323 J. Hu, Y. a. Tang, A. H. Elmenoufy, H. Xu, Z. Cheng and X. Yang, *Small*, 2015, **11**, 5860–5887, DOI: 10.1002/smll.201501923.
324 A. Karnkaew, F. Chen, Y. Zhan, R. L. Majewski and W. Cai, *ACS Nano*, 2016, **10**, 3918–3935, DOI: 10.1021/acsnano.6b01401.
325 H. Chen, G. D. Wang, Y.-J. Chuang, Z. Zhen, X. Chen, P. Biddinger, Z. Hao, F. Liu, B. Shen, Z. Pan and J. Xie, *Nano Lett.*, 2015, **15**, 2249–2256, DOI: 10.1021/nl504044p.
326 X. Yu, X. Liu, W. Wu, K. Yang, R. Mao, F. Ahmad, X. Chen and W. Li, *Angew. Chem., Int. Ed.*, 2019, **58**, 2017–2022, DOI: 10.1002/anie.201812272.
327 X.-D. Ren, X.-Y. Hao, H.-C. Li, M.-R. Ke, B.-Y. Zheng and J.-D. Huang, *Drug Discovery Today*, 2018, **23**, 1791–1800, DOI: 10.1016/j.drudis.2018.05.029.
328 B. Cline, I. Delahunty and J. Xie, *Wiley Interdiscip. Rev.: Nanomed. Nanobiotechnol.*, 2019, **11**, e1541, DOI: 10.1002/wnan.1541.
329 G. Lan, K. Ni, R. Xu, K. Lu, Z. Lin, C. Chan and W. Lin, *Angew. Chem., Int. Ed.*, 2017, **56**, 12102–12106, DOI: 10.1002/anie.201704828.
330 X. D. Ren, X. Y. Hao, H. C. Li, M. R. Ke, B. Y. Zheng and J. D. Huang, *Drug Discovery Today*, 2018, **23**, 1791–1800, DOI: 10.1016/j.drudis.2018.05.029.
331 G. D. Wang, H. T. Nguyen, H. Chen, P. B. Cox, L. Wang, K. Nagata, Z. Hao, A. Wang, Z. Li and J. Xie, *Theranostics*, 2016, **6**, 2295–2305, DOI: 10.7150/thno.16141.
332 C. M. Magalhaes, J. C. Esteves da Silva and L. Pinto da Silva, *ChemPhysChem*, 2016, **17**, 2286–2294, DOI: 10.1002/cphc.201600270.
333 M. Yamaguchi, H. Yoshida and H. Nohta, *J. Chromatogr.*, 2002, **950**, 1–19, DOI: 10.1016/s0021-9673(02)00004-3.
334 C. A. Marquette and L. J. Blum, *Anal. Bioanal. Chem.*, 2006, **385**, 546–554, DOI: 10.1007/s00216-006-0439-9.
335 R. Laptev, M. Nisnevitch, G. Siboni, Z. Malik and M. A. Firer, *Br. J. Cancer*, 2006, **95**, 189–196, DOI: 10.1038/sj.bjc.6603241.
336 Y. Zhang, L. Pang, C. Ma, Q. Tu, R. Zhang, E. Saeed, A. E. Mahmoud and J. Wang, *Anal. Chem.*, 2014, **86**, 3092–3099, DOI: 10.1021/ac404201s.
337 X. Xu, H. An, D. Zhang, H. Tao, Y. Dou, X. Li, J. Huang and J. Zhang, *Sci. Adv.*, 2019, **5**, eaat2953, DOI: 10.1126/sciadv.aat2953.
338 L. Huang, T. C. Chen and F. H. Lin, *Curr. Med. Chem.*, 2013, **20**, 1195–1202, DOI: 10.2174/0929867311320090008.
339 L. Jiang, H. Bai, L. Liu, F. Lv, X. Ren and S. Wang, *Angew. Chem., Int. Ed.*, 2019, **58**, 10660–10665, DOI: 10.1002/anie.201905884.
340 T. Wilson and J. W. Hastings, *Annu. Rev. Cell Dev. Biol.*, 1998, **14**, 197–230, DOI: 10.1146/annurev.cellbio.14.1.197.
341 C. H. Contag and M. H. Bachmann, *Annu. Rev. Biomed. Eng.*, 2002, **4**, 235–260, DOI: 10.1146/annurev.bioeng.4.111901.093336.
342 T. Nakatsu, S. Ichiyama, J. Hiratake, A. Saldanha, N. Kobashi, K. Sakata and H. Kato, *Nature*, 2006, **440**, 372–376, DOI: 10.1038/nature04542.
343 A. Roda, P. Pasini, M. Mirasoli, E. Michelini and M. Guardigli, *Trends Biotechnol.*, 2004, **22**, 295–303, DOI: 10.1016/j.tibtech.2004.03.011.

344 Y. Yang, Q. Shao, R. Deng, C. Wang, X. Teng, K. Cheng, Z. Cheng, L. Huang, Z. Liu, X. Liu and B. Xing, *Angew. Chem., Int. Ed.*, 2012, **51**, 3125–3129, DOI: 10.1002/anie.201107919.

345 C. Y. Hsu, C. W. Chen, H. P. Yu, Y. F. Lin and P. S. Lai, *Biomaterials*, 2013, **34**, 1204–1212, DOI: 10.1016/j.biomaterials.2012.08.044.

346 Y. Yang, W. Hou, S. Liu, K. Sun, M. Li and C. Wu, *Biomacromolecules*, 2018, **19**, 201–208, DOI: 10.1021/acs.biomac.7b01469.

347 D. Kessel and N. L. Oleinick, *Photochem. Photobiol.*, 2018, **94**, 213–218, DOI: 10.1111/php.12857.

348 Z. Zhen, W. Tang, Y.-J. Chuang, T. Todd, W. Zhang, X. Lin, G. Niu, G. Liu, L. Wang, Z. Pan, X. Chen and J. Xie, *ACS Nano*, 2014, **8**, 6004–6013, DOI: 10.1021/nn501134q.

349 W. Gao, Z. Wang, L. Lv, D. Yin, D. Chen, Z. Han, Y. Ma, M. Zhang, M. Yang and Y. Gu, *Theranostics*, 2016, **6**, 1131–1144, DOI: 10.7150/thno.15262.

350 V. Mashayekhi, C. Op'tHooga and S. Oliveira, *J. Porphyrins Phthalocyanines*, 2019, **23**, 1229–1240, DOI: 10.1142/s1088424619300180.

351 G. Canti, A. De Simone and M. Korbelik, *Photochem. Photobiol. Sci.*, 2002, **1**, 79–80, DOI: 10.1039/b109007k.

352 J. H. Sun, I. Cecic, C. S. Parkins and M. Korbelik, *Photochem. Photobiol. Sci.*, 2002, **1**, 690–695, DOI: 10.1039/b204254a.

353 P. Mroz, A. Szokalska, M. X. Wu and M. R. Hamblin, *PLoS One*, 2010, **5**, e15194, DOI: 10.1371/journal.pone.0015194.

354 A. D. Garg and P. Agostinis, *Photochem. Photobiol. Sci.*, 2014, **13**, 474–487, DOI: 10.1039/c3pp50333j.

355 D. R. Green and J. C. Reed, *Science*, 1998, **281**, 1309–1312, DOI: 10.1126/science.281.5381.1309.

356 M. O. Hengartner, *Nature*, 2000, **407**, 770–776, DOI: 10.1038/35037710.

357 S. Elmore, *Toxicol. Pathol.*, 2007, **35**, 495–516, DOI: 10.1080/01926230701320337.

358 A. L. Grilo and A. Mantalaris, *Biotechnol. Adv.*, 2019, **37**, 459–475, DOI: 10.1016/j.biotechadv.2019.02.012.

359 D. Tang, R. Kang, T. V. Berghe, P. Vandenabeele and G. Kroemer, *Cell Res.*, 2019, **29**, 347–364, DOI: 10.1038/s41422-019-0164-5.

360 D. Kessel and Y. Luo, *Cell Death Differ.*, 1999, **6**, 28–35, DOI: 10.1038/sj.cdd.4400446.

361 N. L. Oleinick, R. L. Morris and T. Belichenko, *Photochem. Photobiol. Sci.*, 2002, **1**, 1–21, DOI: 10.1039/b108586g.

362 P. Agostinis, E. Buytaert, H. Breyssens and N. Hendrickx, *Photochem. Photobiol. Sci.*, 2004, **3**, 721–729, DOI: 10.1039/b315237e.

363 R. D. Almeida, B. J. Manadas, A. P. Carvalho and C. B. Duarte, *Biochim. Biophys. Acta, Rev. Cancer*, 2004, **1704**, 59–86, DOI: 10.1016/j.bbcan.2004.05.003.

364 C. Zhou, C. Shunji, D. Jinsheng, L. Junlin, G. Jori and C. Milanesi, *J. Photochem. Photobiol., B*, 1996, **33**, 219–223, DOI: 10.1016/1011-1344(95)07250-0.

365 M. E. Varnes, S. M. Chiu, L. Y. Xue and N. L. Oleinick, *Biochem. Biophys. Res. Commun.*, 1999, **255**, 673–679, DOI: 10.1006/bbrc.1999.0261.

366 J. Usuda, S. M. Chiu, E. S. Murphy, M. Lam, A. L. Nieminen and N. L. Oleinick, *J. Biol. Chem.*, 2003, **278**, 2021–2029, DOI: 10.1074/jbc.M205219200.

367 L. Y. Xue, S. M. Chiu, A. Fiebig, D. W. Andrews and N. L. Oleinick, *Oncogene*, 2003, **22**, 9197–9204, DOI: 10.1038/sj.onc.1207019.

368 J. J. Reiners, Jr., J. A. Caruso, P. Mathieu, B. Chelladurai, X. M. Yin and D. Kessel, *Cell Death Differ.*, 2002, **9**, 934–944, DOI: 10.1038/sj.cdd.4401048.

369 S. M. Chiu, L. Y. Xue, M. Lam, M. E. Rodriguez, P. Zhang, M. E. Kenney, A. L. Nieminen and N. L. Oleinick, *Photochem. Photobiol.*, 2010, **86**, 1161–1173, DOI: 10.1111/j.1751-1097.2010.00766.x.

370 Y. Y. Liu, J. W. Zhang, C. J. Zuo, Z. Zhang, D. L. Ni, C. Zhang, J. Wang, H. Zhang, Z. W. Yao and W. B. Bu, *Nano Res.*, 2016, **9**, 3257–3266, DOI: 10.1007/s12274-016-1204-9.

371 P. Golstein and G. Kroemer, *Trends Biochem. Sci.*, 2007, **32**, 37–43, DOI: 10.1016/j.tibs.2006.11.001.

372 T. Vanden Berghe, A. Linkermann, S. Jouan-Lanhouet, H. Walczak and P. Vandenabeele, *Nat. Rev. Mol. Cell Biol.*, 2014, **15**, 134–146, DOI: 10.1038/nrm3737.

373 S. L. Fink and B. T. Cookson, *Infect. Immun.*, 2005, **73**, 1907–1916, DOI: 10.1128/iai.73.4.1907-1916.2005.

374 L. Ouyang, Z. Shi, S. Zhao, F. T. Wang, T. T. Zhou, B. Liu and J. K. Bao, *Cell Proliferation*, 2012, **45**, 487–498, DOI: 10.1111/j.1365-2184.2012.00845.x.

375 V. Nikoletopoulou, M. Markaki, K. Palikaras and N. Tavernarakis, *Biochim. Biophys. Acta, Mol. Cell Res.*, 2013, **1833**, 3448–3459, DOI: 10.1016/j.bbamcr.2013.06.001.

376 A. P. Castano, T. N. Demidova and M. R. Hamblin, *Photodiagn. Photodyn. Ther.*, 2005, **2**, 1–23, DOI: 10.1016/S1572-1000(05)00030-X.

377 D. A. Al-Mutairi, J. D. Craik, I. Batinic-Haberle and L. T. Benov, *Free Radical Res.*, 2007, **41**, 89–96, DOI: 10.1080/10715760600952869.

378 B. Levine and D. J. Klionsky, *Dev. Cell*, 2004, **6**, 463–477, DOI: 10.1016/s1534-5807(04)00099-1.

379 B. Levine and G. Kroemer, *Cell*, 2008, **132**, 27–42, DOI: 10.1016/j.cell.2007.12.018.

380 N. Mizushima, B. Levine, A. M. Cuervo and D. J. Klionsky, *Nature*, 2008, **451**, 1069–1075, DOI: 10.1038/nature06639.

381 M. C. Maiuri, E. Zalckvar, A. Kimchi and G. Kroemer, *Nat. Rev. Mol. Cell Biol.*, 2007, **8**, 741–752, DOI: 10.1038/nrm2239.

382 F. Janku, D. J. McConkey, D. S. Hong and R. Kurzrock, *Nat. Rev. Clin. Oncol.*, 2011, **8**, 528–539, DOI: 10.1038/nrclinonc.2011.71.

383 E. White and R. S. DiPaola, *Clin. Cancer Res.*, 2009, **15**, 5308–5316, DOI: 10.1158/1078-0432.CCR-07-5023.

384 X. Sui, R. Chen, Z. Wang, Z. Huang, N. Kong, M. Zhang, W. Han, F. Lou, J. Yang, Q. Zhang, X. Wang, C. He and H. Pan, *Cell Death Dis.*, 2013, **4**, e838, DOI: 10.1038/cddis.2013.350.

385 Z. Huang, L. Zhou, Z. Chen, E. C. Nice and C. Huang, *Int. J. Cancer*, 2016, **139**, 23–32, DOI: 10.1002/ijc.29990.

386 Y. Lei, D. Zhang, J. Yu, H. Dong, J. Zhang and S. Yang, *Cancer Lett.*, 2017, **393**, 33–39, DOI: 10.1016/j.canlet.2017.02.012.
387 A. Kumar, U. K. Singh and A. Chaudhary, *Future Med. Chem.*, 2015, **7**, 1535–1542, DOI: 10.4155/fmc.15.88.
388 Y. J. Li, Y. H. Lei, N. Yao, C. R. Wang, N. Hu, W. C. Ye, D. M. Zhang and Z. S. Chen, *Chin. J. Cancer*, 2017, **36**, 52, DOI: 10.1186/s40880-017-0219-2.
389 Y. Chen, M. B. Azad and S. B. Gibson, *Cell Death Differ.*, 2009, **16**, 1040–1052, DOI: 10.1038/cdd.2009.49.
390 N. Rubio, J. Verrax, M. Dewaele, T. Verfaillie, T. Johansen, J. Piette and P. Agostinis, *Free Radical Biol. Med.*, 2014, **67**, 292–303, DOI: 10.1016/j.freeradbiomed.2013.11.010.
391 M. F. Wei, M. W. Chen, K. C. Chen, P. J. Lou, S. Y. Lin, S. C. Hung, M. Hsiao, C. J. Yao and M. J. Shieh, *Autophagy*, 2014, **10**, 1179–1192, DOI: 10.4161/auto.28679.
392 P. Tu, Q. Huang, Y. Ou, X. Du, K. Li, Y. Tao and H. Yin, *Oncol. Rep.*, 2016, **35**, 3209–3215, DOI: 10.3892/or.2016.4703.
393 A. Domagala, J. Stachura, M. Gabrysiak, A. Muchowicz, R. Zagozdzon, J. Golab and M. Firczuk, *BMC Cancer*, 2018, **18**, 210, DOI: 10.1186/s12885-018-4126-y.
394 L. Yu, A. Alva, H. Su, P. Dutt, E. Freundt, S. Welsh, E. H. Baehrecke and M. J. Lenardo, *Science*, 2004, **304**, 1500–1502, DOI: 10.1126/science.1096645.
395 S. Shimizu, T. Kanaseki, N. Mizushima, T. Mizuta, S. Arakawa-Kobayashi, C. B. Thompson and Y. Tsujimoto, *Nat. Cell Biol.*, 2004, **6**, 1221–1228, DOI: 10.1038/ncb1192.
396 J. Zhu, S. Tian, K. T. Li, Q. Chen, Y. Jiang, H. D. Lin, L. H. Yu and D. Q. Bai, *Cancer Med.*, 2018, **7**, 1908–1920, DOI: 10.1002/cam4.1418.
397 Z. M. Markovic, B. Z. Ristic, K. M. Arsikin, D. G. Klisic, L. M. Harhaji-Trajkovic, B. M. Todorovic-Markovic, D. P. Kepic, T. K. Kravic-Stevovic, S. P. Jovanovic, M. M. Milenkovic, D. D. Milivojevic, V. Z. Bumbasirevic, M. D. Dramicanin and V. S. Trajkovic, *Biomaterials*, 2012, **33**, 7084–7092, DOI: 10.1016/j.biomaterials.2012.06.060.
398 Y. Y. Deng, P. Y. Song, X. H. Chen, Y. Huang, L. J. Hong, Q. Jin and J. Ji, *ACS Nano*, 2020, **14**, 9711–9727, DOI: 10.1021/acsnano.0c01350.
399 P. Carmeliet, *Oncology*, 2005, **69**, 4–10, DOI: 10.1159/000088478.
400 P. Carmeliet and R. K. Jain, *Nature*, 2000, **407**, 249–257, DOI: 10.1038/35025220.
401 R. S. Kerbel, *N. Engl. J. Med.*, 2008, **358**, 2039–2049, DOI: 10.1056/NEJMra0706596.
402 R. R. Ramjiawan, A. W. Griffioen and D. G. Duda, *Angiogenesis*, 2017, **20**, 185–204, DOI: 10.1007/s10456-017-9552-y.
403 B. Chen, B. W. Pogue, P. J. Hoopes and T. Hasan, *Crit. Rev. Eukaryotic Gene Expression*, 2006, **16**, 279–305, DOI: 10.1615/CritRevEukarGeneExpr.v16.i4.10.
404 D. Bechet, F. Auger, P. Couleaud, E. Marty, L. Ravasi, N. Durieux, C. Bonnet, F. Plenat, C. Frochot, S. Mordon, O. Tillement, R. Vanderesse, F. Lux, P. Perriat, F. Guillemin and M. Barberi-Heyob, *Nanomed. Nanotechnol. Biol. Med.*, 2015, **11**, 657–670, DOI: 10.1016/j.nano.2014.12.007.
405 Y. Jang, D. Kim, H. Lee, H. Jang, S. Park, G. E. Kim, H. J. Lee, H. J. Kim and H. Kim, *Nanomed. Nanotechnol. Biol. Med.*, 2020, **27**, 14, DOI: 10.1016/j.nano.2020.102194.
406 Z. Wei, P. P. Liang, J. Q. Xie, C. H. Song, C. C. Tang, Y. F. Wang, X. T. Yin, Y. Cai, W. Han and X. C. Dong, *Chem. Sci.*, 2019, **10**, 2778–2784, DOI: 10.1039/c8sc04123g.
407 T. F. Gajewski, H. Schreiber and Y.-X. Fu, *Nat. Immunol.*, 2013, **14**, 1014–1022, DOI: 10.1038/ni.2703.
408 J. B. Swann and M. J. Smyth, *J. Clin. Invest.*, 2007, **117**, 1137–1146, DOI: 10.1172/jci31405.
409 H. Yu, M. Kortylewski and D. Pardoll, *Nat. Rev. Immunol.*, 2007, **7**, 41–51, DOI: 10.1038/nri1995.
410 D. S. Chen and I. Mellman, *Nature*, 2017, **541**, 321–330, DOI: 10.1038/nature21349.
411 P. Sharma and J. P. Allison, *Science*, 2015, **348**, 56–61, DOI: 10.1126/science.aaa8172.
412 S. R. Scheffer, H. Nave, F. Korangy, K. Schlote, R. Pabst, E. M. Jaffee, M. P. Manns and T. F. Greten, *Int. J. Cancer*, 2003, **103**, 205–211, DOI: 10.1002/ijc.10777.
413 L. Zitvogel, N. Casares, M. O. Pequignot, N. Chaput, M. L. Albert and G. Kroemer, *Adv. Immunol.*, 2004, **84**, 131–179, DOI: 10.1016/S0065-2776(04)84004-5.
414 A. Melcher, M. Gough, S. Todryk and R. Vile, *J. Mol. Med.*, 1999, **77**, 824–833, DOI: 10.1007/s001099900066.
415 A. Jalili, M. Makowski, T. Switaj, D. Nowis, G. M. Wilczynski, E. Wilczek, M. Chorazy-Massalska, A. Radzikowska, W. Maslinski, L. Bialy, J. Sienko, A. Sieron, M. Adamek, G. Basak, P. Mroz, I. W. Krasnodebski, M. Jakobisiak and J. Golab, *Clin. Cancer Res.*, 2004, **10**, 4498–4508, DOI: 10.1158/1078-0432.CCR-04-0367.
416 D. Preise, R. Oren, I. Glinert, V. Kalchenko, S. Jung, A. Scherz and Y. Salomon, *Cancer Immunol. Immunother.*, 2009, **58**, 71–84, DOI: 10.1007/s00262-008-0527-0.
417 A. D. Garg, D. V. Krysko, P. Vandenabeele and P. Agostinis, *Photochem. Photobiol. Sci.*, 2011, **10**, 670–680, DOI: 10.1039/c0pp00294a.
418 Y. Yang, Y. Hu and H. Wang, *Oxid. Med. Cell. Longevity*, 2016, 5274084, DOI: 10.1155/2016/5274084.
419 L. Galluzzi, O. Kepp and G. Kroemer, *EMBO J.*, 2012, **31**, 1055–1057, DOI: 10.1038/emboj.2012.2.
420 M. Korbelik, *Photochem. Photobiol. Sci.*, 2011, **10**, 664–669, DOI: 10.1039/c0pp00343c.
421 L. Zheng, Y. Li, Y. Cui, H. Yin, T. Liu, G. Yu, F. Lv and J. Yang, *Lasers Med. Sci.*, 2013, **28**, 1383–1392, DOI: 10.1007/s10103-013-1270-0.
422 Y. Zheng, G. Yin, V. Le, A. Zhang, S. Chen, X. Liang and J. Liu, *Int. J. Biol. Sci.*, 2016, **12**, 120–132, DOI: 10.7150/ijbs.12852.
423 M. W. C. Kang, H. Y. Liu and J. C. Y. Kah, *J. Mater. Chem. B*, 2020, **8**, 10812–10824, DOI: 10.1039/d0tb01953d.
424 H. J. Wang, K. Wang, L. H. He, Y. Liu, H. Q. Dong and Y. Y. Li, *Biomaterials*, 2020, **244**, 14, DOI: 10.1016/j.biomaterials.2020.119964.
425 X. G. Zhang, J. J. Tang, C. Li, Y. Lu, L. L. Cheng and J. Liu, *Bioact. Mater.*, 2021, **6**, 472–489, DOI: 10.1016/j.bioactmat.2020.08.024.
426 C. Zhang and K. Y. Pu, *Chem. Soc. Rev.*, 2020, **49**, 4234–4253, DOI: 10.1039/c9cs00773c.

427 C. W. Ng, J. C. Li and K. Y. Pu, *Adv. Funct. Mater.*, 2018, **28**, 20, DOI: 10.1002/adfm.201804688.
428 J. C. Li, D. Cui, J. G. Huang, S. S. He, Z. B. Yang, Y. Zhang, Y. Luo and K. Y. Pu, *Angew. Chem., Int. Ed.*, 2019, **58**, 12680–12687, DOI: 10.1002/anie.201906288.
429 W. J. Yang, F. W. Zhang, H. Z. Deng, L. S. Lin, S. Wang, F. Kang, G. C. Yu, J. Lau, R. Tian, M. R. Zhang, Z. T. Wang, L. C. He, Y. Ma, G. Niu, S. Hu and X. Y. Chen, *ACS Nano*, 2020, **14**, 620–631, DOI: 10.1021/acsnano.9b07212.
430 W. Q. Yu, X. Q. He, Z. H. Yang, X. T. Yang, W. Xiao, R. Liu, R. Xie, L. Qin and H. L. Gao, *Biomaterials*, 2019, **217**, 119309, DOI: 10.1016/j.biomaterials.2019.119309.
431 A. Casas, G. Di Venosa, T. Hasan and A. Batlle, *Curr. Med. Chem.*, 2011, **18**, 2486–2515, DOI: 10.2174/092986711795843272.
432 Y. Gilaberte, L. Milla, N. Salazar, J. Vera-Alvarez, O. Kourani, A. Damian, V. Rivarola, M. Jose Roca, J. Espada, S. Gonzalez and A. Juarranz, *J. Invest. Dermatol.*, 2014, **134**, 2428–2437, DOI: 10.1038/jid.2014.178.
433 M.-F. Wei, M.-W. Chen, K.-C. Chen, P.-J. Lou, S. Y.-F. Lin, S.-C. Hung, M. Hsiao, C.-J. Yao and M.-J. Shieh, *Autophagy*, 2014, **10**, 1179–1192, DOI: 10.4161/auto.28679.
434 Y. Baglo, B. J. Liang, R. W. Robey, S. V. Ambudkar, M. M. Gottesman and H.-C. Huang, *Cancer Lett.*, 2019, **457**, 110–118, DOI: 10.1016/j.canlet.2019.04.037.
435 W. Tao, X. Zhu, X. Yu, X. Zeng, Q. Xiao, X. Zhang, X. Ji, X. Wang, J. Shi, H. Zhang and L. Mei, *Adv. Mater.*, 2017, **29**, 1603276, DOI: 10.1002/adma.201603276.
436 R. Sakhtianchi, R. F. Minchin, K.-B. Lee, A. M. Alkilany, V. Serpooshan and M. Mahmoudi, *Adv. Colloid Interface Sci.*, 2013, **201**, 18–29, DOI: 10.1016/j.cis.2013.10.013.
437 E. Froehlich, *Environ. Toxicol. Pharmacol.*, 2016, **46**, 90–94, DOI: 10.1016/j.etap.2016.07.003.
438 X. Li, N. Kwon, T. Guo, Z. Liu and J. Yoon, *Angew. Chem., Int. Ed.*, 2018, **57**, 11522–11531, DOI: 10.1002/anie.201805138.
439 D. R. Spahn, *Crit. Care*, 1999, **3**, R93–R97, DOI: 10.1186/cc364.
440 A. R. Kamuhabwa, A. Huygens, T. Roskams and P. A. De Witte, *Int. J. Oncol.*, 2006, **28**, 775–780, DOI: 10.3892/ijo.28.3.775.
441 Y. Cheng, H. Cheng, C. Jiang, X. Qiu, K. Wang, W. Huan, A. Yuan, J. Wu and Y. Hu, *Nat. Commun.*, 2015, **6**, 8785, DOI: 10.1038/ncomms9785.
442 L. Feng, D. Tao, Z. Dong, Q. Chen, Y. Chao, Z. Liu and M. Chen, *Biomaterials*, 2017, **127**, 13–24, DOI: 10.1016/j.biomaterials.2016.11.027.
443 M. Lopez-Lazaro, *Cancer Lett.*, 2007, **252**, 1–8, DOI: 10.1016/j.canlet.2006.10.029.
444 S. Z. F. Phua, G. Yang, W. Q. Lim, A. Verma, H. Chen, T. Thanabalu and Y. Zhao, *ACS Nano*, 2019, **13**, 4742–4751, DOI: 10.1021/acsnano.9b01087.
445 H. Wang, Y. Chao, J. Liu, W. Zhu, G. Wang, L. Xu and Z. Liu, *Biomaterials*, 2018, **181**, 310–317, DOI: 10.1016/j.biomaterials.2018.08.011.
446 J. Liu, T. Liu, P. Du, L. Zhang and J. Lei, *Angew. Chem., Int. Ed.*, 2019, **58**, 7808–7812, DOI: 10.1002/anie.201903475.
447 R. Han, M. Zhao, Z. Wang, H. Liu, S. Zhu, L. Huang, Y. Wang, L. Wang, Y. Hong, Y. Sha and Y. Jiang, *ACS Nano*, 2019, **14**, 9532–9544, DOI: 10.1021/acsnano.9b05169.
448 G. Lan, K. Ni, S. S. Veroneau, X. Feng, G. T. Nash, T. Luo, Z. Xu and W. Lin, *J. Am. Chem. Soc.*, 2019, **141**, 4204–4208, DOI: 10.1021/jacs.8b13804.
449 Y.-Y. Wang, Y.-C. Liu, H. Sun and D.-S. Guo, *Coord. Chem. Rev.*, 2019, **395**, 46–62, DOI: 10.1016/j.ccr.2019.05.016.
450 M. Valko, C. J. Rhodes, J. Moncol, M. Izakovic and M. Mazur, *Chem.-Biol. Interact.*, 2006, **160**, 1–40, DOI: 10.1016/j.cbi.2005.12.009.
451 M. Valko, D. Leibfritz, J. Moncol, M. T. D. Cronin, M. Mazur and J. Telser, *Int. J. Biochem. Cell Biol.*, 2007, **39**, 44–84, DOI: 10.1016/j.biocel.2006.07.001.
452 P. D. Ray, B.-W. Huang and Y. Tsuji, *Cell Signaling*, 2012, **24**, 981–990, DOI: 10.1016/j.cellsig.2012.01.008.
453 C. Gorrini, I. S. Harris and T. W. Mak, *Nat. Rev. Drug Discovery*, 2013, **12**, 931–947, DOI: 10.1038/nrd4002.
454 X. Duan, B. Chen, Y. Cui, L. Zhou, C. Wu, Z. Yang, Y. Wen, X. Miao, Q. Li, L. Xiong and J. He, *Apoptosis*, 2018, **23**, 587–606, DOI: 10.1007/s10495-018-1489-0.
455 H. Fan, G. Yan, Z. Zhao, X. Hu, W. Zhang, H. Liu, X. Fu, T. Fu, X.-B. Zhang and W. Tan, *Angew. Chem., Int. Ed.*, 2016, **55**, 5477–5482, DOI: 10.1002/anie.201510748.
456 W. Zhang, J. Lu, X. Gao, P. Li, W. Zhang, Y. Ma, H. Wang and B. Tang, *Angew. Chem., Int. Ed.*, 2018, **57**, 4891–4896, DOI: 10.1002/anie.201710800.
457 Y. Deng, F. Jia, S. Chen, Z. Shen, Q. Jin, G. Fu and J. Ji, *Biomaterials*, 2018, **187**, 55–65, DOI: 10.1016/j.biomaterials.2018.09.043.
458 A. Ferrario, N. Rucker, S. Wong, M. Luna and C. J. Gomer, *Cancer Res.*, 2007, **67**, 4989–4995, DOI: 10.1158/0008-5472.CAN-06-4785.
459 T. Y. Lin, W. Guo, Q. Long, A. Ma, Q. Liu, H. Zhang, Y. Huang, S. Chandrasekaran, C. Pan, K. S. Lam and Y. Li, *Theranostics*, 2016, **6**, 1324–1335, DOI: 10.7150/thno.14882.
460 M. Broekgaarden, R. Weijer, T. M. van Gulik, M. R. Hamblin and M. Heger, *Cancer Metastasis Rev.*, 2015, **34**, 643–690, DOI: 10.1007/s10555-015-9588-7.
461 E. C. Aniogo, B. P. A. George and H. Abrahamse, *Molecules*, 2020, **25**, 15, DOI: 10.3390/molecules25225308.
462 J. M. Ang, I. B. Riaz, M. U. Kamal, G. Paragh and N. C. Zeitouni, *Photodiagn. Photodyn. Ther.*, 2017, **19**, 308–344, DOI: 10.1016/j.pdpdt.2017.07.002.
463 J. M. Steinbauer, S. Schreml, P. Babilas, F. Zeman, S. Karrer, M. Landthaler and R. M. Szeimies, *Photochem. Photobiol. Sci.*, 2009, **8**, 1111–1116, DOI: 10.1039/b823378k.
464 J. P. Lacour, C. Ulrich, Y. Gilaberte, V. Von Felbert, N. Basset-Seguin, B. Dreno, C. Girard, P. Redondo, C. Serra-Guillen, I. Synnerstad, M. Tarstedt, A. Tsianakas, A. W. Venema, N. Kelleners-Smeets, H. Adamski, B. Perez-Garcia, M. J. Gerritsen, S. Leclerc, N. Kerrouche and R. M. Szeimies, *J. Eur. Acad. Dermatol. Venereol.*, 2015, **29**, 2342–2348, DOI: 10.1111/jdv.13228.

465 Y. Cheng, Y. Chang, Y. Feng, N. Liu, X. Sun, Y. Feng, X. Li and H. Zhang, *Small*, 2017, **13**, 1603935, DOI: 10.1002/smll.201603935.
466 S. H. Ibbotson and J. Ferguson, *Photodermatol., Photoimmunol. Photomed.*, 2012, **28**, 235–239, DOI: 10.1111/j.1600-0781.2012.00681.x.
467 W. J. Cottrell, A. D. Paquette, K. R. Keymel, T. H. Foster and A. R. Oseroff, *Clin. Cancer Res.*, 2008, **14**, 4475–4483, DOI: 10.1158/1078-0432.CCR-07-5199.
468 N. C. Zeitouni, A. D. Paquette, J. P. Housel, Y. Shi, G. E. Wilding, T. H. Foster and B. W. Henderson, *Lasers Surg. Med.*, 2013, **45**, 89–94, DOI: 10.1002/lsm.22118.
469 A. Francois, A. Salvadori, A. Bressenot, L. Bezdetnaya, F. Guillemin and M. A. D'Hallewin, *J. Urol.*, 2013, **190**, 731–736, DOI: 10.1016/j.juro.2013.01.046.
470 J. Fang, H. Nakamura and H. Maeda, *Adv. Drug Delivery Rev.*, 2011, **63**, 136–151, DOI: 10.1016/j.addr.2010.04.009.
471 F. Danhier, *J. Controlled Release*, 2016, **244**, 108–121, DOI: 10.1016/j.jconrel.2016.11.015.
472 H. Kobayashi, R. Watanabe and P. L. Choyke, *Theranostics*, 2013, **4**, 81–89, DOI: 10.7150/thno.7193.
473 A. J. Bullous, C. M. A. Alonso and R. W. Boyle, *Photochem. Photobiol. Sci.*, 2011, **10**, 721–750, DOI: 10.1039/c0pp00266f.
474 M. Broekgaarden, R. van Vught, S. Oliveira, R. C. Roovers, P. M. P. van Bergen en Henegouwen, R. J. Pieters, T. M. Van Gulik, E. Breukink and M. Heger, *Nanoscale*, 2016, **8**, 6490–6494, DOI: 10.1039/c6nr00014b.
475 J. Wang, G. Zhu, M. You, E. Song, M. I. Shukoor, K. Zhang, M. B. Altman, Y. Chen, Z. Zhu, C. Z. Huang and W. Tan, *ACS Nano*, 2012, **6**, 5070–5077, DOI: 10.1021/nn300694v.
476 Q. Liu, L. Xu, X. Zhang, N. Li, J. Zheng, M. Guan, X. Fang, C. Wang and C. Shu, *Chem. – Asian J.*, 2013, **8**, 2370–2376, DOI: 10.1002/asia.201300039.
477 L. Jia, L. Ding, J. Tian, L. Bao, Y. Hu, H. Ju and J.-S. Yu, *Nanoscale*, 2015, **7**, 15953–15961, DOI: 10.1039/c5nr02224j.
478 T.-S. Ding, X.-C. Huang, Y.-L. Luo and H.-Y. Hsu, *Colloids Surf., B*, 2015, **135**, 217–224, DOI: 10.1016/j.colsurfb.2015.07.064.
479 H.-M. Meng, X.-X. Hu, G.-Z. Kong, C. Yang, T. Fu, Z.-H. Li and X.-B. Zhang, *Theranostics*, 2018, **8**, 4332–4344, DOI: 10.7150/thno.26768.
480 N. Yang, W. Xiao, X. Song, W. Wang and X. Dong, *Nano-Micro Lett.*, 2020, **12**, 15, DOI: 10.1007/s40820-019-0347-0.
481 L. Zhang, Y. Gao, S. Sun, Z. Li, A. Wu and L. Zeng, *J. Mater. Chem. B*, 2020, **8**, 1739–1747, DOI: 10.1039/c9tb02621e.
482 W. Yang, F. Zhang, H. Deng, L. Lin, S. Wang, F. Kang, G. Yu, J. Lau, R. Tian, M. Zhang, Z. Wang, L. He, Y. Ma, G. Niu, S. Hu and X. Chen, *ACS Nano*, 2020, **14**, 620–631, DOI: 10.1021/acsnano.9b07212.
483 S. Zhong, C. Chen, G. Yang, Y. Zhu, H. Cao, B. Xu, Y. Luo, Y. Gao and W. Zhang, *ACS Appl. Mater. Interfaces*, 2019, **11**, 33697–33705, DOI: 10.1021/acsami.9b12620.
484 K. Wang, Y. Tu, W. Yao, Q. Zong, X. Xiao, R.-M. Yang, X.-Q. Jiang and Y. Yuan, *ACS Appl. Mater. Interfaces*, 2020, **12**, 6933–6943, DOI: 10.1021/acsami.9b21525.
485 Y. Liu, J. Jing, F. Jia, S. Su, Y. Tian, N. Gao, C. Yang, R. Zhang, W. Wang and X. Zhang, *ACS Appl. Mater. Interfaces*, 2020, **12**, 6966–6977, DOI: 10.1021/acsami.9b22097.
486 G. Yang, S. Z. F. Phua, W. Q. Lim, R. Zhang, L. Feng, G. Liu, H. Wu, A. K. Bindra, D. Jana, Z. Liu and Y. Zhao, *Adv. Mater.*, 2019, **31**, 1901513, DOI: 10.1002/adma.201901513.
487 Y. Xue, J. Tian, L. Xu, Z. Liu, Y. Shen and W. Zhang, *Eur. Polym. J.*, 2019, **110**, 344–354, DOI: 10.1016/j.eurpolymj.2018.11.033.
488 G. Yang, C. Chen, Y. Zhu, Z. Liu, Y. Xue, S. Zhong, C. Wang, Y. Gao and W. Zhang, *ACS Appl. Mater. Interfaces*, 2019, **11**, 44961–44969, DOI: 10.1021/acsami.9b15996.
489 W. Pan, M. Shi, Y. Li, Y. Chen, N. Li and B. Tang, *RSC Adv.*, 2018, **8**, 42374–42379, DOI: 10.1039/c8ra08549h.
490 J. Zhang, X. Zheng, X. Hu and Z. Xie, *J. Mater. Chem. B*, 2017, **5**, 4470–4477, DOI: 10.1039/c7tb00063d.
491 L. Yan, Y. Wang, T. Hu, X. Mei, X. Zhao, Y. Bian, L. Jin, R. Liang, X. Weng and M. Wei, *J. Mater. Chem. B*, 2020, **8**, 1445–1455, DOI: 10.1039/c9tb02591j.
492 X. Jing, Z. Zhi, N. Zhang, H. Song, Y. Xu, G. Zhou, D. Wang, Y. Shao and L. Meng, *Chem. Eng. J.*, 2020, **385**, 123893, DOI: 10.1016/j.cej.2019.123893.
493 J. Zhang, M. Xu, Y. Mu, J. Li, M. F. Foda, W. Zhang, K. Han and H. Han, *Biomaterials*, 2019, **218**, 119312, DOI: 10.1016/j.biomaterials.2019.119312.
494 Z. Xie, S. Liang, X. Cai, B. Ding, S. Huang, Z. Hou, P. A. Ma, Z. Cheng and J. Lin, *ACS Appl. Mater. Interfaces*, 2019, **11**, 31671–31680, DOI: 10.1021/acsami.9b10685.
495 L. Zhou, H. Wang and Y. Li, *Theranostics*, 2018, **8**, 1059–1074, DOI: 10.7150/thno.22679.
496 G. Yang, J. Tian, C. Chen, D. Jiang, Y. Xue, C. Wang, Y. Gao and W. Zhang, *Chem. Sci.*, 2019, **10**, 5766–5772, DOI: 10.1039/c9sc00985j.
497 G. M. Mortimer, N. J. Butcher, A. W. Musumeci, Z. J. Deng, D. J. Martin and R. F. Minchin, *ACS Nano*, 2014, **8**, 3357–3366, DOI: 10.1021/nn405830g.
498 Y. Liu, Z. Wang, Y. Liu, G. Zhu, O. Jacobson, X. Fu, R. Bai, X. Lin, N. Lu, X. Yang, W. Fan, J. Song, Z. Wang, G. Yu, F. Zhang, H. Kalish, G. Niu, Z. Nie and X. Chen, *ACS Nano*, 2017, **11**, 10539–10548, DOI: 10.1021/acsnano.7b05908.
499 R. Shukla, V. Bansal, M. Chaudhary, A. Basu, R. R. Bhonde and M. Sastry, *Langmuir*, 2005, **21**, 10644–10654, DOI: 10.1021/la0513712.
500 M. E. Selim and A. A. Hendi, *Asian Pac. J. Cancer Prev.*, 2012, **13**, 1617–1620, DOI: 10.7314/apjcp.2012.13.4.1617.
501 Y.-J. Gu, J. Cheng, C.-C. Lin, Y. W. Lam, S. H. Cheng and W.-T. Wong, *Toxicol. Appl. Pharmacol.*, 2009, **237**, 196–204, DOI: 10.1016/j.taap.2009.03.009.
502 O. Bar-Ilan, R. M. Albrecht, V. E. Fako and D. Y. Furgeson, *Small*, 2009, **5**, 1897–1910, DOI: 10.1002/smll.200801716.
503 Q. Wu, Y. Zhao, Y. Li and D. Wang, *Nanoscale*, 2014, **6**, 11204–11212, DOI: 10.1039/c4nr02688h.
504 Q. Wu, X. Zhou, X. Han, Y. Zhuo, S. Zhu, Y. Zhao and D. Wang, *Biomaterials*, 2016, **102**, 277–291, DOI: 10.1016/j.biomaterials.2016.06.041.

505 L. Zhao, S. Dong, Y. Zhao, H. Shao, N. Krasteva, Q. Wu and D. Wang, *Ecotoxicol. Environ. Saf.*, 2019, **169**, 1–7, DOI: 10.1016/j.ecoenv.2018.10.106.
506 C. Zhang, K. Zhao, W. Bu, D. Ni, Y. Liu, J. Feng and J. Shi, *Angew. Chem., Int. Ed.*, 2015, **54**, 1770–1774, DOI: 10.1002/anie.201408472.
507 Y. Yang, L. Wang, H. Cao, Q. Li, Y. Li, M. Han, H. Wang and J. Li, *Nano Lett.*, 2019, **19**, 1821–1826, DOI: 10.1021/acs.nanolett.8b04875.
508 M. Kubiak, L. Lysenko, H. Gerber and R. Nowak, *Postepy Hig. Med. Dosw.*, 2016, **70**, 735–742, DOI: 10.5604/17322693.1208196.
509 T. G. St Denis, K. Aziz, A. A. Waheed, Y.-Y. Huang, S. K. Sharma, P. Mroz and M. R. Hamblin, *Photochem. Photobiol. Sci.*, 2011, **10**, 792–801, DOI: 10.1039/c0pp00326c.
510 H. Cao, L. Wang, Y. Yang, J. Li, Y. Qi, Y. Li, Y. Li, H. Wang and J. Li, *Angew. Chem., Int. Ed.*, 2018, **57**, 7759–7763, DOI: 10.1002/anie.201802497.

